CHEMICAL ENGINEERING SCIENCE
GENIE CHIMIQUE

VOL. 7 1958 No. 4

VOL.
7
957/58

Studies on ion-exchange—I

General introduction

K. KLAMER and D. W. VAN KREVELEN
Central Laboratory, Staatsmijnen, Geleen, Holland

(*Received* 27 *August* 1957)

Abstract—This paper forms an introduction to a series dealing with the characterization of ion-exchangers both as regards their equilibria with electrolyte solutions and their kinetic behaviour. An outline is given of the development of ion-exchangers with reference to their principal field of application, the purification of water.

For the quantitative description of the behaviour of a column use will be made of an equation giving the differential material balance, and of data on equilibria and kinetics. When commercial products are examined it is, in general, found that the equilibria in which H^+-ions play a part cannot be described by the known formulae, e.g., that of the law of mass action, while the determination of their equilibria by known methods also meets with difficulties.

The ion-exchange phenomenon is studied in the light of the theory of adsorptive percolation or chromatography. If there is an instantaneous establishment of equilibrium, the differential material balance may be used for demonstration how a chromatogram can alter its shape depending on the form of the isotherm. *Mutatis mutandis*, the same formulae as used for chromatography may be employed for ion-exchange.

Experiments and applications, which will be discussed later, relate to the use of ion-exchangers in water purification practice.

Résumé—La présente documentation est une introduction à une série relative aux caractéristiques d'échangeurs d'ions tant en ce qui concerne leurs équilibres avec des solutions électrolytiques que leur comportement cinétique. On donne une vue générale du développement des échangeurs d'ions par rapport à leur domaine principal d'application, à savoir l'épuration d'eau.

Pour la description quantitative du comportement d'une colonne on utilise une équation représentant le bilan-matière differentiel et des données relatives aux équilibres et à la cinétique. En examinant des produits de commerce on constate, en général, que l'équilibre dans lequel les ions H^+ jouent un rôle ne peut-être décrit moyennant les formules connues, par exemple, celle de la loi sur l'action de la masse, parce que la détermination de leur équilibre par les méthodes connues se heurte à des difficultés.

On étudie le phénomène de l'échange d'ions à la lumière de la théorie de la filtration adsorptive ou la chromatographie. En cas d'un établissement instantané de l'équilibre on peut utiliser un bilan-matière differentiel pour démontrer comment un chromatogramme peut modifier sa forme en fonction de la forme de l'isotherme. Les formules utilisées pour la chromatographie s'appliquent, *mutatis mutandis*, aussi à l'échange d'ions.

Les expérimentations et les applications qui seront traitées plus tard portent sur l'emploi d'échangeurs d'ions pour l'épuration d'eau.

Zusammenfassung—Dieser Aufsatz stellt eine Einführung zu einer Serié dar, die sich mit den charakteristischen Eigenschaften von Ionenaustauschern beschäftigt und zwar sowohl hinsichtlich ihrer Gleichgewichte mit elektrolytischen Lösungen als auch ihres kinetischen Verhaltens. Ferner wird ein Überblick gegeben über die Entwicklung von Ionenaustauschern in Bezug auf ihre hauptsächliche Anwendung, die Wasserreinigung.

Für die quantitative Beschreibung des Verhaltens einer Kolonne wird von einer differenziellen Mengenbilanz und von den Werten des Gleichgewichts und der Kinetik Gebrauch gemacht. Bei der Untersuchung handel süblicher Produkte stellt man fest, dass im allgemeinen die Gleichgewichte, in denen H^+-Ionen eine Rolle spielen, nicht durch bekannte Gleichungen beschrieben werden können, z.B. durch das Massenwirkungsgesetz, da auch die Bestimmung ihrer Gleichgewichte durch bekannte Methoden auf Schwierigkeiten stösst.

Der Ionenaustausch wird unter dem Gesichtspunkt der adsorptiven Filtration oder Chromatographie untersucht. Sofern sich das Gleichgewicht augenblicklich einstellt, kann die differenzielle Mengenbilanz benutzt werden, um die Änderung der Form eines Chromatogramms in Abhängigkeit von der Form der Isothermen zu zeigen. Dieselben Gleichungen, die für die Chromatographie benutzt werden, können auch mutatis mutandis auf den Ionenaustausch angewendet werden.

Experimente und Anwendugen, die später diskutiert werden sollen, beziehen sich auf den Gebrauch von Ionenaustauschern in der Praxis der Wasserreinigung.

1. OBJECT OF THE INVESTIGATION

ION-EXCHANGE, i.e. the process in which equivalent amounts of ions are exchanged between a solid and a solution, was discovered about a century ago by THOMPSON [12] and WAY [14]. A few years later EICHHORN [5] established the reversibility of the process. Nearly 50 years after this discovery GANS [6] realized the first technical application of ion-exchangers, water-softening, which is still their principal field.

Up to about 20 years ago natural zeolites and synthetic silicates, for which GANS introduced the name permutites, were the only products used for this process. Gradually the permutites were superseded by ion-exchangers prepared from sulphonated coal (SMIT [11] and LIEBKNECHT [10]) and by completely synthetic products derived from phenosulphonic acid and formaldehyde (ADAM and HOLMES [1]) which have the advantage of permitting regeneration with acids. The latter authors also developed the first anion-exchangers on the basis of polyamides and formaldehyde, while the range of ion-exchangers, as far as their functional groups are concerned, was completed by the strongly basic anion-exchangers (D'ALELIO [2]) which are capable even of binding weak acids such as silicic acid.

As in other fields of technology, preparation and utilization of ion-exchangers has been far ahead of the theoretical knowledge. We may say that it was not until 1943, when de VAULT [13] advanced his theory of chromatography, that a basis was provided permitting a theoretical interpretation of the process. Of the problems attending the application of ion-exchangers, their characterization is one of the most important; unfortunately, this is still very incompletely understood. The cause of this is to be sought in the complicated character of the problem. For complete comprehension it is essential that information be available about the equilibrium and the kinetics of the process, and these data should be combined with the material balance of the column expressed in the two variables place and time. Since even in relatively simple cases the results are already extremely complicated from a mathematical point of view, it is obvious that kinetic investigations in a column are almost exclusively restricted to those processes of which the equilibria either can be represented by a linear [4] or a Langmuir [9] isotherm or satisfy the law of mass action [3].

However, the results of this study of industrially applicable commercial products have shown that the above equilibria usually fail to fit the experimental results adequately. This also

VOL. 7 957/58

appears from the literature dealing for example with equilibrium measurements on cation-exchangers in which H^+-ions are involved (KRISHNAMOORTY and OVERSTREET [8]); it is just these equilibria which occur frequently in connection with the use of ion-exchangers for water purification.

Furthermore it will be seen that the customary procedures of determining the equilibria are not, in general, applicable to all types of ion-exchangers. Therefore, another method has been developed starting from the theory of chromatography. The final results have been expressed in graphs which were used afterwards to give a graphical interpretation of the kinetic measurements, a method not previously used in this field.

The object of the investigation to be discussed in this series of articles is to describe the behaviour of ion-exchangers in the preparation of boiler-feed water. As the treatment has been kept as general as possible the conclusions are also applicable to other fields.

2. Relative Data from the Theory of Chromatography

To obtain a clear insight into the phenomena taking place in a column filled with ion-exchanger, it is useful to fall back upon those considerations in the theory of chromatography (de VAULT [13], GLUECKAUF [7]) in which these phenomena are brought into connection with the relative adsorption isotherm(s). Starting from the well-known differential material balance (for piston-flow):

$$v\left(\frac{\delta c}{\delta x}\right)_t + \gamma\left(\frac{\delta c}{\delta t}\right)_x + S\left(\frac{\delta q}{\delta t}\right)_x = 0 \qquad (1)$$

it can be derived that in the case of instantaneous establishment of equilibrium in the column, the rate of displacement v_e of a given concentration c satisfies the relation:

$$\left(\frac{\delta x}{\delta t}\right)_e = \frac{v}{\gamma + Sf'(c)} \qquad (2)$$

Here $f'(c)$ is the derivative of the isotherm $q = f(c)$. Differentiation of equation 2 gives:

$$\frac{d\left(\frac{\delta x}{\delta t}\right)_e}{dc} = \frac{-vSf''(c)}{\{\gamma + Sf'(c)\}^2} \qquad (3)$$

This equation is very useful for describing the shape, or changes in the shape, of a chromatogram. When the isotherm is linear the rate of displacement v_e is independent of concentration; a given chromatogram retains its shape.

When the *curvature* of the isotherm is *positive* (Fig. 1), loading of an empty column will result in a diffuse front since v_e decreases with increasing

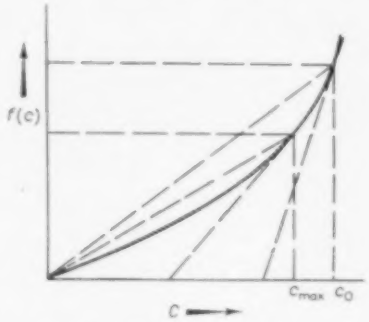

FIG. 1. $f''(c) > 0$. Tangents and chords.

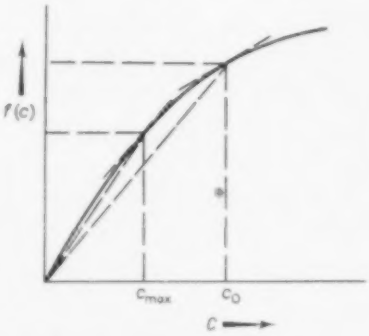

Fig. 2. $f''(c) < 0$. Tangents and chords.

concentration. If, on the other hand, the isotherm shows a *negative curvature* (Fig. 2), v_e would, according to equation 3, increase with increasing concentration which would lead to an impossible situation. It must be concluded, therefore, that the front is sharp and that all concentrations move at the same rate:

$$\frac{dx}{dt} = \frac{v}{\gamma + S\dfrac{f(c_0)}{c_0}}. \qquad (4)$$

When the column is eluted with a pure solvent, an isotherm with a positive curvature will, in

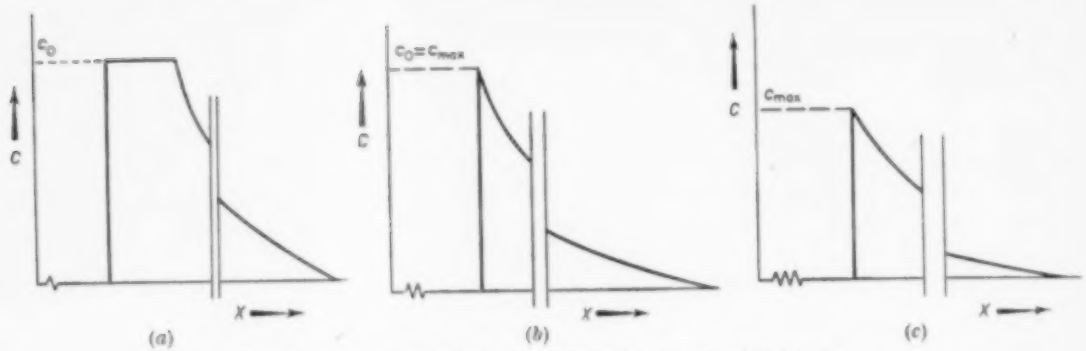

FIG. 3. Development of chromatogram for the case $f''(c) > 0$.

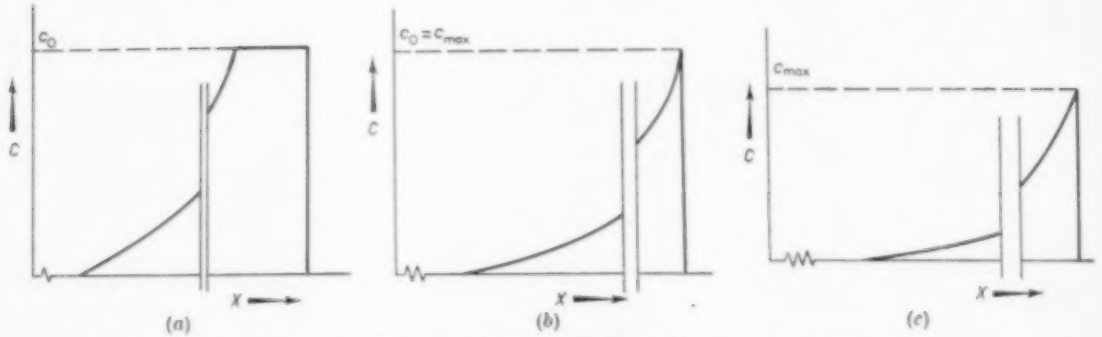

Fig. 4. Development of chromatogram for the case $f''(c) < 0$.

analogy with the foregoing, develop a sharp rear boundary, whereas an isotherm with a negative curvature will develop a diffuse one (Figs. 3a and 4a).

With either type of isotherm the rear catches up with the front; when the isotherm has a positive curvature the rate of c_0 in the (sharp) rear is higher than that of c_0 in the (diffuse) front since the slope of the chord through $(c_0, f(c_0))$ and (0,0) is smaller than that of the tangent in $(c_0, f(c_0)$ to the isotherm see equations (2) and (4) and Fig. 1). *Mutatis mutandis*, this also holds for the isotherms with negative curvatures (Fig. 2). The further concentration changes are shown in Fig. (3)b, (c) and 4(b), (c).

If the isotherm shows an *inflection point* as in Fig. 5 ($f'''(c) > 0$), loading at instantaneous equilibrium proceeds differently. It might be concluded from the foregoing that with $c < c_b$ the front tends to adopt a sharp shape and with

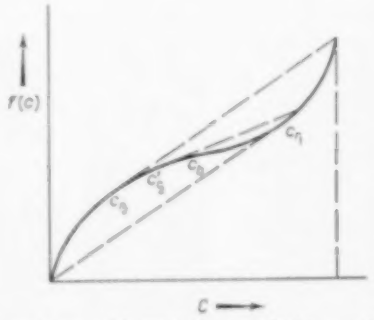

FIG. 5. Isotherm with $f'''(c) > 0$ ($f''(c) = 0$ if $c = c_b$).

$c > c_b$ a diffuse one. However, the slope of the tangent ($f'(c_b)$) in c_b is smaller than that of the chord for (0·0) and $(c_b, f(c_b))$; as a result the rate of c_b in the sharp part of the front would be lower than that in the diffuse part. Consequently, the front will be straightened up to c_{r_1} which point is defined by :

$$f'(c_{r_1}) = f(c_{r_1})/c_{r_1}$$

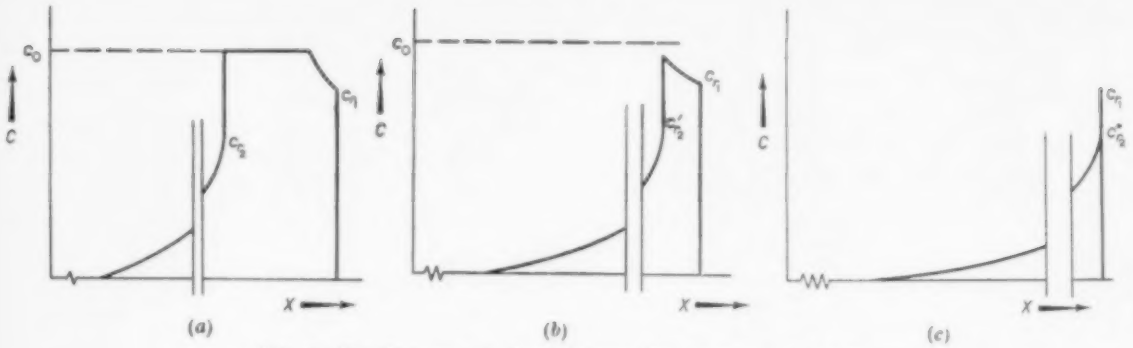

FIG. 6. Development of chromatogram for the case $f'''(c) > 0$.

Here again elution leads to rear formation as described above and finally the chromatogram is transformed as shown in Fig. 6(a), (b), (c). The rear overtakes the front and c_{r_2} increases (c_{r_2}'). When the two sharp parts have caught up with each other, c_{r_2} is given by the tangent drawn from c_{r_1} to the top of the isotherm :

$$f'(c_{r_2}'') = [f(c_{r_1}) - f(c_{r_2}'')]/[c_{r_1} - c_{r_2}''] \quad (5)$$

When this point has been reached the further course of the curve is as shown in Figs. 6b and c.

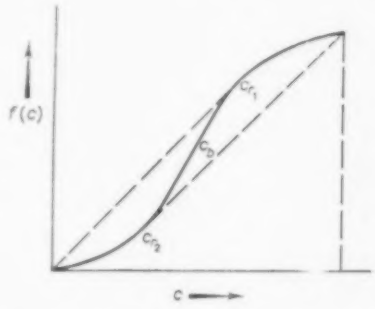

FIG. 7. Isotherm with $f'''(c) < 0$ ($f''(c) = 0$ if $c = c_b$).

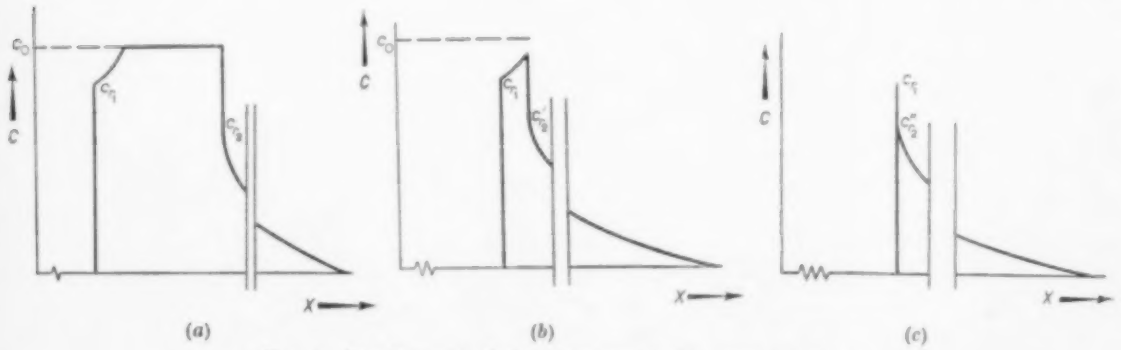

FIG. 8. Development of chromatogram for the case $f'''(c) < 0$.

An analogous description can be given for the case $f'''(c) < 0$ (Fig. 7). In Fig. 8 (a, b, c) the development of the chromatogram is indicated.

3. Ion-Exchange as a Form of Adsorptive Percolation

Ion-exchange in a column bears some resemblance to a chromatographic process. An example of ion-exchange reactions is the equilibrium between a sodium chloride solution and a cation-exchanger in the H^+– form :

$$NaCl + HR \rightleftharpoons NaR + HCl \quad (6)$$

$$\text{or } Na_L^+ + H_R^+ \rightleftharpoons Na_R^+ + H_L^+ \quad (7)$$

In many theories these equilibria are represented by a formula ; however, these will not be discussed here because, like the empirical formulations, they

have only a limited validity. Therefore, we shall restrict ourselves to giving a graphical representation of the equilibria in a following paper. With the above equilibrium the loading of the ion-exchanger q_{Na}^{+} is a function of the concentrations of Na^+ and H^+ in the solution :

$$q_{Na}^{+} = f(c_{Na}^{+}, c_{H}^{+}) \tag{8}$$

During the ion-exchange process the total concentration of the solution remains constant since every Na^+-ion leaving the solution is replaced by an H^+-ion.

This is why q_{Na}^{+} for different total concentrations in solution (a) is represented as a function of the equivalent fraction* of one ion type (e.g. Na^+) in solution (α) :

$$q_a = f_a(\alpha) \tag{9}$$

The formulae and observations mentioned above then continue to be valid provided c is replaced by αa and it is borne in mine that in a column experiment a is constant. The material balance (equation 1) then changes into :

$$av\left(\frac{\delta\alpha}{\delta x}\right)_t + a\gamma\left(\frac{\delta\alpha}{\delta t}\right)_x + S\left(\frac{\delta q_a}{\delta t}\right)_x = 0 \tag{10}$$

the equation for the rate of displacement of the equivalent fraction in a diffuse part of the chromatogram at instantaneous equilibrium (equation 2) into :

$$\left(\frac{\delta x}{\delta t}\right)_a = \frac{av}{a\gamma + Sf_a'(\alpha)} \tag{11}$$

and the corresponding equation for a sharp part (equation 4) into :

$$\frac{dx}{dt} = \frac{av}{a\gamma + \dfrac{Sf_a(\alpha_0)}{\alpha_0}} \tag{12}$$

Here α_0 = the equivalent fraction of Na^+-ions in the liquid which is flowing in.

In analogy to the substitution of αa for c, q_a might be replaced by the equivalent fraction of the ion in the exchanger multiplied by the total capacity ; as the latter quantity is often difficult to determine this substitution will not be made here.

With these equations, the ion-exchange mechanism has been expressed in formulae which are normally used in chromatography.

Acknowledgement—The authors thank Dr. C. VAN HEERDEN for valuable discussions about this subject.

NOTATION

a = total ion concentration in solution $(M\,L^{-3})$
c = concentration in the liquid $(M\,L^{-3})$
$f(c)$ = concentration in the absorbent at equilibrium $(M\,L^{-3})$
$f_a(\alpha)$ = concentration in the ion-exchanger at equilibrium $(M\,L^{-3})$
q = concentration in the absorbent $(M\,L^{-3})$
q_a = concentration in the ion-exchanger $(M\,L^{-3})$
S = cross-sectional area of the column (L^2)
t = time (T)
v = rate of flow $(L^3\,T^{-1})$
v_c = displacement rate of the concentration c in the column $(L\,T^{-1})$
x = distance to the point where the liquid enters the column (L)
α = equivalent fraction of one ion type in solution
γ = free space per unit length in the column (L^2)

Subscripts

o = condition before the liquid enters the column
b = inflection point in the isotherm
L = liquid
R = ion-exchanger
r = tangent point

*The equivalent fraction in ion-mixtures of equal valency is of course equal to the molecular fraction ; this does not apply, however, when the ions differ in valency.

REFERENCES

[1] ADAM B. A. and HOLMES E. L. *J. Soc. Chem. Ind. Lond.* 1935 **54** 1-6T.
[2] D'ALELIO G. F. *U.S. Pat.* 2,366,008.
[3] BADDOUR R. F. and GILLILAND E. R. *Industr. Engng. Chem.* 1953 **45** 330.
[4] BOYD G. E. MYERS, L. S. Jr. and ADAMSON A. W. *J. Amer. Chem. Soc.* 1947 **69** 2849.
[5] EICHHORN H. *Pogg. Ann. Phys., Chem.* p3 1858 **105** 126.

[6] Gans R. *Jb. königl. preuss. geol. Landesanstalt* 1905 **26** 179 ; 1906 **27** 63.

[7] Glueckauf E. *J. Chem. Soc.* 1947 1302.

[8] Krishnamoorty C. and Overstreet R. *Soil Sci.* 1950 **69** 87.

[9] Lapidus L. and Rosen J. B. *Chem. Eng. Progr. Symp. Series* 1954 Na14 **50** 97.

[10] Liebknecht O. *Ger. Pat.* 763,926 ; *U.S. Pat.* 2,191,060 ; 2,206,007.

[11] Smit P. *Dutch Pat.* 49,741 ; *U.S. Pat.* 2,191,063 ; 2,205,635.

[12] Thompson H. S. *J. R. Agric. Soc.* 1850 **11** 68.

[13] de Vault D. *J. Amer. Chem. Soc.* 1943 **65** 532.

[14] Way T. T. *J. R. Agric. Soc.* 1850 **11** 313 ; 1852 **13** 123.

VOL.
7
957/58

Chemical Engineering Science, 1958, Vol. 7, pp. 204 to 214. Pergamon Press Ltd.

Studies on ion-exchange—II

Determination of ion-exchange equilibria

K. KLAMER, J. C. H. LINSSEN and D. W. VAN KREVELEN
Central Laboratory, Staatsmijnen, Geleen, Holland

(*Received* 27 *August* 1957)

Abstract—A description is given of current methods for the determination of the equilibria of ion exchangers in electrolyte solutions, by means of which the behaviour of a column can be accounted for; among these, the "column method" is to be preferred. However, it is found that experiments carried out according to the column method easily lead to results that are inaccurate or even wrong. It is shown that this disadvantage can be eliminated by the use of buffer solutions having the ion concentration for which the equilibrium is required, for a buffering anion has a great influence on the way in which the equilibrium is reached with cation exchangers, and the same influence is exerted by a buffering cation on anion exchangers.

The determination of a number of equilibria with cation and anion exchangers is described with reference to the purification of water. It is striking that in the resulting isotherms inflection points occur very frequently; these points are attributable to the polyfunctionality of the products. In general, an isotherm may have a great variety of shapes, dependent on the structure of the exchanger and on the composition of the solution. A classification of isotherms on this basis is given. The exchange of uni – univalent ions proves to be independent of the total ion concentration of the solution.

Résumé—On donne une description de méthodes courantes pour la détermination des équilibres d'échangeurs d'ions dans des solutions électrolytiques, équilibres qui permettent de calculer le comportement d'une colonne; de toutes ces méthodes on préfère appliquer la méthode de la colonne. Cependant, on a constaté que les expérimentations effectuées selon la méthode de la colonne entrainent facilement des résultats inexacts et même faux.

On démontre que ce désavantage peut-être évité par l'emploi de solutions tampons qui ont une concentration d'ions pour laquelle on désire connaître l'équilibre. C'est qu'un anion tampon exerce une grande influence sur la manière dont on atteint l'équilibre avec des échangeurs de cations, et un cation tampon exerce la même influence sur les échangeurs d'anions.

La détermination d'un nombre d'équilibres avec des échangeurs de cations et d'anions se trouve décrite par rapport à la purification d'eau. Il est remarquable que les isothermes qui en résultent manifestent très souvent des points d'inflexion, points qui sont dus à la polyfonctionnalité des produits. En général, une isotherme peut avoir une grande diversité de formes en fonction de la structure de l'échangeur et de la composition de la solution. On donne une classification d'isothermes à cette base.

L'échange d'ions uni – univalents s'avère indépendante de la concentration totale d'ions de la solution.

Zusammenfassung—Die heute üblichen Methoden für die Bestimmung der Gleichgewichte von Ionenaustauschern in elektrolytischen Lösungen werden beschrieben, mit deren Hilfe das Verhalten einer Kolonne ermittelt werden kann. Unter diesen wird die "Säulenmethode" bevorzugt. Man findet indessen, dass Versuche, die gemäss der Säulenmethode ausgeführt werden, leicht zu ungenauen oder sogar falschen Ergebnissen führen. Es zeigt sich, dass dieser Nachteil durch die Verwendung von Pufferlösungen vermieden werden kann, welche diejenige Ionenkonzentration besitzen, für die das Gleichgewicht gesucht wird. Ein pufferndes Anion hat einen grossen Einfluss auf die Art, in der das Gleichgewicht mit Kationenaustauschern erreicht wird, und der gleiche Einfluss wird durch ein pufferndes Kation auf Anionaustauscher ausgeübt.

Die Verfasser beschreiben die Bestimmung einer Anzahl von Gleichgewichten mit Kationen- und Anionen-Austauschern im Hinblick auf die Wasserreinigung. Es fällt auf, dass die sich ergebenden Isothermen sehr häufig Wendepunkte besitzen. Diese Punkte lassen sich durch die sehr verschiedene Natur der Produkte erklären. Im allgemeinen kann eine Isotherme sehr verschiedene Formen haben, abhängig von der Struktur des Austauschers und der Zusammensetzung der Lösung. Auf dieser Grundlage wird eine Klassifikation von Isothermen mitgeteilt. Der Austausch von ein-einwertigen Ionen erweist sich als unabhängig von der gesamten Ionenkonzentration der Lösung.

VOL. 7 957/58

IN PART I it has been proved that in chromatography, in the case of an instantaneous equilibrium in the column, the change in the shape of the chromatogram can be quantitatively and qualitatively predicted from the shape of the adsorption isotherm. A similar observation applies to ion exchange.

In reality, the establishment of the equilibrium is, of course, not instantaneous, but even so, knowledge of the position of the equilibrium is of the utmost importance for calculating the driving force of the process.

In this part, attention will be paid to the determination of the equilibria and to the classification of ion exchangers according to the shapes of the equilibrium curves.

1. METHODS OF DETERMINING EQUILIBRIUM

The relation $q_a = f_a(\alpha)$ can be determined by the following methods :

(1.1) *The batch method*

This method was used for instance by GREGOR and BREGMAN [8]. While being stirred continuously, a given quantity of exchanger is allowed to reach equilibrium with a solution containing the ions of which the equilibrium is to be determined. Once equilibrium has been reached, the compositions of the solution and the exchanger are determined. The disadvantage of this method is that it is impossible to predict the value of α which the solution will eventually have, so that it is often necessary to carry out several experiments in order to scan a certain range.

(1.2) *The derivation from a continuous elution curve*

This less widely used method has been elaborated by GLUECKAUF [5], [6], SILLÉN [15], [16] and YANOWSKI [18]. By integration of the following equation (equation 11 in our first paper [10]) :

$$\left(\frac{\partial x}{\partial t}\right)_{\alpha} = \frac{av}{a\gamma + Sf_a'(\alpha)} \qquad (1)$$

a relation is obtained between $f_a'(\alpha)$ and the volume of liquid passed through the column. From the elution curve α can be determined as a function of this volume, and by graphical integration of $f_a'(\alpha)$ it is then possible to determine $f_a(\alpha)$.

The disadvantage of this method, already pointed out by GLUECKAUF and COATES [7], is the probability of rather serious errors in the case of isotherms deviating little from linearity. If for some reason the chromatogram is disturbed, or if a kinetic process is involved, such a disturbance may give rise to the erroneous conclusion that there is a diffuse front, as with linear isotherms all concentrations have the same velocity.

(1.3) *The column method*

A solution having a known value of α is passed over a column containing an ion exchanger until the composition of the effluent becomes equal to that of the incoming solution. A disadvantage is that, if a widening front is involved (with a sharp front the experiment in general proceeds rapidly), there is a chance that a large amount of liquid has to be passed over before the correct equilibrium is reached ; for, if a certain α is accompanied by a high $f_a'(\alpha)$, the rate at which α moves through the column will, according to equation (1), be low.

That this is not an imaginary danger may be seen from the fact that, whereas the $Na^+ - H^+$ equilibrium for a monofunctional strongly acid exchanger can easily be determined with a solution of hydrochloric acid and common salt, this method cannot be used for a polyfunctional

exchanger possessing both strongly acid and weakly acid groups. Later it will be seen that with the latter type of exchangers $f'_a(\alpha)$ is high if α has a high value. One cause is that, on the strength of analysis, there is a tendency to think that the effluent has the same composition as the incoming solution, while owing to a small error in the analysis a large error in $f_a(\alpha)$ may occur if $f'_a(\alpha)$ has a high value.

It will be shown that also with the latter exchangers the equilibria may well be determined, provided use is made of buffer solutions.

(1.4) *The column method using buffer solutions*

In itself the use of buffer solutions is not a novel technique : these solutions have long been used in the determination of the relation between pH and total capacity [8]. In the present case, however, buffer solutions are to be used for determining equilibrium curves, so that care will have to be taken that the α values show a wide spread and that the total ion concentration in the *inflowing solution* in the various tests is always the same and equal to the ion concentration for which the equilibrium curve is to be determined.

However, if buffer solutions are used, not only the equilibrium :

$$Na^+_L + H^+_R \rightleftharpoons Na^+_R + H^+_L \qquad (2)$$

but also the equilibrium :

$$H^+ + X^- \rightleftharpoons HX \qquad (3)$$

plays a part, which implies that *in the column* $c_{Na^+} + c_{H^+}$ is no longer constant, but $c_{Na^+} + c_{H^+} + c_{HX} = c^\circ$.

In addition to the previously determined equivalent fraction :

$$\alpha_1{}^\circ = (c^\circ_{Na^+})/(c^\circ_{Na^+} + c^\circ_{H^+}) \qquad (4)$$

in which the index 1 relates to the isotherm to be determined (Fig. 1), the auxiliary quantity α_2 is now introduced :

$$\alpha_2 = (c_{Na^+})/(c_{Na^+} + c_{H^+} + c_{HX}) \qquad (5)$$

corresponding to a second isotherm $f_{c^\circ}(\alpha_2)$ (*cf.* Fig. 1, curve 2) ; this indicates by its shape

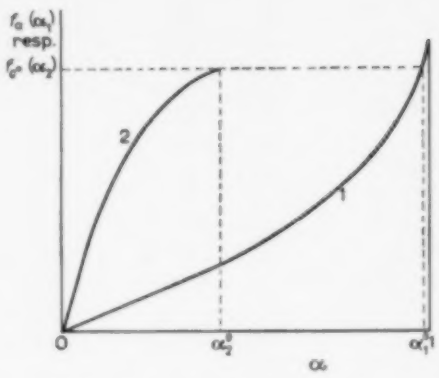

FIG. 1. Curves of types 1 and 2.

whether or not a sharp front is formed in the column.

A sharp front ($f''_{c^\circ}(\alpha_2) < 0$) is ideal ; the only requirement is that $f'_{c^\circ}(\alpha_2)$ be not too great ; in any case α_2 must be small, and hence, in accordance with equation (5), c_{HX} great. This requirement can be fulfilled by a correct choice of HX – i.e. by ensuring that this acid is sufficiently weak.

It will be clear that *without a buffer* $f_a(\alpha_1{}^\circ)$ *cannot be reached, because* $f_a'(\alpha_1{}^\circ)$ *is very great, whereas, if a buffer is used, this load can be realized* ($f_a(\alpha_1{}^\circ) = f'_{c^\circ}(\alpha_2{}^\circ)$), *because* $f_{c^\circ}(\alpha_2{}^\circ)$ *is small.* Each point to be determined of the isotherm 1, i.e. each value of the equivalent fraction in the solution ($\alpha_1{}^\circ$), has its own curve 2, whose shape indicates how the $f_a(\alpha)$ value corresponding to $\alpha_1{}^\circ$ is reached ; consequently there is a series of curves of type 2 relating to each isotherm to be determined.

The above observations can be illustrated by describing how a second isotherm can be calculated if the first should be known. For equilibrium (3) the following equation holds :

$$K = (c_{H^+} \cdot c_{X^-})/(c_{HX}) \qquad (6)$$

and, owing to the electric neutrality of the solution :

$$c_{Na^+} + c_{H^+} = c_{X^-} \qquad (7)$$

Finally it is assumed that :

$$c_{Na^+} + c_{H^+} + c_{HX} = c^\circ \qquad (8)$$

If c_{Na^+} and c_{HX} are eliminated from equation (5) by means of equations (6), (7) and (8), it follows that :

$$\alpha_2 = \frac{K}{c_{N^+} + K} - \frac{c_{H^+}}{c^\circ} \tag{9}$$

Next, c_{H^+} is chosen and α_2 calculated from equation (9), bearing in mind that to α_2 there belongs the same $f(\alpha)$ as to :

$$\alpha_1 = (\alpha_2 c^\circ)/(\alpha_2 c^\circ + c_{H^+}) \tag{10}$$

It is clear that α_2 is smaller according as the dissociation constant K is lower, and depending on the value of K, calculation results in an isotherm similar in shape to curve 2 in Fig. 1.

An additional advantage of buffer solutions is that α_1° is more strongly fixed, which contributes to the accuracy of the experiment, particularly for high α (low H^+ ion concentration) and $f'(\alpha)$; this advantage is also obtained if the batch method is used.

From these considerations if is concluded that the column method with buffer solutions is to be preferred to all others.

2. Experiments to Determine the Equilibrium

(2.1) *Cation exchangers*

Of the cations contained in natural waters Ca^{2+} and Na^+ are the most numerous and qualitatively the most important, as usually Ca^{2+} has the highest and Na^+ the lowest affinity for cation exchangers of all the positive ions contained in water [12]. Equilibria were determined for these two kinds of ions. The total ion concentrations chosen were 0·01 and 0·003 g equiv/l; these concentrations represent about the maximum and mean salt contents of natural waters. The following exchangers were examined [2].

(a) Imac C 12, a sulphonated polystyrene, corresponding to Dowex 50 and Amberlite IR 120. It is considered a monofunctional strongly acid exchanger.

(b) Dusarit S, a sulphonated coal with both strongly acid and weakly acid groups.

(c) Dusarit VKG, likewise a sulphonated coal, which has, however, more weakly acid and fewer strongly acid groups.

(d) Lewatit, a polyfunctional exchanger on a synthetic resin basis.

(e) Stamion, a weakly acid exchanger obtained by a treatment of oxidized coal with a solution of sodium hydroxide [4].

(f) Amberlite IRC 50, a monofunctional weakly acid exchanger, probably a copolymer of metacrylic acid and divinyl benzene [3].

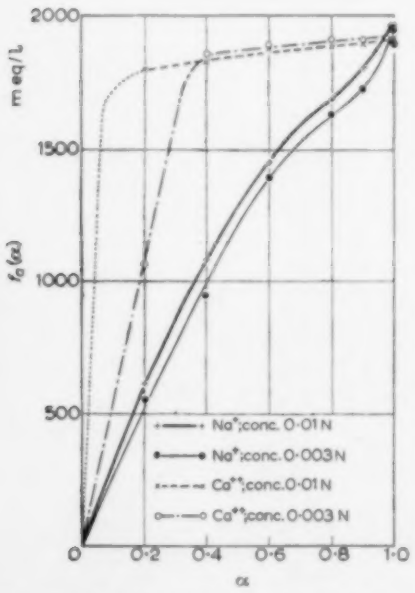

Fig. 2a. Equilibrium curves of Imac C 12.

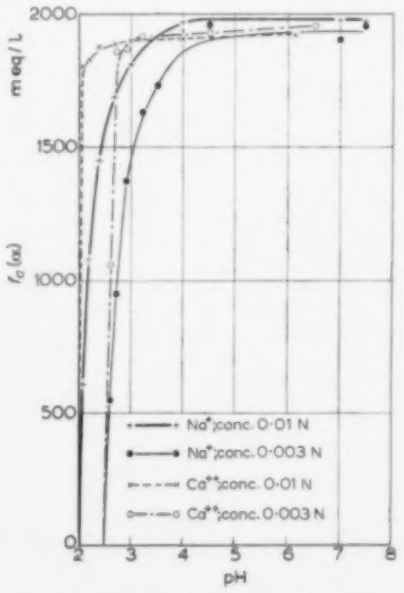

Fig. 2b. Capacity-pH curves of Imac C 12.

Samples consisting of 25–35 ml of ion exchanger were treated in small columns containing solutions of buffer salts, until the effluent had the same composition as the incoming solution, which was checked by measuring the pH value.

The buffer solutions were prepared as follows. If the equilibrium curve for Na^+ ions was to be determined at a total concentration of Na^+ and H^+ ions = 0·003 N, (where N (normal)

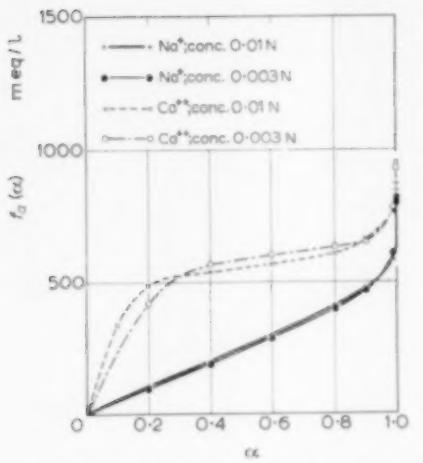

FIG. 3a. Equilibrium curves of Dusarit S.

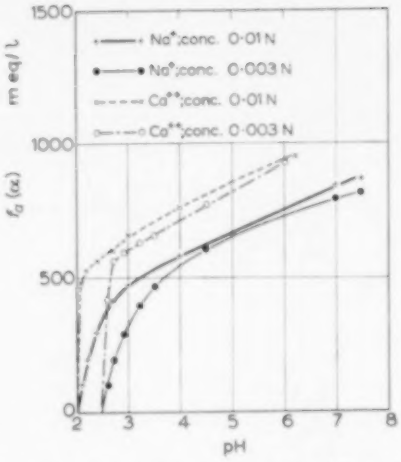

FIG. 3b. Capacity-pH curves of Dusarit S.

refers to 1 g equiv/l.), use was made, (e.g. for a value of $\alpha = 0{\cdot}6$), of a solution of sodium hydroxide of $0{\cdot}6 \times 0{\cdot}003 = 0{\cdot}0018$ N. By adding 1 : 1 phosphoric acid the solution was brought to a $pH = -\log 0{\cdot}003\,(1 - 0{\cdot}6) = 2{\cdot}92$. The adjustment was made by means of a pH-meter (radiometer). For the concentration 0·01 N an analogous method of preparation may be used. The Ca^{2+} buffers were prepared from calcium acetate solutions.

After the experiment the exchanger was regenerated with excess hydrochloric acid; the Na^+ ion in the regenerating solutions was determined by precipitation with zincuranylacetate, and the Ca^{2+} ion by titration, for which the complexone method was used. The f_a value corresponding to the α value given above could then be calculated directly as m equiv/l.

The results are given in Figs. 2a–7a which show the loads of the exchangers as functions of the equivalent fractions α_{Na} and α_{Ca}; as these graphs are not very clear at high values of α, in Figs. 2b–7b the loads are shown as functions of the pH value.

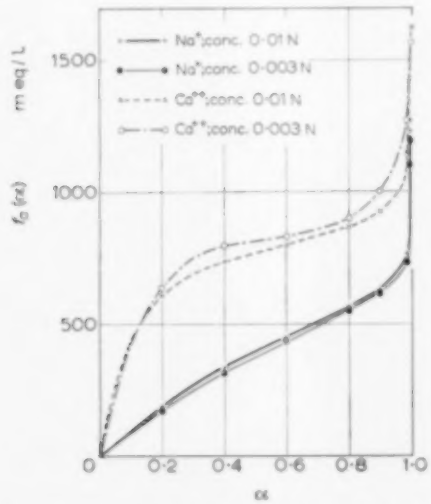

FIG. 4a. Equilibrium curves of Dusarit VKG.

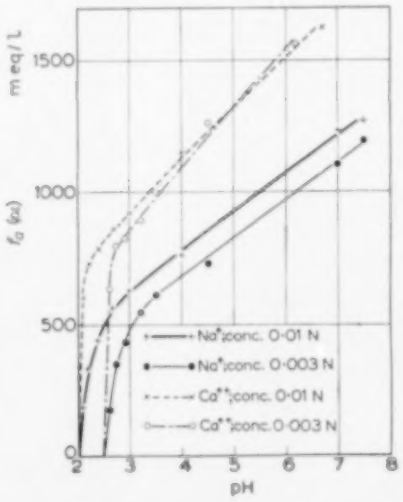

FIG. 4b. Capacity-pH curves of Dusarit VKG.

VOL.
7
957/58

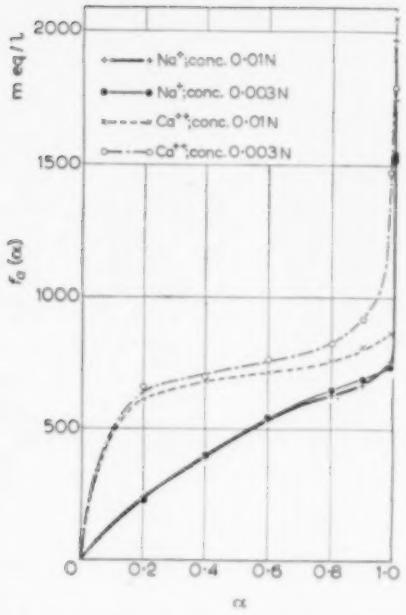

FIG. 5a. Equilibrium curves of Lewatit.

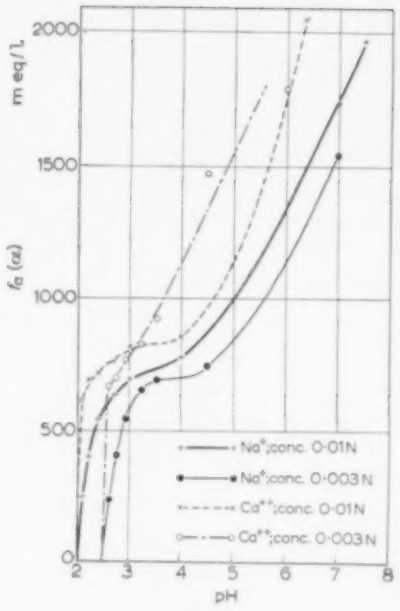

FIG. 5b. Capacity-pH curves of Lewatit.

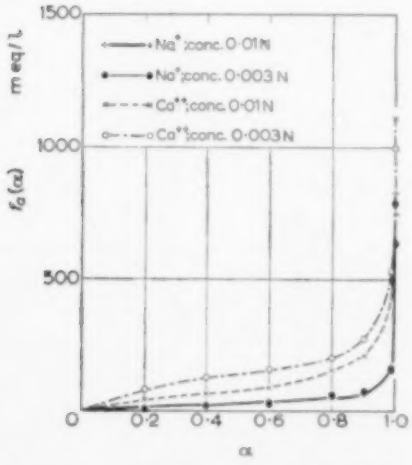

FIG. 6a. Equilibrium curves of Stamion.

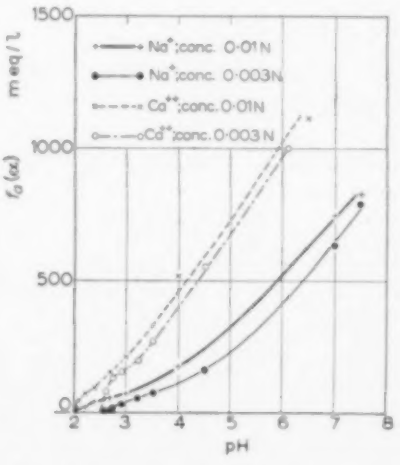

FIG. 6b. Capacity-pH curves of Stamion.

(2.2) *Anion exchangers*

The measurement of equilibria for anion exchangers is, in principle, subject to the same considerations as those given for cation exchangers; in this case also buffer solutions have to be used. There are, however, two practical difficulties.

In the first place it is the cation that has to act as a buffer with anion exchangers, and the choice of cations is limited. After some searching we found as suitable cations piperidine and homo-piperidine, the basicity of which corresponds to the acidity of phosphoric acid, and mono-ethanolamine with a basicity corresponding to the acidity of acetic acid.

In the second place the pH adjustment of the

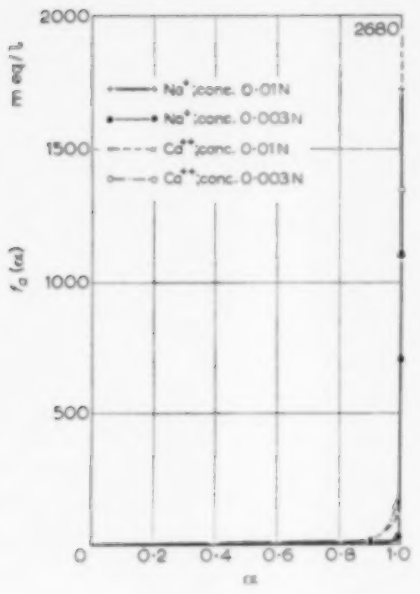

FIG. 7a.
Equilibrium curves of Amberlite IRC 50.

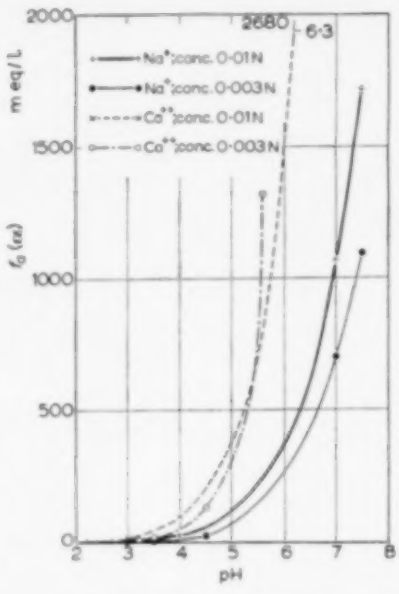

FIG. 7b.
Capacity-pH curves of Amberlite IRC 50.

solutions to be used for determining the equilibria in the alkaline range cannot be made by means of a glass electrode, owing to the wide variation in the range covered. With a hydrogen electrode reproducible results were obtained. The OH^-–Cl^- equilibria were measured, and those for the following anion exchangers are mentioned [2]:

(a) Amberlite IRA 401, an exchanger with quaternary (alkylated) ammonium groups on a polystyrene basis.

(b) Permutit ES, like (a), but not monofunctional as, in addition to alkyl groups, there are probably also alkylol groups (corresponding to Dowex 2 and Amberlite IRA 410).

(c) Dowex 3, like (a), but containing only weakly basic groups.

The equilibria were determined in the same way as for cation exchangers. Solutions with total OH^- and Cl^- ion concentrations of 0·01 N, were prepared by adjusting solutions of α 0·01 N hydrochloric acid to a pH value of 14–log 0·01 $(1 - \alpha)$ by addition of monoethanolamine (for lower OH^- ion concentrations) and piperidine or homo-piperidine (for higher OH^- ion concentrations). After regeneration with an excess amount of sodium hydroxide solution the Cl^- ion concentration was determined by titration according to Mohr. Results are shown in Figs. 8 and 9.

Not so much for the characterization as for the practice of ion exchange it is desirable to know also the acid adsorption equilibria for anion exchangers. Some experiments which were made to determine the hydrochloric acid equilibria for Dowex 3 and Permutit ES will therefore be described.

The determination of these equilibria was carried out in a similar manner to that used for the OH^-–Cl^- equilibria, except that instead of buffer solutions, solutions of hydrochloric acid (which may be considered as limiting cases of buffer solutions) of various concentrations were used.

It was found that with Dowex 3 the equilibrium was only established very slowly: even after some days had elapsed, the concentration of the hydrochloric acid in the effluent was lower than that in the incoming solution. Therefore the method was slightly altered: first the exchanger was loaded with 1 N hydrochloric acid and

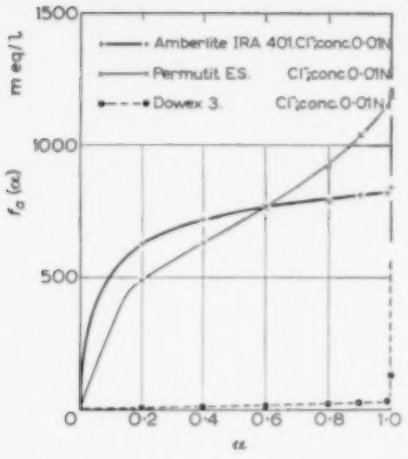

FIG. 8.
Equilibrium curves of anion exchangers.

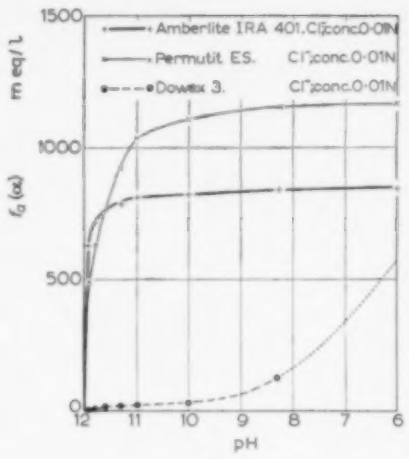

FIG. 9.
Capacity-pH curves of anion exchangers.

next with solutions of lower concentrations ($< 0{\cdot}02$ N) for which the isotherm had to be determined. With the altered method the concentration in the effluent (which was at first higher) after a reasonable time became equal to the concentration in the fresh solution. An explanation of the effect of this alteration of the method of determining the equilibrium will be given at a later stage.

The hydrochloric acid adsorption equilibria for Dowex 3 and Permutit ES are given in Fig. 10.

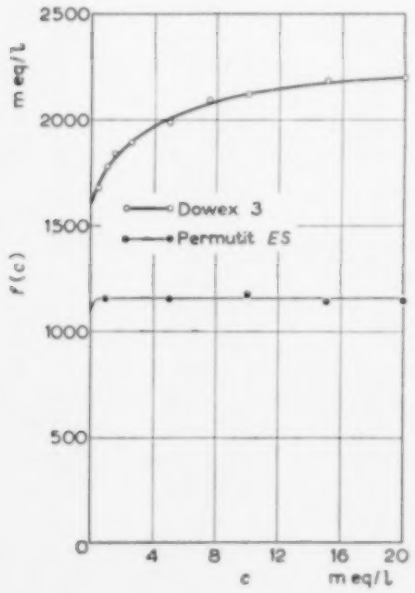

FIG. 10.
Acid adsorption curves of Dowex 3 and Permutit ES.

(2.3) *Discussion*

(a) *Inspection of the isotherms of Figs.* 2–8 *shows a striking number of inflection points.* GLUECKAUF was the first to find this type of isotherm for ion exchangers, viz. with the equilibrium $Cu^{2+} - H^+$ for Zeo-Karb which is presumably a polyfunctional exchanger [6]. Further examples are the equilibria $Cl^- - NO_3^-$ for Dowex 2, found by WHEATON and BAUMAN [17] (cf. ZEEGERS [19]). GLUECKAUF suggests that this type of curve will be found where the affinities of the competing ions for the exchanger are of the same order. By way of example he refers to the systems examined by ROTHMUND and KORNFELD [13], viz. $Ag^+ - Tl^+$ and $Na^+ - NH_4^+$ for aluminium silicate exchangers. Against GLUECKAUF's opinion it may be adduced that, if the affinities of the various ions for the exchanger are of the same order, a linear isotherm is to be expected. If the experiments of ROTHMUND and KORNFELD are plotted graphically it is, indeed, seen that these authors found linear isotherms in the α region they investigated.

Like SELKE [14] *the authors believe that this type of curve is inherently bound up with the polyfunctionality of an exchanger.*

From Figs. 2–7 the impression is obtained that the curves for Dusarit VKG, for example, might have been formed by superposition of the curves for Imac C 12 on those for Stamion. A mixture of exchangers such as Imac C 12 and Stamion, or an exchanger containing acid groups of different strengths will, in the case of equilibria in which H^+ ions take part, give curves with inflection points. It may be said that if the metal ion in solution has a small equivalent fraction, when the strongly acid groups on the exchanger are chiefly involved, the affinity of the metal ion for the exchanger is smaller than that of the H^+ ion, whereas at high values of α, when the weakly acid groups also play a part, the affinity of the metal ion for the exchanger will become predominant. The course of the equilibrium curves of Imac C 12 at high α, and the analogy with the polyfunctional exchangers, suggest that this exchanger also contains a certain number of weakly acid groups. This conclusion would agree with what BOYD [1] presumed in connection with the sulphonated polystyrenes.

(b) *Mathematical representation of equilibrium curves.* In general it is impossible to represent the equilibrium curves in a formula. The only regularity is that the $Na^+ - H^+$ equilibrium is in most cases independent of the total concentration in the solution and hence exclusively depends on the proportion between the ion concentrations.

This has been observed by HONDA [9] among others. Perhaps this relation has a deeper cause. If we assume the occurrence of a Donnan equilibrium, the following equilibria must be established in a system containing Na^+, H^+ and Cl^- ions :

$$c_{H_R^+} \cdot c_{Cl_R^-} = c_{H_L^+} \cdot c_{Cl_L^-} \qquad (11)$$

$$c_{Na_R^+} \cdot c_{Cl_R^-} = c_{Na_L^+} \cdot c_{Cl_L^-} \qquad (12)$$

from which follows, after division :

$$c_{H_R^+}/c_{Na_R^+} = c_{H_L^+}/c_{Na_L^+} \qquad (13)$$

If it is further assumed that $c_{H_R^+}$ depends only on the load of Na^+ ions ($c_{Na_R^+}$), it will immediately be clear that :

$$c_{Na_R^+} = f(c_{Na_L^+}/c_{H_L^+}) \qquad (14)$$

Unfortunately, $c_{H_R^+}$ can only be calculated from equation (13), and cannot be determined independently, as the number of non-dissociated groups on the exchanger is not known.

If equation (13) is assumed to be correct one may get an impression of the *dissociation constants of the acid groups on the exchanger in dependence on* α_{Na}, from $c_{H_R^+}$ and from a determination of the total number of exchangeable groups q°, using the equation :

$$K = \left[c_{H_R^+}(c_{Na_R^+} + c_{H_R^+})\right]/\left[q^\circ - c_{Na_R^+} - c_{H_R^+}\right] \qquad (15)$$

Table 1.
Dussarit VKG

α	$f(\alpha)$	K (*g mol/l.*)	α	$f(\alpha)$	K (*g mol/l.*)
0·2	180	2·1	0·9	630	0·092
0·4	330	1·0	0·99	760	0·013
0·6	440	0·44	0·999	900	0·0027
0·8	560	0·16	0·9999	1070	0·00072

For anion exchangers the following relation, corresponding to equation (14), holds :

$$c_{Cl_R^-} = f(c_{Cl_L^-}/c_{OH_L^-})$$

and, for a preponderantly acid medium :

$$c_{Cl_R^-} = f(c_{HCl_L}) \qquad (16)$$

which corresponds to the results of KUNIN and MYERS [11] and to the results of the present authors (Fig. 10).

(c) *The position of the capacity-pH curves depends on the total ion concentration in solution.* GREGOR and BREGMAN [8] came to the above conclusion, and therefore used high salt concentrations in solution, with the result that the capacity-pH curves became relatively less dependent on the salt content. This effect is easily understood; from Fig. 2b–7b it can be seen that at a high pH value the capacity usually becomes less dependent on the salt concentration. If now the concentration is raised, the capacity-pH curve shifts

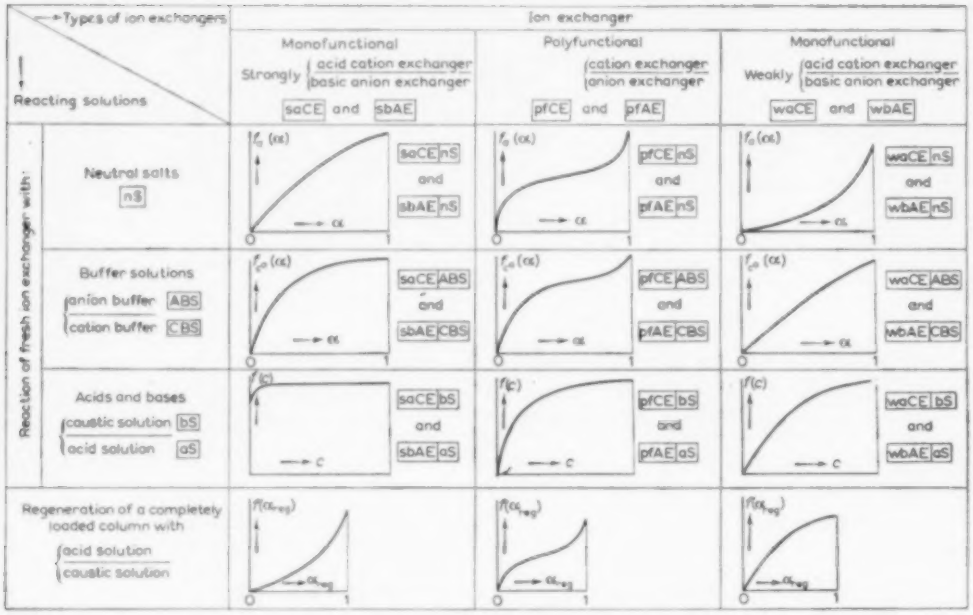
Types of ion exchangers
Reacting solutions
Ion exchanger
Monofunctional
Strongly {acid cation exchanger / basic anion exchanger
saCE and sbAE
Polyfunctional
{cation exchanger / anion exchanger
pfCE and pfAE
Monofunctional
Weakly {acid cation exchanger / basic anion exchanger
waCE and wbAE
Reaction of fresh ion exchanger with:
Neutral salts
nS
saCE nS and sbAE nS
pfCE nS and pfAE nS
waCE nS and wbAE nS
Buffer solutions
{anion buffer ABS / cation buffer CBS
saCE ABS and sbAE CBS
pfCE ABS and pfAE CBS
waCE ABS and wbAE CBS
Acids and bases
{caustic solution bS / acid solution aS
saCE bS and sbAE aS
pfCE bS and pfAE aS
waCE bS and wbAE aS
Regeneration of a completely loaded column with
{acid solution / caustic solution

FIG. 11. Classification of ion exchange equilibrium curves.

to the left. Doubling the concentration results in a shift of the curve of 0·3 pH unit (= log 2), so that a measurement in the normal pH range (pH > 2) will then show the capacity to be relatively little dependent on the total concentration in solution.

The use of high salt concentrations provides comparative information on the acidity distribution of the groups in the exchanger. This information cannot be used for calculating equilibrium curves, as it gives capacity values for very high α only.

3. Classification of Ion Exchangers and of Ion Exchange Isotherms

On the basis of the foregoing it is possible to classify ion exchangers according to the shapes of their equilibrium curves; this classification is shown in Fig. 11.

It is seen that, depending on the nature of the exchanger (monofunctional, strong or weak; or polyfunctional) and of the type of the solution (neutral salts, acids and bases, buffered or unbuffered), and on the question whether loading or regeneration takes place, a great variety of isotherms can be obtained.

In Part III it will be seen what quantitative data on the capacity follow immediately from the shape of the equilibrium curve.

Notation

a = total ion concentration in solution (ML^{-3})

c = concentration in the liquid (ML^{-3})

c° = for definition, see eq. (8)

$f(\alpha)$ = concentration in ion exchanger at equilibrium (ML^{-3})

K = dissociation constant (ML^{-3})

q = total number of groups in the exchanger (whether or not dissociated) (ML^{-3})

S = cross-sectional area of column (L^2)

t = time (T)

v = rate of flow $(L^3\,T^{-1})$

x = distance to the point where the liquid enters the column (L)

α = equivalent fraction of a given ion in solution = $\frac{c_{Na^+}}{a}$

γ = free space per unit length in the column (L^2)

Indices and subscripts

L = liquid

R = exchanger

o = condition before the liquid enters the column

References

[1] Boyd G. E. *Ann. Rev. Phys. Chem.* 1951 **2** 309.

[2] Buser W. *Chimia* 1955 **9** 73.

[3] Conway D. E., Green J. H. S. and Reichenberg D. *Trans. Faraday. Soc.* 1954 **50** 511.

[4] *Dutch pat.* 75,735.

[5] Glueckauf E. *Nature* 1945 **156** 748.

[6] Glueckauf E. *J. Chem. Soc.* 1947 1302

[7] Glueckauf E. and Coates J. I. *J. Chem. Soc.* 1947 1315.

[8] Gregor H. P. and Bregman J. I. *J. Amer. Chem. Soc.* 1948 **70** 2370.

[9] Honda M. *J. Amer. Chem. Soc.* 1951 **73** 2943.

[10] Klamer K. and van Krevelen D. W. Part I, *Chem. Engng. Sci.*, 1958 **7** 197.

[11] Kunin R. and Myers R. J. *J. Amer. Chem. Soc.* 1947 **69** 2874.

[12] Kunin R. and Myers R. J. *Ion Exchange Resins*, p. 25. Wiley, New York 1950.

[13] Rothmund V. and Kornfeld G. *Z. Anorg. Chem.* 1918 **103** 129.

[14] Selke W. A. *Ion Exchange Technology* (Ed. Nachod and Schubert), p. 61. Academy Press, New York 1956.

[15] Sillén L. G. *Ark. Kemi* 1950 **2** 477.

[16] Sillén L. G. *Ark. Kemi* 1950 **2** 499.

[17] Wheaton R. M. and Bauman W. C. *Industr. Engng. Chem* (*Industr.*) 1951 **43** 1087.

[18] Yanowsky M. I. *Zh. prikl. Khim., Leningr.* 1951 **24** 745.

[19] Zeegers J. A. *Chem. Eng. Sci.* 1953 **2** 74.

Chemical Engineering Science, 1958, Vol. 7, pp. 215 to 221. Pergamon Press Ltd.

The hydrodynamics of flow between horizontal concentric cylinders—I

Flow due to rotation of cylinder

D. B. Brewster and A. H. Nissan*

Department of Textile Industries, The University, Leeds 2

(*Received* 3 *May* 1957)

Abstract—The approximate velocity distributions for laminar flow between horizontal concentric cylinders with the inner cylinder only rotating have been studied for liquid levels other than when the system is completely full. The stability of the laminar flow has been shown to depend on the parameters S and d_0/d as used by Di Prima, where d_0 is the distance of the surface of zero velocity from the inner cylinder and d is the width of the gap. The secondary motion resulting from instability has been investigated and the wavelength of the vortices produced between the inner cylinder and d_0 agrees with that for the same value of d_0/d due to rotation of both cylinders in opposite directions when the annulus is full of liquid.

Résumé—Les auteurs étudient la répartition approximative des vitesses dans le cas d'un écoulement laminaire entre des cylindres concentriques horizontaux, le cylindre intérieur tournant. Les mesures ont été faites pour des niveaux différents de liquide, le système n'étant jamais entièrement noyé. Ils ont montré que la stabilité de cet écoulement laminaire dépend des paramètres S et d_0/d, comme l'a indiqué Di Prima : d_0 est la distance de la surface de vitesse nulle, le cylindre intérieur étant pris comme origine, et d la largeur de l'espace annulaire.

Le mouvement secondaire résultant de l'instabilité a été étudié, et la longueur d'onde du tourbillon produit entre le cylindre intérieur et d_0, concorde avec celle correspondant à la même valeur de d_0/d, dans le cas de la rotation de deux cylindres en sens inverse, quand l'éspace annulaire est remplie de liquide.

Zusammenfassung—Es wurden die angenäherten Geschwindigkeitsverteilungen für laminare Strömung zwischen waagerechten, konzentrischen Zylindern, von denen nur der innere rotierte, bei nicht vollständig gefülltem System untersucht. Die Stabilität der laminaren Strömung erwies sich als abhängig von den Parametern S und d_0/d, wie von Di Prima angegeben, wobei d_0 die Entfernung der Schicht mit der Geschwindigkeit Null vom inneren Zylinder und d die Spaltweite ist. Die von der Instabilität herrührende Sekundärbewegung wurde untersucht; die Wellenlänge der zwischen dem Innenzylinder und d_0 erzeugten Wirbel stimmte mit jener für gleiche d_0/d-Werte bei entgegengesetzter Rotation beider Zylinder und vollständig gefülltem Ringspalt überein.

Introduction

The flow of liquids in curved passages is of interest in a number of chemical engineering problems. A rotating drum filter, for instance, consists of a large cylinder which rotates inside a container, the suspension to be filtered being in the annulus. The suspension has a complicated form of motion : it is rotated by the drum, is pumped through the annulus under a positive head, and is finally given a radial component in the filtering region. Similarly, in paper- and board-making, a sheet of fibre is taken off a suspension on to a drum covered with wire gauze which rotates in a vat full of a fibre suspension.

In these and similar flow systems there are essentially two problems : (1) the distribution of velocity and pressure heads across and along the system under different regimes of flow ; and (2) the critical speeds at which the flow changes from laminar to a more complicated pattern. For example, in paper-making, longitudinal streaks can arise in the formed sheet when a certain type

*Present address : Rensselaer Polytechnic Institute, Troy, New York

of vortex motion predominates in the flow, due to its instability in a curved passage.

In this paper will be discussed the motion of a liquid contained between two concentric cylinders with the inner cylinder rotating. The axis of the cylinders is horizontal and a free liquid surface is present.

Theory of Flow between Rotating Concentric Cylinders

It will be assumed that the annulus between two concentric cylinders contains an incompressible, homogeneous Newtonian fluid. The problem consists of determining the character of the laminar motion existing at slow speeds and secondly the speed at which this motion becomes unstable. Consideration of the type of motion produced when instability occurs—vortex or turbulent motion—is important but will only be briefly dealt with in this paper.

Laminar Motion (slow speeds)

When the annulus is completely full of liquid the mode of flow is well known and the tangential (Couette) velocity distribution between the cylinders is given by Lamb [1]. If the cylinders rotate in opposite directions there is a cylindrical surface of radius r_0 between the two cylinders at which the tangential velocity is zero. This is given by

$$r_0^2 = \frac{b^2 (1 - \mu)}{1 - \mu (b^2/a^2)} \qquad (1)$$

If the common axis of the cylinders is horizontal it is possible to drain liquid from the annulus between the cylinders until the top of the inner cylinder is "dry". The Couette velocity distribution will not longer hold between a and b for this system.

Consider the flow when the outer cylinder is stationary and the inner rotates ($\mu = 0$).

It will be assumed that as the rotating cylinder passes through the free horizontal liquid surface it carries with it a liquid film of negligible thickness compared with the annulus width d. The rotating liquid, next to the moving inner cylinder, on reaching the free horizontal liquid surface, cannot continue in the same direction and must return in the opposite direction as shown in Fig. 1.

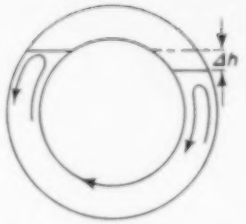

Fig. 1. Rotation of inner cylinder with complete reversed flow.

The free liquid surfaces at the two sides of the cylinder will be at different levels and Δh, the difference in height, will be a measure of the pressure head required to produce this "reverse flow."

This simple picture of a "dry" top will only hold for liquids of low viscosity. If the viscosity is high a film of liquid of significant thickness will be carried over the top of the cylinder. It is hoped to deal with this more complicated case in later work.

The velocity distribution between a and b will be approximately as shown by Fig. 2.

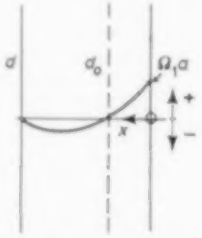

Fig. 2. Approximate velocity distribution between concentric cylinders with complete reversed flow.

For values of $d/a \ll a$ we may consider the problem as one of flow between parallel plates, one of which moves at velocity $\Omega_1 a$ relative to the other.

The velocity distribution [1] is given by

$$v = \frac{(d - x)}{d} \Omega_1 a - \frac{x (d - x)}{2 \nu\rho} \frac{dp}{ad\theta} \qquad (2)$$

If the net flow is zero,

$$\int_0^d v dx = \tfrac{1}{2} d \Omega_1 a - \frac{d^3}{12 \nu\rho} \frac{dp}{ad\theta} = 0$$

VOL. 7 957/58

or $$\frac{1}{2\nu\rho}\frac{dp}{ad\theta} = \frac{3\,\Omega_1\,a}{d^2} \qquad (3)$$

When $v = 0$, from equations (2) and (3):

$$d_0/d = 1/3 \qquad (4)$$

These relationships apply when there is a complete reversal of flow. For a fluid of low viscosity it is possible to drain liquid from between cylinders until the liquid level lies *between* the highest points of the two cylinders and to obtain a steady state of flow. Rotation of the inner cylinder in this case will produce incomplete reverse flow as shown by Fig. 3*.

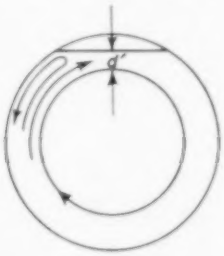

FIG. 3. Rotation of inner cylinder with partially reversed flow.

Assuming an approximate velocity distribution as in Fig. 4 and assuming that the velocity at d' (Fig. 3) is the same for any point at this distance from the inner cylinder, the equation of

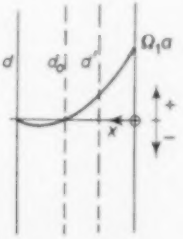

FIG. 4. Approximate velocity distribution between concentric cylinders with partially reversed flow.

continuity is given for the region between d' and d, in the body of the liquid and far from the free surface, by:

$$\int_{d'}^{d_0} v\,dx = \int_{d_0}^{d} v\,dx$$

We shall assume from equation (4) that in this case

$$\frac{d_0 - d'}{d - d'} = 1/3$$

or $$\frac{d_0}{d} = (1/3)\left[1 + \frac{2d'}{d}\right] \qquad (5)$$

Stability of Laminar Motion

Full annulus

The stability of laminar flow between rotating concentric cylinders has been studied by many workers. G. I. TAYLOR [2] was the first to show analytically and experimentally that for cylinders of given radii and a liquid of a certain viscosity there were definite angular velocities of the outer and inner cylinders at which instability would occur. He further showed that the motion resulting from instability was three-dimensional and consisted of pairs of toroid-shaped vortices, the rotation within each being in the opposite direction to its neighbour. The spacing of these toroids along the axis of the cylinders is constant for a particular apparatus and speeds of rotation of the cylinders. The wavelength or width of adjacent pairs of vortices depends on the cylinder radii and speeds of rotation.

TAYLOR showed that when only the inner cylinder was rotating the critical angular velocity was given by

$$\frac{\Omega_c^{\,2}\,a^2\,d^3}{\frac{1}{2}(a+b)\,\nu^2} = \frac{\pi^4 f}{0{\cdot}0571\,f^2 + 0{\cdot}00056} \qquad (6)$$

where $f = 1 - 0{\cdot}652\,(d/a)$

and $d = (b - a)$.

LEWIS [3] confirmed TAYLOR's work experimentally and showed that approximations involving $(d/a) < a$ used by TAYLOR in his theoretical analysis held for (d/a) as high as 0·7.

The solution of the stability problem mathematically has been further studied by several workers.

SYNGE [4] has shown that for stability of a rotating fluid the circulation must increase

*When the viscosity is high the "bubble" is pumped bodily or partly around between the cylinders.

outwards. That is for angular velocities ω_1, ω_2 at r_1 and r_2 the flow is stable if

$$\omega_2 r_2^2 > \omega_1 r_1^2$$

When the cylinders rotate in opposite directions there is an inner section where the angular velocity is *decreasing* outwards and this section will tend towards instability. The outer section where the angular velocity is *increasing* outwards will tend towards stability.

More recent work, mainly on the theory of instability is reviewed by Lin [5] and Oppenheim and Hughes [6].

Dean [7] has shown theoretically that disturbances of the same type as those described by Taylor [2] for Couette flow can exist for a parabolic velocity distribution. He showed that the critical velocity for instability is

$$\bar{v}_c = 36 \sqrt{\frac{a}{d}} \cdot \frac{\nu}{d}.$$

There has been no direct experimental verification of this criterion, but it appears to explain why the Reynolds number for instability in a curved pipe is lower than that for a straight pipe.

Di Prima [8] has plotted the results of experiments carried out by Taylor [2]. He has expressed the angular velocities (Ω_2 and Ω_1) in terms of

$$S = \frac{8\Omega_c^2 \left[1 - \mu\,(b^2/a^2)\right]^2 d_0^5}{\nu^2 \left[1 - (b^2/a^2)\right]^2 r_0} \qquad (7)$$

and plotted experimental values of S against d_0/d (see Fig. 9) where Ω_c is the critical angular velocity of the inner cylinder.

We may express S in terms of d_0 by use of equation (1)

$$S = \frac{8\,\Omega_c^2\, d_0^3 a}{\nu^2 \left[4 + 8\,(d_0/a) + 5\,(d_0/a)^2 + (d_0/a)^3\right]} \qquad (7a)$$

for $d_0/a < 1$ this may be approximated by

$$S = \frac{2\,\Omega_c^2\, d_0^3\, a}{\nu^2}$$

$$\text{or } \Omega_c = \sqrt{\frac{S}{2a\,d_0}} \frac{\nu}{d_0} \qquad (8)$$

The wavelength of the vortex motion parallel to the axis of the cylinders resulting from instability is given by Fig. 5 where $\frac{2\pi}{\lambda}$ is the wavelength [8].

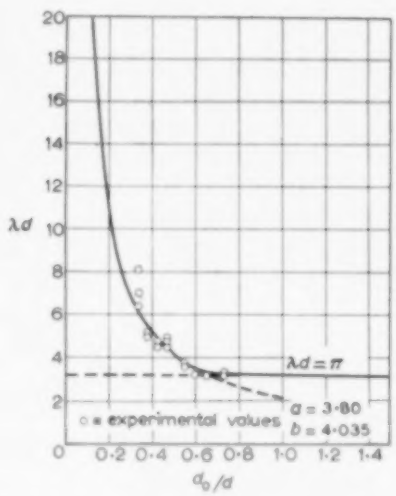

Fig. 5. Wavelength of the vortex motion.

For complete reverse flow, Synge's criterion [4] would suggest that the inner (Couette) section tends towards instability. The outer section, not having a simple Couette velocity distribution, but a parabolic distribution, may affect the stability of the inner section in a different way from Couette flow and may tend towards instability itself.

In order to compare approximately the stabilities of the sections a to $(a + d_0)$ and $(a + d_0)$ to $(a + d)$ we must calculate the average velocity in the reverse flow section $(a + d_0)$ to $(a + d)$.

From equations (2) and (3)

$$\bar{v} = \frac{1}{d - d_0} \int_{d_0}^{d} v\, dx$$

$$= \frac{\Omega_1 a}{d(d - d_0)} \int_{d_0}^{d} \left\{(d - x) - \frac{3x\,(d - x)}{d}\right\} dx$$

$$\bar{v} = -\,\Omega_1\, a\,(d_0/d)\,(1 + d_0/d)$$

From equation (4)

$$\bar{v} = -\,(2/9)\,\Omega_1\, a \qquad (9)$$

VOL. 7 1957/58

DEAN's criterion may be applied to the reverse flow or outer section

$$v_c = 36 \sqrt{\frac{a}{(d - d_0)}} \cdot \frac{\nu}{(d - d_0)} \qquad (10)$$

From equations (9), (4) and (10)

$$\Omega_c a = 297{\cdot}4 \sqrt{\frac{\bar{a}}{\bar{d}}} \cdot \frac{\nu}{\bar{d}} \qquad (11)$$

Assuming that TAYLOR's criterion, equation (6), holds for the inner section a to $(a + d_0)$ and that the section behaves like an inner cylinder of radius a rotating in a stationary outer cylinder of radius $(a + d_0)$, the approximate critical velocity for instability is

$$\Omega_c a = 41{\cdot}1 \sqrt{\frac{\bar{a}}{\bar{d}_0}} \cdot \frac{\nu}{\bar{d}_0} = 214 \sqrt{\frac{\bar{a}}{\bar{d}}} \cdot \frac{\nu}{\bar{d}} \qquad (12)$$

Comparison of (11) and (12) shows that as Ω_1 increases instability will first occur in the section a to $(a + d_0)$.

It will be shown that TAYLOR's criterion calculated for a full gap cannot be applied in this way for accurate prediction of critical velocity.

For partial reverse flow a similar prediction that instability will occur in the section a to $(a + d_0)$ can be made.

In the comparison just made between the stabilities of the two sections a to $(a + d_0)$ and $(a + d_0)$ to $(a + d)$ TAYLOR's criterion was used assuming that there was a stationary solid surface at $(a + d_0)$; this is equivalent to a value of $\mu = 0$ for cylinders of radii a and $(a + d_0)$ and would correspond to a value of S of the order of 3,400. It appears more reasonable to assume that the liquid flowing between $(a + d_0)$ and $(a + d)$ has an effect on the stability of the inner section and as a first approximation we could assume that its effect is similar to that of the liquid in the section $(a + d_0)$ to $(a + d)$ between cylinders rotating in opposite directions at such a value of μ that $d_0/d = 1/3$.

This would give a value of Ω_c characterized by $S \simeq 1{,}000$ and the critical velocity would be reduced by $\sqrt{\frac{1000}{3400}}$ or a factor of $\frac{1}{1{\cdot}85}$ from that given by TAYLOR's criterion for a stationary outer cylinder of radius $(a + d_0)$.

It will be shown experimentally that the use of the value of S given by Fig. 9 for the particular value of d_0/d considered gives good agreement and is

$$\Omega_c a = 116{\cdot}5 \sqrt{\frac{\bar{a}}{\bar{d}}} \cdot \frac{\nu}{\bar{d}} \qquad (13)$$

when calculated from equation (8) using $S = 1{,}000$.

EXPERIMENTAL

Calibration of apparatus

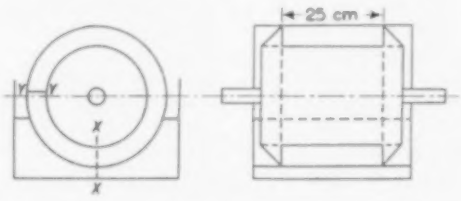

FIG. 6. Diagram of experimental apparatus showing position of optical tank and end seals.

The two cylinders of the apparatus (Fig. 6) were set horizontally. The inner cylinder was metallic and the outer made of Perspex. Built round the outer cylinder was an optical tank so that Section XX of the annulus could be observed. The speed of rotation of the inner cylinder could be varied over a wide range. Circumferential or end seals were used to limit the flow to a 25-cm length of cylinder.

The apparatus was first calibrated by obtaining the critical speeds for liquids of different viscosities when the annulus was full. Indication of vortex formation was by dye injection when the liquid was water and by self-indication properties described by HAGERTY [9] with water/glycerine solutions. This effect could be observed with solution of viscosities as low as 8 centistokes at room temperature.

Values of Ω_c obtained for different values of viscosity are plotted in Fig. 7.

By application of TAYLOR's criterion, equation (6), the effective value of d was found.

$$d = 0{\cdot}867 \text{ cm.}$$

This value of d was used as the constant for the apparatus.

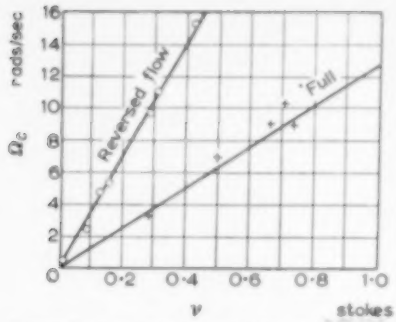

Fig. 7. Experimental critical angular velocity for Couette (full) flow and complete reversed flow. $a = 15{\cdot}6$ cm, $b = 16{\cdot}467$ cm (Calibrated by Taylor's criterion).

Completely Reversed Flow

This experiment could be carried out quite simply with water, but with high viscosity glycerine solutions a thick film was carried over the top of the inner cylinder. Consequently, in order to have complete reversed flow with glycerine solutions a stationary barrier seal was inserted across the apparatus at YY, Fig. 6.

Values of critical speed were obtained for various values of viscosity and are given in Fig. 7.

By the method of least squares

$$\Omega_c = 35{\cdot}27\ \nu.$$

$$\Omega_c^2 = 1{,}244\ \nu^2.$$

S was computed from equation (7a) using $d_0/d = 1/3$

$$S = 933$$

The vortices produced were photographed (Fig. 8) using parallel transmitted light for illumination. Measurement of the spacing of the vortices gave

$$\lambda d = 5{\cdot}45 \text{ cm}.$$

This falls very nearly on the curve in Fig. 5.

Partially Reversed Flow

The critical velocities were found for water for various free surface levels d' between a and b and are plotted in Fig. 9.

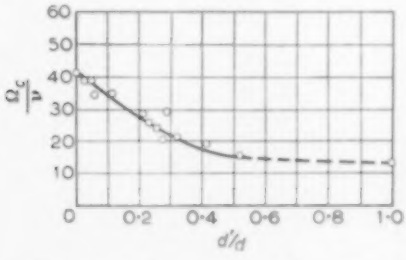

Fig. 9. Experimental values of Ω_c/ν against reduced liquid depth d'/d for partially reversed flow.
$a = 15{\cdot}6$ cm $\quad b = 16{\cdot}467$ cm

Using the relation between d_0/d and d'/d given in equation (5) the curve in Fig. 9 was converted to one of Ω_c/ν against d_0/d. From this curve were calculated corresponding values of S from equation (7a).

Fig. 10 gives Di Prima's plot of Taylor's results. On this the results of the present work are also shown. It is apparent that good agreement, in general, exists except at the value of $d_0/d = 1$ where present results fall lower than predicted values.

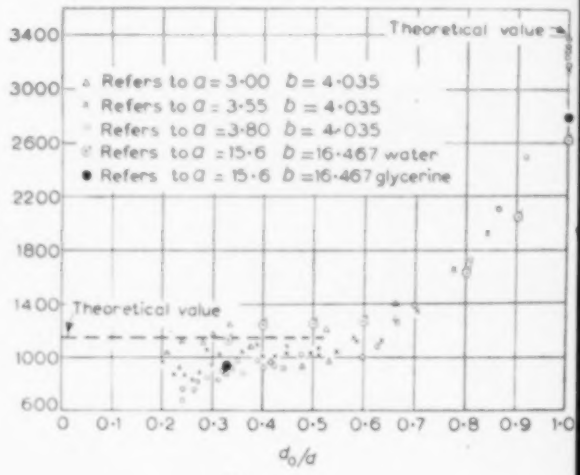
Theoretical value
Refers to a = 3·00 b = 4·035
Refers to a = 3·55 b = 4·035
Refers to a = 3·80 b = 4·035
Refers to a = 15·6 b = 16·467 water
Refers to a = 15·6 b = 16·467 glycerine
S
Theoretical value
d_0/d

Fig. 10.
ø refers to $a = 15{\cdot}6$ $b = 16{\cdot}467$ water
• refers to $a = 15{\cdot}6$ $b = 16{\cdot}467$ glycerine

Discussion

Although a detailed mathematical analysis of the reversed and partially reversed flow problems would be desirable to establish the stability criterion, the simple laminar flow analysis together with the experiments performed have shown that the stability criterion may be obtained from the curve of S against (d_0/d).

Divergence of the author's experimental values from those of Taylor as shown on Fig. 10, especially at $d_0/d = 1$, are probably due to the inaccuracy of the apparatus used. The effective value of $d = 0{\cdot}867$ cm. was calculated from Taylor's criterion using the experimentally determined value of Ω_c/ν for full flow. This value of d when substituted in equation (7a) should have given a value of $S = 3{,}400$ if

VOL.
7
957/58

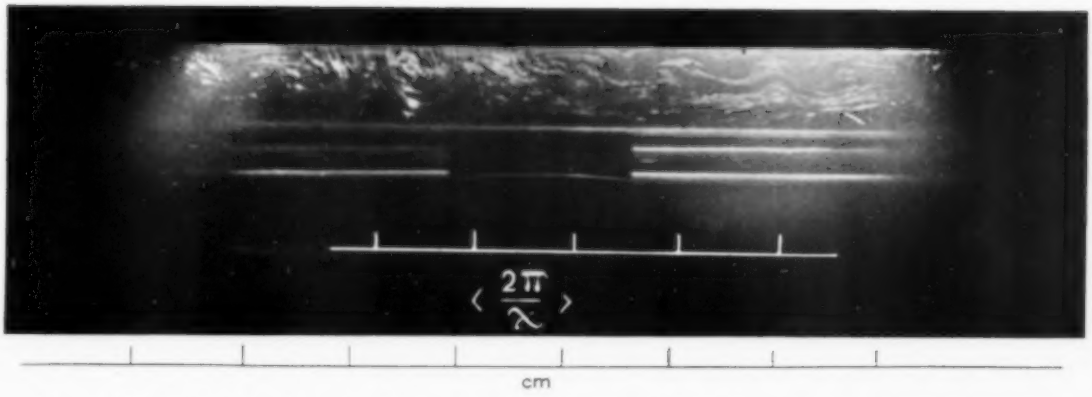

FIG. 8. Vortices produced by instability of completely reversed flow in 70 per cent glycerine solution.

VO
7
1957

TAYLOR's criterion were exactly obeyed by the apparatus. In fact, as indicated in Fig. 10 for $d_0/d = 1$, $S = 2800$. This error is probably due to the eccentricity of the cylinders, the inner being made from a 12in. i.d. copper pipe covered with 80 mesh wire gauze and the outer moulded in two halves from Perspex. No precautions were taken to reduce vibrations from the driving motor.

CONCLUSIONS

It has been established that the curve of S against d_0/d provides the correct criteria for the instability of laminar flow between two concentric cylinders both when flow is of the Couette type and when reversed flow occurs. The calculation of d_0/d using the approximate laminar flow equation is satisfactory.

Acknowledgements—The authors wish to thank Mr. F. CASS of the Department of Chemical Engineering and their colleagues in the Department of Textile Industries at the University of Leeds for their helpful criticism, and the Wool Textile Research Council for financing the investigation. Thanks are also due to the Referee whose criticisms and suggestions were most helpful.

NOTATION

a = radius of inner cylinder
b = radius of outer cylinder
r = radial distance
r_0 = radius of lamina with zero velocity
$d = (b - a)$
$d_0 = (r_0 - a)$
d' = depth of liquid above inner cylinder
$x = (r - a)$
Ω_1 = angular velocity of inner cylinder
Ω_2 = angular velocity of outer cylinder
$\mu = \Omega_2/\Omega_1$ = ratio of angular velocity of outer and inner cylinders
v = tangential velocity
ν = kinematic viscosity
p = pressure
θ = angle
ρ = density
Ω_c = critical angular velocity of inner cylinder

REFERENCES

[1] LAMB H. *Hydrodynamics* (6th Ed.). Cambridge (1932).
[2] TAYLOR G. I. *Phil. Trans.* A 1922 **223** 289.
[3] LEWIS J. W. *Proc. Roy. Soc.* A 1923 **117** 388.
[4] SYNGE J. L. *Proc. Roy. Soc.* A 1938 **167** 250.
[5] LIN C. C. *Theory of Hydrodynamic Stability.* Cambridge (1955).
[6] OPPENHEIM A. K. and HUGHES R. R. *Industr. Engng. Chem.* (*Industr.*) 1957 **49** 593.
[7] DEAN W. R. *Proc. Roy. Soc.* A 1928 **121** 402.
[8] DI PRIMA R. C. *Quart. Appl. Math.* 1955 **XIII** 55.
[9] HAGERTY W. W. *J. Appl. Mech.* 1950 **17** 54.

VOL. 7
957/58

Chemical Engineering Science, 1958, Vol. 7, pp. 222 to 228. Pergamon Press Ltd.

On the mechanism of interfacial resistance to mass transfer in liquid-liquid extraction

G. Boye-Christensen and S. G. Terjesen

The Technical University of Norway, Chemical Engineering Laboratory, Trondheim, Norway

(*Received* 16 *May* 1957; *revised* 30 *August* 1957)

Abstract—The additional resistance to the transfer of *o*-nitrophenol from an aqueous solution to falling drops of carbon tetrachloride caused by the addition of the surface-active agent sodium oleyl-*p*-anisidine sulphonate has been determined, and the results compared with those previously reported with iodine as the diffusing solute.

The results are adequately described by the adsorption isotherm previously developed, but the adsorption equilibrium appears to be more closely approached with smaller drops than with large ones. The equation of state for the adsorbed molecules, however, applies irrespective of the degree of approach to equilibrium.

The percentage reduction in the rate of mass transfer is shown to be 66-69 per cent for this system both with iodine and *o*-nitrophenol as diffusing solutes and for drop sizes between 7·5 and 18·5 mm³. It is concluded that there is no specific chemical or physical interaction between the adsorbed surface-active molecules and the diffusing solute, and that the results favour a hydrodynamic type of mechanism for interfacial resistance.

Résumé—Dans le cadre de l'étude de l'échange entre l'o-nitrophenol en solution aqueuse et une pluie de gouttes de tétrachlorure de carbone, les auteurs ont étudié la résistance supplémentaire causée par l'adjonction de l'agent tensio-actif oleyl-p-anisidinesulphonate. De plus, les valeurs obtenues ont été comparées avec celles déjà obtenues en employant l'oide comme soluté diffusant.

Les résultats sont correctement rapportés par l'isotherme d'adsorption déjà décrit; toutefois l'équilibre paraît être plus rapproché avec des petites gouttes qu'avec des grandes.

L'équation d'état pour les molécules adsorbées s'applique cependant, sans tenir compte du degré d'approche de l'équilibre.

La réduction affectant l'échange massique, exprimée en pour cent, est de 66 – 69 pour les deux solutés diffusant utilisés—l'iode et l'o-nitrophénol—et pour des gouttes de 7,5 à 18,5 mm3. Les auteurs en concluant qu'il n'y a pas d'action chimique ou physique spécifique, entre les molécules actives de la surface d'adsorption et du soluté diffusant. Ces résultats les amènent à conclure en faveur d'un mécanisme du type hydrodynamique pour la résistance interfaciale.

Zusammenfassung—Es wurde der zusätzliche Widerstand auf die Übertragung von o-Nitrophenol aus einer wässrigen Lösung auf fallende Tropfen von Tetrachlorkohlenstoff bestimmt, der durch die Zugabe des oberflächenaktiven Stoffes Natrim-Oleyl-p-Anisidinsulfonat hervorgerufen wurde. Die Ergebnisse wurden mit den früher mitgeteilten verglichen, bei denen Jod der diffundierende Stoff war.

Die Ergebnisse werden hinreichend durch die früher mitgeteilte Adsorptions-isotherme beschrieben, jedoch scheint das Adsorptionsgleichgewicht besser bei kleineren als bei grösseren Tropfen erreicht zu werden. Die Zustandsgleichung der adsorbierenden Moleküle scheint unabhängig von der Annäherung an das Gleichgewicht zu sein.

Die prozentuelle Verringerung der Grösse der Stoffübertragung ergibt sich zu 66 bis 69% für dieses System mit Jod und ϕ-Nitrophenol als diffundierende Substanz und für Tropfengrössen zwischen 7,5 und 18,5 mm³. Daraus kann man schliessen, dass es keine chemische oder physikalische Wechselwirkung zwischen den adsorbierten oberflächenaktiven Molekülen und der diffundierenden Substanz gibt und dass die Ergebnisse auf einen hydrodynamischen Mechanismus für den Grenzflächenwiderstand hindeuten.

VOL.
7
957/58

Introduction

The nature of the additional resistance to mass transfer in liquid-liquid extraction caused by the presence of surface-active substances has been discussed by several authors. For convenience, the term interfacial resistance is used for this phenomenon. The term implies that the resistance is caused by surface-active molecules adsorbed at the interface, but it must not be taken to give any indication of the responsible mechanism. The explanations advanced can be classified either as barrier theories or as hydrodynamic theories. The former category is based on the assumption that surface-active molecules adsorbed at a liquid-liquid interface form a kind of barrier which interferes with the passage of diffusing solute molecules, whereas the latter presupposes that the adsorbed molecules are somehow capable of modifying the hydrodynamic conditions in the vicinity of the interface.

Hutchinson [1] found that the resistance was highly specific. He favoured the barrier theory, and suggested that the action is not mechanical, but involves forces of a physical or chemical nature. West, Robinson, Morgenthaler, Beck and McGregor [2] found that the rate of extraction of acetic acid from benzene by drops of water was greatly reduced by traces of plasticizer extracted from Tygon tubing in the benzene feed line. They concluded that this effect is associated with a reduction of the internal circulation in the aqueous drops. In a later paper West, Herrman, Chong and Thomas [3] studying the effect of impurities in the benzene phase made the highly tentative suggestion that the surface-active substances act as a kind of interfacial barrier.

Garner and Hale [4] adopted the view of Hutchinson that the interfacial resistance is caused by physical or chemical interaction between the diffusing solute and the surface-active molecules at the interface. Garner and Hale [4] and Garner and Skelland [5] have shown that additions of surface-active agents reduce the rate of internal circulation in the drops, but that diffusing solute can counteract this effect to some extent. They found, however, that in extracting diethylamine from toluene by drops of water no internal circulation could be observed even in the absence of surface-active agent. On this basis they rejected the hydrodynamic theory in favour of a barrier type of theory.

According to Lewis [6] transfer of turbulence across an interface constitutes an important element in mass transfer, and he explains interfacial resistance as a result of a reduction in the transfer of turbulence caused by adsorbed surface-active molecules. The effect of adsorbed molecules on the spontaneous interfacial turbulence described by Lewis and Pratt [7] must also be included among the possible explanations. The situation has recently been discussed by Lindland and Terjesen [8], but the experimental material so far available has been insufficient for any firm conclusions to be drawn.

Some advances have, however, been made along more general lines. Garner and Hale [4] have shown that there is no parallelism between interfacial resistance and interfacial tension, and Melhus and Terjesen [9] have concluded that interfacial resistance and interfacial tension are two different manifestations of adsorption, unrelated to each other except for the fact that they both originate in adsorption. Whereas Garner and Hale [4] did not find any direct connection between adsorption and interfacial resistance, the latter authors developed a theory of interfacial resistance, assuming, as a first approximation, proportionality between the two phenomena.

Extensive determinations of interfacial resistance are available for the system water – carbon tetrachloride with iodine as diffusing solute and sodium oleyl-*p*-anisidine sulphonate as surface active agent [8]. This system appears to be particularly suitable for studies of interfacial resistance, and it is the purpose of the present investigation to extend this work by substituting *o*-nitrophenol for iodine as diffusing solute. Dissolved molecules of iodine and *o*-nitrophenol have very different physical and chemical properties, and any physical or chemical forces operating at the interface must be expected to interfere differently with the passage of the two substances. A comparison of results obtained with these substances should therefore yield

additional information about the nature of interfacial resistance.

Experimental

The apparatus and experimental procedure has been described in detail elsewhere [8]. Some difficulties were experienced in maintaining constant drop volume throughout a run, but capillaries drawn from thin-wall glass tubing gave satisfactory performance. An observation of Garner and Skelland [13] that the time of drop formation is important was confirmed, and their suggestion to work with fairly low drop frequencies was adopted. The temperature was 25°C as before, and the concentration of *o*-nitrophenol about 0·020 g/100 ml aqueous phase.

Materials

The carbon tetrachloride was of technical quality, and fractionated in a column of 5–10 theoretical plates with a reflux ratio of about 6 : 1. The fraction used distilled between 76 and 77°C and had a refractive index of $n_D^{25} = 1{\cdot}4568$ as compared with the value of 1·4571 given in the *International Critical Tables*. When a sample was distilled in an analytical column of 60–80 theoretical plates at a reflux ratio of 99 : 1 at the beginning and end of distillation and 49 : 1 in the middle, about 97 per cent went over at 76·8°C (760 mm Hg). The forerunnings and the residue had boiling points very close to this value and approximately the correct refractive indices, showing that the solvent phase consisted of practically pure carbon tetrachloride.

The *o*-nitrophenol was *Merck Pro Analysi*. It is an acid with a dissociation constant of about $7{\cdot}5 \times 10^{-8}$ and in order to reduce dissociation to a negligible value the pH of all aqueous solutions was adjusted to 3·15 by making the solution 0·002 N with regard to citric acid (*Merck Pro Analysi*).

The sodium oleyl-*p*-anisidine sulphonate was purified and stock solutions prepared with sodium sulphate and sodium chloride as described previously [10]. Stock solutions older than one week were discarded.

Methods of Analysis

Solutions of *o*-nitrophenol in water at pH = 3·15 and in carbon tetrachloride were analysed photometrically using a Beckman DU quartz spectrophotometer. The readings were taken at the absorption maximum which was found to be located at 3500 Å for both aqueous and solvent solutions.

Results and Discussion

Experiments were carried out with drops varying from 5 to 22 mm^3 in volume and with bulk concentrations of surface active-agent up to $3{\cdot}5 \times 10^{-4}$ g/100 ml of aqueous phase. Larger drops gave poor reproducibility, and at higher concentrations of surface-active agent the drops coalesced rather slowly in the receiver at the bottom of the column.

During the earlier part of the work it was not possible to maintain constant drop volume from one run to another, and it was necessary to determine the percentage approach to equilibrium p as a function of drop volume for each concentration of surface active-agent. The volumes were, however, kept as close to 7·5 and 18·5 mm^3 as possible. The values of p for these two selected volumes were then determined by graphical interpolation. This applies also to the rate of fall of the drops. The results are given in Table 1 together with the corresponding total and interfacial resistances R_E and R_{Ei} calculated on a time and extract or solvent basis as described previously [8]. In addition, the resistances are given also on a raffinate or aqueous basis :

$$R_R = R_E/m \text{ and } R_{Ri} = R_{Ei}/m$$

The distribution coefficient for *o*-nitrophenol between water and carbon tetrachloride was required for the calculations. It was determined by alternately shaking and leaving in a thermostat at 25°C a glass-stoppered bottle containing 50 ml of 0·002 N aqueous citric acid and 50 ml of carbon tetrachloride to which was added a suitable amount of *o*-nitrophenol. Within the range of 0·011 to 0·022 g of *o*-nitrophenol per 100 ml of aqueous phase the result was :

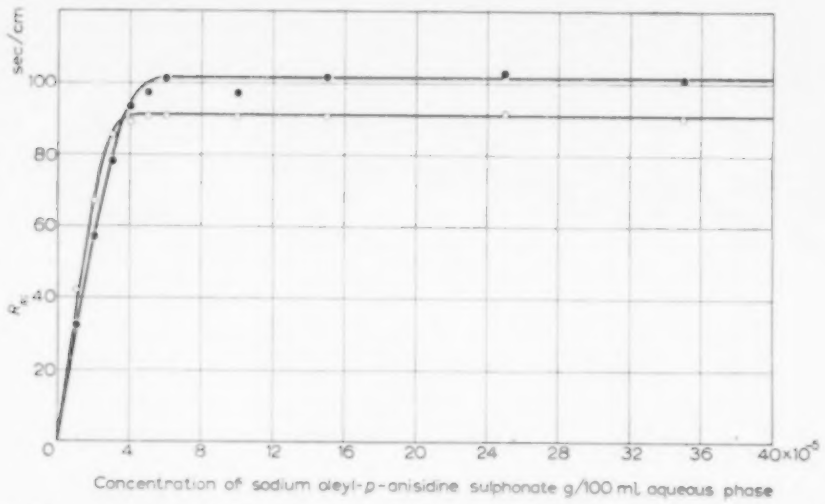

FIG. 1. Interfacial resistance coefficients on a raffinate or aqueous basis with *o*-nitrophenol as diffusing solute.
○ Drop volume 7·5 mm³ ● Drop volume 18·5 mm³

VOL. 7 1957/58

$$m = 126{\cdot}5 \pm 2{\cdot}5$$

$$= \frac{\text{mg of } o\text{-nitrophenol per ml of solvent phase}}{\text{mg of } o\text{-nitrophenol per ml of aqueous phase}}$$

The distribution equilibrium is so greatly in favour of the solvent phase that the resistance to mass transfer can be considered to be located almost entirely on the aqueous side, as was the case also with iodine as diffusing solute.

The interfacial resistances have been plotted on Fig. 1 where the curves represent the best fitting equation of the type developed previously [8] :

$$C_S = K \frac{R_i}{\left(1 - \frac{R_i}{R_{i\infty}}\right)^{0{\cdot}1}} \qquad (1)$$

Values of the constant K in equation (1) are given in Table 2 together with the limiting interfacial and total resistances $R_{i\infty}$ and R_∞, based on present work and previous results with iodine as diffusing solute [8]. The values have been calculated on a raffinate or aqueous basis as well as on an extract or solvent basis. The limiting values of the resistances represent the average for the concentration range $C_S = 10 - 35 \times 10^{-5}$ g/100 ml. The constants in the corresponding isotherm :

$$C_S = K_{\text{isotherm}} \frac{A_0\Gamma}{(1 - A_0\,\Gamma)^{0{\cdot}1}} \qquad (2)$$

are included also.

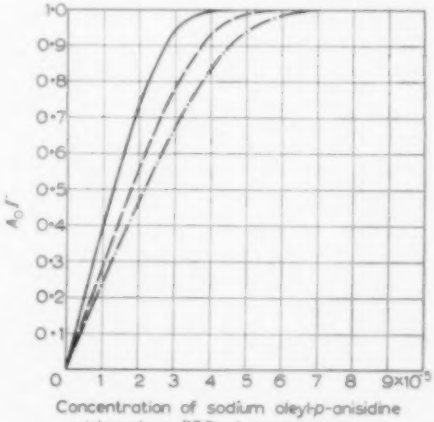

FIG. 2. Adsorption isotherms.
——— *o*-nitrophenol, drop volume 7·5 mm³
– – – – – *o*-nitrophenol, drop volume 18·5 mm³
— · — · — Iodine, average for drop volumes 4·2, 9·5 and 22·3 mm³

It can be seen from Fig. 1 that the theoretical equation is capable of describing the results within the limits of experimental error. The results, which are more accurate than the

Table 1. *Summary of results*

$C_E \times 10^5$ (g/100 ml)	v (cm/sec)	$p = \frac{C_E \times 100}{m \times C_{RA}}$	$R_E \times 10^{-3}$ (sec/cm)	$R_{Ei} = 10^{-3}$ (sec/cm)	R_R (sec/cm)	R_{Ri} (sec/cm)
	Drop volume : 7·5 mm³, *equivalent radius* : 1·21 mm					
0	18·8	3·12	5·9	0	47	0
1	17·0	1·84	11·2	5·3	89	42
2	16·8	1·46	14·4	8·5	114	67
3	16·6	1·27	16·7	10·8	132	85
5	16·5	1·23	17·3	11·4	137	90
10	16·5	1·23	17·3	11·4	137	90
25	16·3	1·23	17·6	11·7	139	92
35	16·3	1·25	17·3	11·4	137	90
	Drop volume : 18·5 mm³, *equivalent radius* : 1·64 mm					
0	22·0	2·03	5·8	0	46	0
1	19·7	1·34	9·8	4·0	78	32
2	19·3	1·04	13·0	7·2	103	57
3	19·2	0·87	15·7	9·9	124	78
4	19·2	0·78	17·6	11·8	139	93
5	19·2	0·76	18·0	12·2	143	97
6	19·2	0·73	18·7	12·9	148	102
10	19·2	0·75	18·2	12·4	144	97
15	19·2	0·73	18·7	12·9	148	102
25	19·1	0·73	18·8	13·0	149	103
35	18·9	0·75	18·6	12·8	147	101

previous ones, also show the effect of drop size on the action of the surface active-agent. This becomes particularly clear from an inspection of the slope of the adsorption isotherms in Fig. 2. For a given bulk concentration of the surface-active agent the fraction of the interface covered by adsorbed molecules is considerably larger for drop volumes of 7·5 mm³ than of 18·5 mm³. With the smaller drops the interface is practically completely covered when the bulk concentration

Table 2. *Limiting resistances and values of the constants in the equations* (1) *and* (2)

Reference	*Present work*		*Lindland and Terjesen*		
Diffusing solute	*o-nitrophenol*		*Iodine*		
Drop volume (mm³)	18·5	7·5	22·3	9·5	4·2
$R_{E\infty}$, sec/cm	18600	17400	11900*	10800	10600*
$R_{E,\infty}$, sec/cm	12800	11400	Average value 7400		
$R_{R\infty}$, sec/cm	147	138	130	120	119
$R_{Ri\infty}$, sec/cm	101	91	Average value 82		
K_E, g cm/sec 100 ml	$2·6 \times 10^{-9}$	$2·1 \times 10^{-9}$	Average value $5·4 \times 10^{-9}$		
K_R, g cm/sec 100 ml	$3·3 \times 10^{-7}$	$2·6 \times 10^{-7}$	Average value $4·9 \times 10^{-7}$		
K_{isotherm}, g/100 ml	$3·3 \times 10^{-5}$	$2·4 \times 10^{-5}$	Average value $4·0 \times 10^{-5}$		

*In ref. [8], in the second column on page 8, these values are incorrectly called the overall resistances without addition of surface-active agent.

is about $4{\cdot}5 \times 10^{-5}$ g/100 ml of aqueous phase whereas about $5{\cdot}5 \times 10^{-5}$ g/100 ml is necessary with the larger drops. The adsorption equilibrium is thus more closely approached the smaller the drops.

The exponent in the denominator of equations (1) and (2) is an expression of the sharpness of the transition between the rising and the horizontal branch of the curves. It can be seen from Fig. 1 that the value 0·1 fits very well in both cases. It has previously been shown [9] that the exponent, but not the constant, in the isotherm enters into the equation of state for the adsorbed film and therefore must be expected to be invariant with respect to the degree of approach to adsorption equilibrium.

The average isotherm obtained previously with iodine as diffusing solute exhibits a somewhat slower approach to equilibrium. It must, however, be remembered that the surface-active agent in that case had added two molecules of iodine to the double bond, and therefore really it was a slightly different substance.

For the purpose of comparing the different results the interfacial resistance R_i has been expressed as per cent of the total limiting resistance R_∞ and plotted in Fig. 3. The total limiting resistance given in Table 2 has been used as a basis rather than the resistance without addition of surface-active agent because the former appears to be more accurate, particularly in the case of the previous work. The resistance without addition of surface-active agent is rather sensitive to traces of impurities. It can be seen from Fig. 3 that for concentrations of surface-active agent below 6×10^{-5} g/100 ml there is a small, but systematic deviation from the fully drawn curve representing the average of all observations.

For higher concentrations, on the other hand, the interfacial resistance amounts to 66–69 per cent of the total limiting resistance, irrespective of diffusing solute and drop size. This is equivalent to stating that the percentage reduction in the rate of mass transfer caused by additions of surface-active agent greater than 6×10^{-5} g/100 ml is 66–69 per cent. Since the two solutes differ considerably in physical and

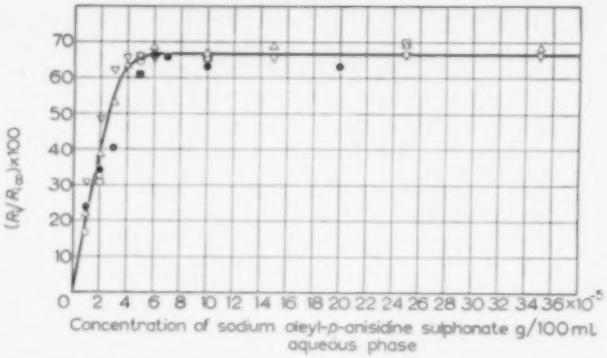

FIG. 3. Interfacial resistance coefficients R_i expressed as per cent of the total limiting resistance coefficients R_∞.
▽ *o*-nitrophenol, drop volume 7·5 mm³
△ *o*-nitrophenol, drop volume 18·5 mm³
□ Iodine, drop volume 4·2 mm³
○ Iodine, drop volume 9·5 mm³
● Iodine, drop volume 22·3 mm³

chemical properties the retardation of mass transfer therefore appears to be caused by a general mechanism not involving any specific chemical or physical interaction between the diffusing solute and the adsorbed surface-active molecules.

The observation that a change from one solute to another affects the interfacial resistance and the normal resistance in approximately the same proportions can be explained most easily by assuming that interfacial resistance is the result of modifications to the normal mechanism of mass transfer rather than an introduction of a new and additional mechanism. Such a modification to the normal mechanism of mass transfer can take place through changes in the hydrodynamic conditions in the vicinity of the interface caused by the adsorbed surface-active molecules.

The limiting total resistances $R_{R\infty}$ are fairly accurate for iodine as well as for *o*-nitrophenol. It is of interest to consider the ratio of these resistances for the two different diffusing solutes, but for approximately the same drop size. The result of such a comparison is given in Table 3.

It is generally agreed that liquid phase diffusivities are inversely proportional to the molar volume of the solute to the power of 0·6. The molar volumes of iodine and *o*-nitrophenol have been calculated according to the method of WILKE [11]

VOL. 7 957/58

Table 3. Comparison of limiting resistances with iodine and o-nitrophenol

Drop size, mm³ :		
For iodine	22·3	9·5
For *o*-nitrophenol	18·5	7·5
$\frac{R_{R\infty \text{ iodine}}}{R_{R\infty \text{ o-nitrophenol}}}$	0·88	0·87

and Wilke and Chang [12], and found to be 71·5 and 130·7 cm³/g mole respectively. The ratio of the diffusivity of *o*-nitrophenol to that of iodine is therefore 0·70. On the assumption that the difference between the experiments with the two solutes is represented entirely by the two diffusivities the results can be expressed by the equation :

$$R_{R\infty} \sim D^{-0.38} \qquad (3)$$

Conclusions

(1) Both the additional resistance caused by the presence of the surface-active agent and the normal resistance are affected in the same proportions when *o*-nitrophenol is substituted for iodine as diffusing solute. This indicates that the additional resistance is a result of a modification to the normal mechanism of mass transfer rather than an introduction of a new mechanism. The results thus favour a hydrodynamic type of theory.

(2). The rates of mass transfer is proportional to the diffusivity to the power of 0·38.

(3) The absorption equilibrium is more closely approached with smaller drops than with large ones.

Acknowledgement—The authors are indebted to the Royal Norwegian Council for Scientific and Industrial Research for a grant which has made this work possible.

Notation

A_0 = effective cross-sectional area of adsorbed surface-active molecules — cm²/g mol

a_0 = effective cross-sectional area of adsorbed surface-active molecules — Å²/molecule

C_E = concentration of *o*-nitrophenol in solvent phase — mg/cm³

C_E^* = equilibrium concentration in solvent phase — mg/cm³

C_R = concentration of *o*-nitrophenol in aqueous phase — mg/cm³

C_{RA} = average of initial and final concentration in aqueous phase — mg/cm³

C_S = concentration of surface-active agent in aqueous phase — g/100 ml

D = diffusivity — cm²/sec

m = distribution coefficient : $\frac{\text{mg } o\text{-nitrophenol per ml solvent phase}}{\text{mg } o\text{-nitrophenol per ml aqueous phase}}$

R_E = total resistance to mass transfer on a time and extract or solvent basis — sec/cm

R_{Ei} = interfacial resistance on a time and solvent basis — sec/cm

R_R = total resistance on a time and raffinate or aqueous basis — sec/cm

R_{Ri} = interfacial resistance on a time and aqueous basis — sec/cm

R_∞ = limiting resistance i.e. resistance reached when further additions of surface-activeagent caused no further increase — sec/cm

v = drop velocity — cm/sec

Γ = surface concentration of surface-active agent — g mol/cm²

References

[1] Hutchinson E. *J. Phys. Chem.* 1948 **52** 897.
[2] West F. B., Robinson P. A., Morgenthaler A. C., Beck T. R. and McGregor D. K. *Industr. Engng. Chem. (Industr.)* 1951 **43** 234.
[3] West F. B., Herrman A. J., Chong A. T. and Thomas L. E. K. *Industr. Engng. Chem. (Industr.)* 1952 **44** 625.
[4] Garner F. H. and Hale A. R. *Chem. Engng. Sci.* 1953 **2** 157.
[5] Garner F. H. and Skelland A. H. P. *Chem. Engng. Sci.* 1955 **4** 149.
[6] Lewis J. B. *Chem. Engng. Sci.* 1954 **3** 248, 260.
[7] Lewis J. B. and Pratt H. R. C. *Nature, Lond.* 1953 **171** 1155.
[8] Lindland K. P. and Terjesen S. G. *Chem. Engng. Sci.* 1956 **5** 1.
[9] Melhus J. B. and Terjesen S. G. *Chem. Engng. Sci.* In print.
[10] Holm A. and Terjesen S. G. *Chem. Engng. Sci.* 1955 **4** 265.
[11] Wilke C. R. *Chem. Engng. Progr.* 1949 **45** 218.
[12] Wilke C. R. and Chang P. *Amer. Inst. Chem. Engrs. J.* 1955 **1** 264.
[13] Garner F. H. and Skelland A. H. P. *Industr. Engng. Chem. (Industr.)* 1954 **46** 1235.

Chemical Engineering Science, 1958, Vol. 7, pp. 229 to 234. Pergamon Press Ltd.

Diffusion controlled reaction in a laminar boundary layer

S. K. Friedlander* and Mitchell Litt†

*Department of Chemical Engineering, The Johns Hopkins University, Baltimore, Md.

†Department of Chemical Engineering, Columbia University, N.Y.

(*Received* 1 *August* 1957)

Abstract—A simple, exact (boundary-layer) solution is obtained to the equations of diffusion and and energy for a rapid reaction occurring in the laminar boundary layer on a flat plate. The velocity distribution is assumed to be given by the Blasius solution to the Prandtl boundary-layer equations. Expressions are derived for rates of interphase transfer, and concentration and temperature distributions. Applications are to problems of absorption, extraction, dissolution and combustion.

Résumé—C'est la solution exacte et simple des équations de diffusion et d'énergie qui est ici obtenue pour une réaction rapide ayant lieu dans la couche limite laminaire d'une plaque plane. Il est admis que la distribution des vitesses est celle fournie par la solution de Blasius aux équations de la couche limite de Prandtl. Ceci permet de déduire des expressions pour les taux d'échanges dans l'interphase, et la répartition des températures et des concentrations. Des applications peuvent être faites aux problèmes d'absorption, d'extraction, de dissolution et de combustion.

Zusammenfassung—Für die Gleichungen der Diffusion und der Energie bei einer schnellen Reaktion in der laminaren Grenzschicht einer ebenen Platte wird eine einfache, exakte (Grenzschicht–) Lösung angegeben. Die Geschwindigkeitsverteilung wird gemäss der Blasius-Lösung der Grenzschichtgleichungen von Prandtl angenommen. Für den Austausch zwischen den Phasen und die Verteilungen von Konzentration und Druck werden Ausdrücke abgeleitet. Anwendungen stellen dar: Probleme der Absorption, Extraktion, Auflösung und Verbrennung.

VOL. 7 957/58

Introduction

During the last two decades a considerable amount of information, both theoretical and experimental, has become available on the dynamics of real fluids. Much of this information is summarized in the monographs on turbulent flow by Batchelor [1] and Townsend [15] and on boundary-layer theory by Schlichting [10]. Recently, investigators have sought to apply these results to moving fluids in which chemical reactions are taking place, systems of great practical importance. Thus Corrsin [3] has begun the development of a statistical theory for chemical reaction in a turbulent fluid, and Chambré and Acrivos [2] have applied boundary-layer theory to heterogeneous catalysis in a flow system. Kiser and Hoelscher [7] describe a water tunnel constructed to facilitate hydrodynamically controlled studies of catalytic surface reactions.

Another important class of chemical changes in flow systems is the rapid, irreversible second-order reaction. Examples are the absorption of carbon dioxide by dilute solutions of base [4] or the dissolution of solid acids in basic solutions [5, 6]. A similar model is used in combustion calculations for the burning of single fuel drops [8, 14] but here the picture is further complicated by large heat effects.

As pointed out by Sherwood and Pigford [13], two approaches are commonly employed in

making quantative predictions for these systems. In one, a modification of the old Nerst-Brunner theory, it is postulated that a stagnant film exists next to the interface. The component which is dissolving, evaporating, or being absorbed diffuses across the phase boundary to a point within the film where it meets the other reactant diffusing in from the main body of the liquid or gas. Reaction is instantaneous. In the steady state, the reaction zone takes up a position which depends on the diffusivities and concentrations of the components.

Alternatively, absorption in packed columns has been pictured as an unsteady state phenomenon in which packets of liquid contact the interface for a short time and then return to the main body. During the period of contact, unsteady molecular diffusion to the reaction zone (as defined above) takes place but the position of the reaction zone changes with time.

These models, while easily pictured and mathematically tractable, are not faithful representations of any real flow system. As a guide to the influence of convective effects it would be useful to have theoretical predictions for an actual system, well defined hydrodynamically. It is shown below that with some not too restrictive assumptions it is possible to obtain a simple, exact (boundary-layer) solution to the problem of rapid chemical reaction in the laminar boundary layer on a flat plate.

Analysis

As an example, the steady state dissolution of a slightly soluble solid, such as benzoic acid, in a flowing dilute solution of a base may be considered. The geometry is that of a flat plate of acid at zero incidence to the flow. The process is practically isothermal, and the properties of the fluid are independent of position. The rate at which dissolution takes place as a function of distance from the leading edge of the plate and concentration of reactant in the mainstream (at infinity) will now be discussed.

For low rates of dissolution, the normal velocity at the interface is small. Provided the Reynolds number is sufficiently large, the velocity distribution is given by the Blasius solution of the Prandtl boundary-layer equations [10] :—

$$ff'' + 2f''' = 0 \tag{1}$$

where f' (η) represents the (dimensionless) boundary-layer velocity and $\eta = y\sqrt{U/\nu x}$. Values of f and its derivatives are tabulated in Schlichting [11].

Substance A dissolves from the plate and diffuses to the reaction zone while B diffuses into the reaction zone from the main body of the solution. In the reaction region, which is considered to be of negligible thickness, the two substances meet, and the rapid, irreversible reaction :—

$$aA + bB \rightarrow \text{products} \tag{2}$$

takes place. In the region between the reaction zone and the surface the diffusional process is described by the expression :—

$$u\frac{\partial C_A}{\partial x} + v\frac{\partial C_A}{\partial y} = D_A\frac{\partial^2 C_A}{\partial y^2} \tag{3}$$

Here the term representing diffusion in the x direction is neglected in accordance with the usual boundary-layer assumptions. Similarly in the region outside the reaction zone :—

$$u\frac{\partial C_B}{\partial x} + v\frac{\partial C_B}{\partial y} = D_B\frac{\partial^2 C_B}{\partial y^2} \tag{4}$$

Transforming to the η co-ordinate system, it is easily shown [12] that these equations become :—

$$\frac{1}{S_A}\frac{d^2c_A}{d\eta^2} + \frac{f}{2}\frac{dc_A}{d\eta} = 0 \tag{5}$$

and

$$\frac{1}{S_B}\frac{d^2c_B}{d\eta^2} + \frac{f}{2}\frac{dc_B}{d\eta} = 0 \tag{6}$$

where

$$c_A = \frac{C_A}{C_{AS}}, \quad c_B = \frac{C_B}{C_{BM}} \tag{7}$$

The boundary conditions imposed on the system are as follows :—

$$\left.\begin{array}{ll} \text{At} & \eta = 0, \quad c_A = 1 \\ & \eta = \eta_R, c_A = c_B = 0 \\ & \eta = \infty, c_B = 1 \end{array}\right\} \tag{8}$$

Stated in words, it is assumed that the reaction takes place along a surface of constant $\eta = \eta_R$.

This assumption is necessary to preserve the similarity postulated in the transformation to the η co-ordinate system. The final condition necessary to fix the position of η_R results from the assumption that the materials enter the reaction zone in stoichiometric proportions :—

At $\eta = \eta_R$

$$D_A \frac{\partial C_A}{\partial y_A} = \frac{-a}{b} D_B \frac{\partial C_B}{\partial y_B} \tag{9}$$

or

$$c_A' = \frac{-a}{b} \frac{S_A}{S_B} \frac{C_{BM}}{C_{AS}} c_B' \tag{9a}$$

Since $f = -2f'''/f''$, equations (5) and (6) can be integrated between limits to give :—

$$c_A = 1 - \frac{\int_0^\eta f''^{S_A} \, d\eta}{\int_0^{\eta_R} f''^{S_A} \, d\eta}, \quad \eta_R > \eta > 0 \tag{10}$$

and

$$c_B = \frac{\int_{\eta_R}^\eta f''^{S_B} \, d\eta}{\int_{\eta_R}^\infty f''^{S_B} \, d\eta}, \quad \infty > \eta > \eta_R \tag{11}$$

Substituting in (10) for c_A' and c_B' and rearranging the following equation is obtained :—

$$\frac{aC_{BM}}{bC_{AS}} = \left(\frac{S_B}{S_A}\right)^{\frac{1}{2}} \left(\frac{f_R''}{0{\cdot}332}\right)^{S_A - S_B} \left[\frac{\theta_{1BR}}{1 - \theta_{1AR}}\right] \tag{12}$$

using the approximation (12) :—

$$\int_0^\infty f''^S \, d\eta = \frac{(0{\cdot}332)^S}{0{\cdot}332 S^{\frac{1}{2}}} \tag{13}$$

The parameter θ_1 is defined by the expression:—

$$\theta_1(\eta, S) = \frac{\int_\eta^\infty f''^S \, d\eta}{\int_0^\infty f''^S \, d\eta} \tag{14}$$

and is plotted by Schlichting [12] after Pohlhausen [9]. From equation (10) the local Sherwood number is :—

$$N_x = -\left(\frac{\partial c_A}{\partial y}\right)_0 x = \frac{0{\cdot}332 \, S_A^{\frac{1}{2}} \, R_x^{\frac{1}{2}}}{1 - \theta_{1AR}} \tag{15}$$

and the mean Sherwood number for the entire plate up to x is given by :—

$$N_M = 2N_x = \left[\frac{1}{1 - \theta_{1AR}}\right] \left[0{\cdot}664 \, S_A^{\frac{1}{2}} \, R_x^{\frac{1}{2}}\right] \tag{16}$$

The quantity $1/1 - \theta_{1AR}$ represents a correction factor for reaction when applied to the term $0{\cdot}664 \, S_A^{\frac{1}{2}} \, R_x^{\frac{1}{2}}$, the Sherwood number for pure diffusion. Since $\theta \leqslant \theta_1 \leqslant 1$, the mass transfer rate for simultaneous reaction will always be greater than that for diffusion alone.

For a given system, with S_A, S_B and C_{AS} fixed, the reaction factor can be obtained as a function of main stream concentration in the following way : A value of η_R is assumed and θ_{1AR}, θ_{1BR}, and f_R'' read off the appropriate curves and tables [11, 12]. The reaction factor can be calculated immediately and the corresponding value of aC_{BM}/bC_{AS} can be obtained from equation (12). Fig. 1 shows the results of a calculation of this type taking $S = 900$ for benzoic acid and 524 for sodium hydroxide in water at 25°C. The values of S are based on the data given by King and Brodie [6].

For the important case of $S_A = S_B$, $\theta_{1AR} = \theta_{1BR} = \theta_{1R}$ and from equation (12) :—

$$1 - \theta_{1R} = \frac{1}{1 + \dfrac{aC_{BM}}{bC_{AS}}} \tag{17}$$

and

$$N_M = \left(1 + \frac{aC_{BM}}{bC_{AS}}\right) 0{\cdot}664 \, S_A^{\frac{1}{2}} \, R_x^{\frac{1}{2}} \tag{18}$$

It is interesting to note that the reaction factor $1 + \{(aC_{BM})/(bC_{AS})\}$ is identical with that obtained for the simplified model of constant film thickness without convection (13). The factor for $S_A = S_B$ is also shown in the Figure.

When C_{BM}/C_{AS} is very large the reaction zone approaches the surface, $f_R'' \to f_S'' = 0{\cdot}332$ and $\theta_{1AR} \to 1$. Equation (12) can be rearranged to give

$$\frac{1}{1-\theta_{1AR}} \approx \frac{aC_{BM}}{bC_{AS}}\left(\frac{S_A}{S_B}\right)^{\frac{1}{2}},\ \eta_R \to 0 \qquad (19)$$

This explains the linearity of the curves in Fig. for large values of C_{BM}/C_{AS}.

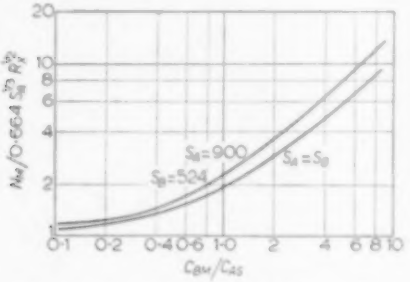

Fig. 1. Reaction factor as a function of concentration ratio.

Extension to Non-Isothermal Systems

This approach can be extended to the steady state non-isothermal case with constant fluid properties to permit calculation of the temperature of the reaction zone and the distribution near the surface. The energy equivalent to equation (5) is :—

$$\frac{1}{P}\frac{d^2T}{d\eta^2} + \frac{f}{2}\frac{dT}{d\eta} = 0 \qquad (20)$$

assuming that dissipation by viscous friction is negligible. If the surface temperature T_S and main stream temperature T_M are constant, the temperature T_R of the reaction zone must also be constant to preserve similarity. Under these conditions, the solution to equation (20) for each side of the reaction zone is identical with the form for the concentration distributions :—

$$t_A = \frac{T_R - T_A}{T_R - T_S} = 1 - \frac{\int_0^{\eta} f''^{P_A}\,d\eta}{\int_0^{\eta_R} f''^{P_A}\,d\eta},\ \eta_R > \eta > 0 \qquad (21)$$

$$t_B = \frac{T_R - T_B}{T_R - T_M} = \frac{\int_{\eta_R}^{\eta} f''^{P_B}\,d\eta}{\int_{\eta_R}^{\infty} f''^{P_B}\,d\eta},\ \infty > \eta > \eta_R \qquad (22)$$

The position of the reaction surface η_R can be calculated from the flow-diffusion equation in a manner described in the previous section. Its value depends on the temperature distribution through the solubility or vapour pressure relationship $C_S = F(T_S)$.

The temperature of the reaction zone is obtained by assuming that the heat generated at $\eta = \eta_R$ is conducted away from both sides of the zone according to the expression :—

$$\Delta H_R D_A C_{AS}\left(\frac{\partial c_A}{\partial y}\right)_R = k\left[\left(\frac{\partial T_A}{\partial y}\right)_R - \left(\frac{\partial T_B}{\partial y}\right)_R\right] \qquad (23)$$

or

$$\frac{\Delta H_R D_A}{k} C_{AS}\, c'_{AR} = -(T_R - T_S)\, t'_{AR} + (T_R - T_M)\, t'_{BR} \qquad (23a)$$

(Since the reaction zone is of vanishing thickness, the heat convected in and out is equal). Rewriting equation (23*a*) in terms of θ_1 :—

$$\frac{-\Delta H_R D\ C_{AS}}{k(1-\theta_{1AR})}\left(\frac{S_A}{P}\right)^{\frac{1}{2}}\left[\frac{0{\cdot}332}{f_R''}\right]^{P-S_A} = \left[\frac{T_R - T_S}{1-\theta_{1R}} + \frac{T_R - T_M}{\theta_{1R}}\right] \qquad (24)$$

where $\theta_{1AR} = \theta_1(S_A, \eta_R)$ and $\theta_{1R} = \theta_1(P, \eta_R)$.

If η_R is known from the diffusion calculation T_R can be obtained from equation (24). Assuming that the surface and mainstream temperatures were both 25°C, a calculation of this type was made for the system benzoic acid–sodium hydroxide solution. For dilute solutions of the base, the temperature rise of the reaction zone was found to be negligible.

For a gaseous reaction $S \approx P$ and equation (24) becomes :—

$$-\Delta H_R D_A C_{AS}/k = (T_R - T_S) + \frac{1-\theta_{1R}}{\theta_{1R}}(T_R - T_M) \qquad (25)$$

Flame front temperatures for combustion processes can be estimated from equation (25) provided that mean fluid properties can be used in the equations of motion, diffusion and energy.

VOL. 7 1957/58

Application to Other Geometries

The "exact" method developed above for the laminar boundary layer on a flat plate can be extended to other laminar flows for which similar (one space parameter) solutions to the boundary-layer equations exist. Examples are flow past a wedge and free jet flow. Application to turbulent systems (such as free jets) may also be possible provided the reaction takes place over a sufficiently narrow region.

For shapes such as cylinders or spheres which do not permit similarity transformations, the von Karman integral method can be applied. Here it is necessary to assume the existence of two boundary layers; at the edge of the inner layer, the boundary conditions are given by equations of the type (8) and (9) and a polynomial form can be assumed for the concentration in each layer. A calculation of this type was made for the flat plate and the results were found to compare well with those of the exact solution.

Over a large Reynolds number range most of the transfer for such shapes as cylinders and spheres occurs in a laminar boundary layer extending back from the forward stagnation point; here the Sherwood number for pure diffusion is given by :—

$$N_M = AS^{\frac{1}{3}} R^{\frac{1}{2}} \qquad (26)$$

The quantity A is a constant which depends on the geometry but is usually near 0·664, the flat plate value. Thus, as a first approximation, it seems reasonable to assume that the reaction factor for other geometries will be of a form similar to that for the flat plate.

Acknowledgement—The authors wish to express their appreciation to E. I. du Pont de Nemours and Co. Inc., for the fellowship held by one of them (M.L.) during the investigation.

Notation

a, b = stoicheiometric coefficients of chemical reaction
c_A, c_B = boundary-layer concentration parameters for reactants A and B, dimensionless
C_A, C_B = boundary-layer concentrations of reactants A and B, moles/l
C_{AS} = surface concentration of A, moles/l
C_{BM} = mainstream concentration of B, moles/l
c_P = specific heat of fluid, cal/g°C
D_A, D_B = diffusivities of reactants A and B in fluid, cm.^{2}/sec
f' = boundary-layer velocity, dimensionless
ΔH_R = standard heat of reaction, kcal/g mole
k = thermal conductivity of fluid, cal/sec (cm^2) (°C)/cm
k_X = local mass transfer coefficient, cm/sec
N_M = mean Sherwood number, $2N_X$, dimensionless
N_X = local Sherwood number, $k_x x/D_A$, dimensionless
P = Prandtl number for fluid, $c_P \rho \nu/k$
R_X = distance Reynolds number, Ux/ν
S_A = Schmidt number for reactant A, ν/D_a
S_B = Schmidt number for reactant B, ν/D_B
t_A, t_B = boundary-layer temperature parameters, dimensionless
T_S = temperature of surface, °C
T_R = temperature of reaction zone, °C
T_M = temperature of fluid main stream, °C
u, v = boundary-layer velocity in x and y directions, respectively, cm/sec
U = main stream fluid velocity, cm/sec
x = direction parallel to plate
y = direction perpendicular to plate
ν = kinematic viscosity, cm^2/sec
η = dimensionless coordinate, $y\sqrt{U/x\nu}$
ρ = density of fluid, g/cm^3

Notes :—Primed quantities denote differentiation with respect to η; the subscript "R" refers to values taken at $\eta = \eta_R$.

References

[1] Batchelor G. K. *The Theory of Homogeneous Turbulence*. University Press, Cambridge 1953.

[2] Chambré P. L. and Acrivos A. *J. Appl. Phys.* 1956 **27** 1322.

[3] Corrsin S. Statistical behaviour of a reacting mixture in isotropic turbulence,. Paper presented at Amer. Chem. Soc. symposium on Fluid Mechanics in Chemical Engineering, 27–8 December 1956.

[4] Hatta S. *Technol. Rep. Tôhoku Imp. Univ.* 1928-9 **8** 1; 1932 **10** 119.

[5] Hixson A. W. and Baum S. J. *Industr. Engng. Chem.* 1944 (*Industl.*) **36** 528.

[6] King C. V. and Brodie S. S. *J. Amer. Chem. Soc.* 1937 **59** 1375.

[7] Kiser K. M. and Hoelscher H. E. *Industr. Engng. Chem.* (*Industr.*) 1957 **49** 970.

[8] Penner S. S. *Introduction to the Study of Chemical Reactions in Flow Systems* p. 67. Butterworth Scientific Publications, London 1955.

[9] Pohlhausen E. *Z. Angew. Math. Mech.* 1921 **1** 115.

[10] Schlichting H. *Boundary Layer Theory* p. 103. McGraw-Hill, New York, 1955.

[11] Schlichting H. *Boundary Layer Theory* p. 107. McGraw-Hill, New York 1955.

[12] Schlichting H. *Boundary Layer Theory* pp. 264-5. McGraw-Hill, New York 1955.

[13] Sherwood T. K. and Pigford R. L. *Absorption and Extraction* p. 320. McGraw-Hill, New York, 1952.

[14] Spaulding D. B. *Selected Combustion Problems.* N.A.T.O. Advisory Group for Aeronautical Research and Development, p. 340. Butterworth Scientific Publications, London 1954.

[15] Townsend A. A. *The Structure of Turbulent Shear Flow.* University Press, Cambridge 1956.

VO
7
1957

Chemical Engineering Science, 1958, Vol. 7, pp. 235 to 240. Pergamon Press Ltd.

Countercurrent gas–liquid flow

Stability of a spherical liquid film in an infinite airstream

J. E. Howkins and J. F. Davidson
Chemical Engineering Department, Cambridge

(*Received* 8 *August* 1957)

Abstract—A liquid film runs symmetrically under gravity over a string of spheres suspended in an upward stream of air. At a certain air velocity a standing wave forms on the film covering the lowest hemisphere. The wave is formed at about 30° to the vertical, where the pressure gradients within the airstream, due to its acceleration over the sphere, are a maximum.

Experiments with spheres of 1·0 and 1·5 in. diam. suspended in a 5·75 in. tube gave good agreement with theory. Wave formation of this kind is thought to be responsible for loading in packed towers of high voidage.

Résumé—Les auteurs considèrent un film liquide s'écoulant symétriquement par gravité sur un chapelet de sphères suspendues dans un courant d'air ascendant. Une onde stable se forme sur le film couvrant l'hémisphère inférieure, pour une certaine vitesse de l'air. Cette onde est placée à 30° environ sur la verticale à l'endroit où les variations de pression dans le courant d'air, dûes à l'accélération sur la sphère, sont maximum.

Des sphères de 1 à 1,5 pouce de diamètre suspendues dans un tube de 5,75 pouces donnent des résultats en accord avec la théorie. C'est sans doute cette onde que détermine le point de charge dans les colonnes à garnissage ayant un grand degré de vide.

Zusammenfassung—Ein flüssiger Film läuft symmetrisch unter dem Einfluss der Schwerkraft über ein Band aus Kugeln, das in aufwärts strömender Luft aufgehängt ist. Bei einer bestimmten Geschwindigkeit bildet sich auf dem Film, der die unterste Halbkugel bedeckt, eine stehende Welle. Die Welle bildet sich bei einem Winkel von etwa 30° von der Senkrechten, wo die Druckgradienten des Luftstromes, hervorgerufen durch seine Beschleunigung längs der Kugel, ein Maximum haben.

Versuche mit Kugeln von 25 und 38 mm Durchmesser, aufgehängt in einem Rohr von 146 mm lichter Weite, ergaben gute Übereinstimmung mit der Theorie. Wellenbildung dieser Art kann die Belastung von Füllkörpersäulen mit grossem Leervolumen beeinflussen.

1. Introduction

In a previous paper [1] it was suggested that loading in packed towers is caused by the formation on the liquid film of standing waves supported by pressure gradients within the gas stream. These pressure gradients are due to the acceleration of the gas as it passes up through regions of the packing where the flow area is contracting.

The present paper deals with the formation of similar waves, but the pressure gradients were produced differently. Fig. 1 shows the arrangement. A jet of liquid is put on to the top of a vertical string of spheres, and forms a symmetrical film which runs down freely under gravity, the liquid leaving as a jet at the bottom. When the surrounding air is moved vertically upwards the air velocity just above the liquid surface at *A*

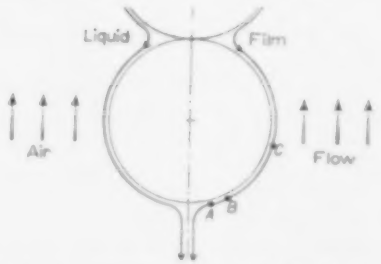

Fig. 1. Sphere covered by a liquid film in an upward airstream.

will be less than at B. Consequently the pressure at A will be greater than at B, and the liquid film between A and B will be subjected to a tangential force caused by the pressure gradient.

The mechanism of wave formation due to this pressure gradient is similar to that previously described [1]; if we consider the equilibrium of an element of the liquid film between A and B in Fig. 1, the force of gravity must always be balanced by the sum of the pressure gradient and viscous forces. The latter force is inversely proportional to film thickness, and this will become very large at an airflow such that the gravity force is balanced entirely by the pressure gradient force. This balance produces the large wave shown in Fig. 2 which has formed on the hemispherical end of a 1·5 in. diam. cylinder covered by a liquid film; this arrangement was used to find the effect of altering the airflow pattern above the lowest hemisphere.

Experiments were also made with vertical strings of spheres of diameters 1·0 and 1·5 in. The spheres and the cylinder were suspended on the axis of a tube of 5·75 in. i.d., which is large enough to give a small wall effect.

When the clearance between the balls and the tube is small [1] the wave formation is different. In this case the pressure gradient on the bottom ball in the region AB Fig. 1 is small compared with the pressure gradient in the region C. At C the contracting area between the ball and the tube, as the air moves up, causes a pressure gradient, with wave formation just below the equator of each ball. This is thought to be the mechanism of loading in packed towers of moderate voidage. A detailed treatment of this case is given elsewhere [2] and will be published later. With high voidages it is thought that loading will begin at the bottom of the tower, as in the present experiments.

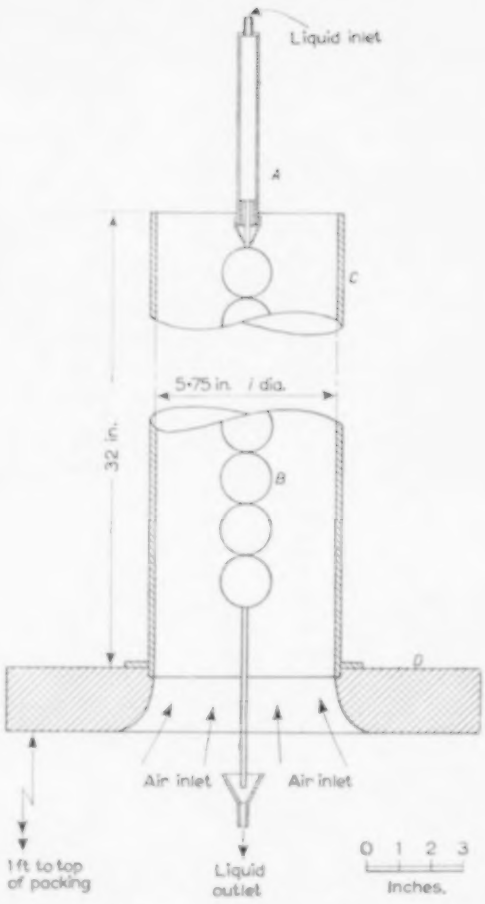

Fig. 3. The apparatus (to scale).

2. Experimental

Apparatus and procedure.

A sectional scale drawing of the apparatus is shown in Fig. 3. Here A is the liquid distributor, B the string of balls, and C the tube of 5·75 in. i.d. The entry piece D was designed to have the same form as the I.S.A. nozzle in B.S.1042 [3]. The entry piece D fitted on top of a 1 ft^2 packed tower, with a space of 1 ft between the bottom of D and the top of the packing. With these precautions it was assumed that the air velocity would be uniform at the bottom of the tube C. The liquid, after running as a film over the balls, ran down a rod through the axis of the balls, and was collected by the small funnel and taken out by a small tube through the packing below.

Experiments were carried out with three liquids; water, water + 1 per cent Lissapol, and liquid paraffin. The water rate was measured by a rotameter, the liquid paraffin rate by timing a measured volume, and the air rate by a calibrated entry flume of the type described by Ower [4].

VOL.
7
957/58

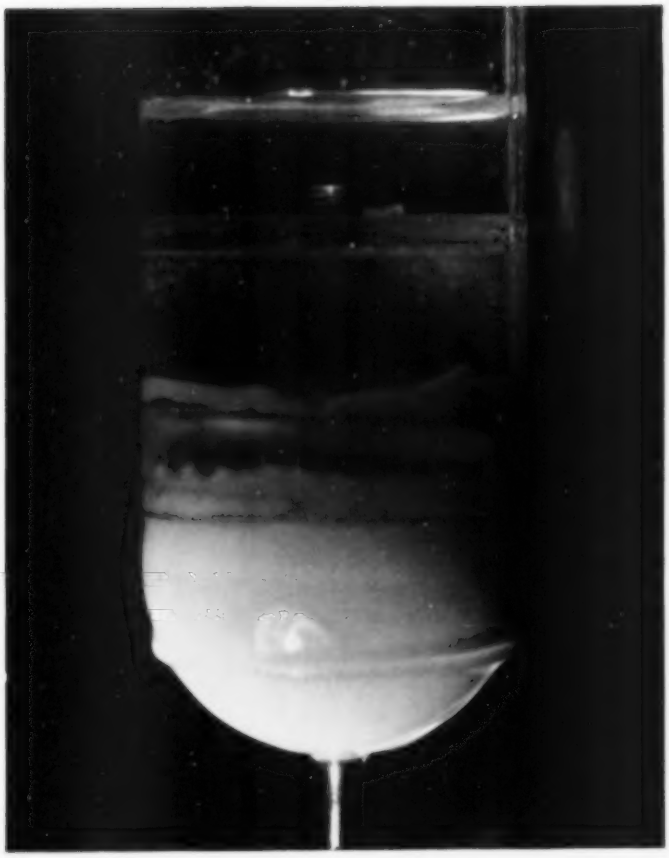

FIG. 2. Wave forming on a film of liquid paraffin (rate = 0·023 ml/sec) due to the upward flow of air (velocity = 17·5 ft/sec).

VO
7
1957

With the liquid film running steadily, the air rate was gradually increased until a wave formed on the lowest hemisphere.

3. Theory

The airflow round the outside of a sphere covered by a liquid film was analysed approximately by using Stokes' stream function, with various combinations of sources and sinks superposed on a uniform stream, as described by Milne-Thomson [5]. Typical air streamlines are shown in Fig. 4; here (a) shows the streamlines

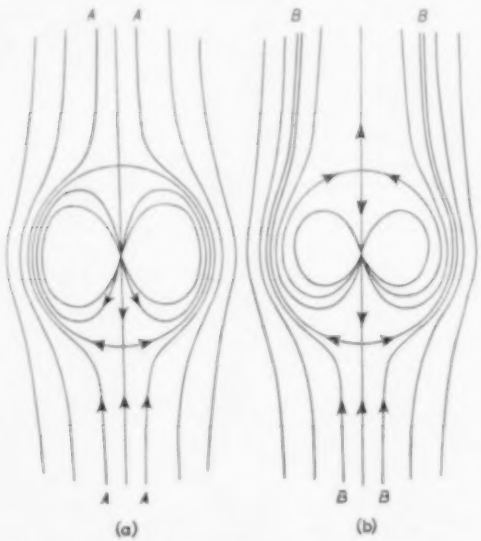

Fig. 4. Inviscid motion (to scale). (a) Flow round a sphere, produced by a doublet in a uniform stream. (b) Doublet and a point source in a uniform stream.

due to a doublet—that is, an equal source and sink at the same point—combined with a uniform infinite stream. This combination of doublet and uniform stream gives the flow round a sphere. By appropriate choice of doublet strength and main stream velocity, one of the streamlines AA can be made to have nearly the same shape as the surface of the liquid film. Over the lower half of the sphere the actual air streamlines are similar to those shown in Fig. 4(a), and consequently the pressure gradients along the first part of the streamline AA will be similar to those which actually act on the liquid film.

On account of separation of the main airstream, and the formation of a wake behind the sphere, an element of air starting in contact with the water surface flows along a path BB rather than AA. The change in the pressure gradients over the lower half of the sphere is not large and was estimated from the streamlines in Fig. 4(b). These streamlines are due to a coincident source and doublet with a uniform stream.

The stream function for the flow round a sphere (Fig. 4a) is:

$$\psi = \frac{Ur^2 \sin^2\theta}{2}\left(1 - \frac{a^3}{r^3}\right). \qquad (1)$$

Here U is the main stream velocity, r is the radius measured from the doublet, a is the radius of the sphere, and θ is the angle measured from the axis. The streamlines of Fig. 4(b) are obtained by adding a term $m \cos\theta$ to equation [1], m being the strength of the additional source at the origin.

Boundary conditions

(a) The streamlines AA and BB are chosen to coincide with the surface of the film far below the sphere. This means that if R_0 is the radius of the rod plus the asymptotic film thickness, in Fig. 4 the value of ψ along AA is $UR_0^2/2$ and is $(UR_0^2/2) + m$ along BB.

(b) When $\theta = 90°$ the distance of the streamline from the axis must be R_1, the radius of the sphere plus the liquid film thickness. For the streamline AA, the resulting equation is $R_1R_0^2 = R_1^3 - a^3$, and for the streamline BB there is the same equation with $2m\,R_1/U$ subtracted from the right hand side.

(c) For the streamlines in Fig. 4a the boundary conditions (a) and (b) determine the motion completely, but a third condition is required when separation is considered as in Fig. 4b. Rather arbitrarily, it was decided to equate to R_1 the distance of the streamline BB from the axis at $\theta = 100°$. The resulting equation is $UR_0^2R_1 = U(R_1^3 - a^3\sin^3 100°) - 2mR_1(1 - \cos 100°)$ and this, together with boundary condition (b), determines a and U/m. In this case a is nearly equal to the radius of the actual sphere.

Pressure gradient

The radial and tangential velocities u and v along the streamlines AA and BB were calculated by substituting equation (1) into the expressions $u = -(\partial\psi/\partial\theta)/r^2 \sin\theta$ and $v = (\partial\psi/\partial r)/r \sin\theta$. The pressure p at any point was then calculated from Bernoulli's theorem, and plotted as a function of θ. The slope of the resulting graph is $(\partial p/\partial\theta)_\psi$.

Condition for wave formation

The airflow at which the pressure gradient forces entirely balance the gravity forces on the liquid film is calculated by putting :

$$-\frac{1}{r}\left(\frac{\partial p}{\partial\theta}\right)_\psi = \rho_l g \sin\theta. \qquad (2)$$

Here ρ_l is the liquid density. This equation is derived by a balance on an element of the liquid film, and gives an upper limit to the airflow for stability. A similar upper limit calculated in the previous paper [1] for a vertical water film was about 25 per cent above the true critical airflow.

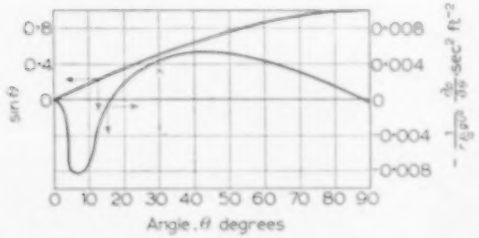

Fig. 5. Functions for determining the critical airflow.

Fig. 5 shows how equation (2) was satisfied, and gives $\sin\theta$ and $(\partial p/\partial\theta)/r\,\rho_a g U^2$ as functions of θ. To satisfy (2), $\sin\theta$ is multiplied by $\rho_l/\rho_a U^2$, ρ_a being the density of air. The value of U was adjusted to give contact between the curves in the region X Fig. 5. This is the critical value of U and the wave forms at the point of contact. In the case of the 1·0 in. sphere the angle is 29° and is indicated in Fig. 6 with the streamline BB which was assumed to coincide with the surface of the liquid film. In deriving (2), it has been assumed that the liquid film is very thin, that is, that the streamline BB is nearly tangential to the ball. This is only approximately true at 29° in Fig. 6, so too much accuracy must not be ascribed to these calculations.

The procedure when using the streamlines of Fig. 4a, not allowing for separation, is similar, and results from both methods are given in Table 1.

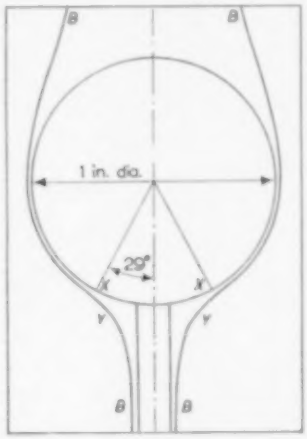

Fig. 6. Air streamline round a 1 in. diam. ball. Liquid paraffin rate = 0·03 ml/sec.

4. Results

Table 1 shows the results for two strings of spheres and for the cylinder with hemispherical ends. The latter was used to get an experimental measure of the effect of altering the airflow above the lowest hemisphere. Three liquids were used, water and liquid paraffin because of their widely differing viscosities, and water with 1 per cent of Lissapol because of its low surface tension, about 30 dyn/cm, its other characteristics being the same as water. The liquid flow rates were adjusted to give roughly the same film thickness for each liquid.

It was not possible to measure the angle at which the wave initially became large, because the wave broke into spray with water, and moved round the ball with liquid paraffin. Thus in Fig. 2, where the initial formation was at about 30° to the vertical, the wave as photographed is at about 45° to the vertical.

Table 1. *Wave formation on a sphere in an air stream*

Viscosity of the liquid paraffin ≃ 300 cP

Sphere dia., in.	*Liquid*	*Liquid rate*, ml/sec	*Theoretical*				*Experimental*	*Col. 8* / *Col. 6*
			No separation		*Separation*			
			velocity, ft/sec	*angle*, deg	*velocity*, ft/sec	*angle*, deg	*Air velocity* ft/sec	
1·0	Liquid paraffin	0·03	23·3	32	24·3	29	17·9	0·74
1·0	Water	3·5			25·8	26	22·3	0·87
1·0	Water + 1% Lissapol	3·5			25·8	26	19·2	0·74
1·5	Liquid paraffin	0·03			28·4	24	17·3	0·61
1·5	Water	1·76 to 8·7			30·2	24	22·6 to 23·8	0·76
1·5	Water + 1% Lissapol	3·5			30·2	24	19·3	0·64
Cylinder dia.								
1·5	Liquid paraffin	0·023					17·5	
1·5	Water	1·76 to 8·7					22·6 to 23·8	
1·5	Water + 1% Lissapol	3·5					19·1	

5. Discussion

Effect of separation behind the lowest sphere

The results given in Table 1 from the two theoretical methods, the streamlines being those in Fig. 4(a) and 4(b), are in good agreement, showing that the effect of separation is small. Further evidence is provided by the excellent agreement between the results for the string of 1·5 in. spheres and the results for the 1·5 in. cylinder with hemispherical ends. In these two cases the airflow pattern above the lowest hemisphere must be different although the difference may not be great.

These results are what would be expected, since the flow pattern round the nose of a streamlined object is not much influenced by the shape of its back.

Another effect of separation is to ensure that the wave formation is only on the lowest sphere. Every other sphere is in the wake of the one below, and since a wake is a region of constant pressure, no wave is formed.

Interaction between the air and water streams

In the previous paper [1] elaborate relaxation calculations were necessary to determine the critical airflow for wave formation, 0·115 ft^3/sec. These calculations were necessary because the pressure gradients inducing the wave were influenced by the shape of the wave and vice versa. When this interaction was ignored, as in the present paper, a value of 0·145 ft^3/sec was obtained, the ratio of the two values being 0·79. This is of the same order as the ratio of the experimental to the theoretical velocities given in the last column of the Table. Therefore it seems likely that the difference between theory and experiment in the present case is largely due to interaction.

Surface tension

In the previous experiments [1], the critical airflow was *raised* about 5 per cent when Teepol was added to the water, and this was explained as

being the result of eliminating travelling ripples. These ripples, in passing through the standing waves, were thought to cause premature instability.

In the present case, although the Lissapol eliminates travelling ripples, the critical velocity is *lowered* about 13 per cent. A likely explanation is that the pressure gradients are quite sensitive to the shape of the liquid surface near *Y*, Fig. 6, and this shape is affected by surface tension. This explanation is supported by the agreement between the results for liquid paraffin and water + Lissapol, both liquids having a surface tension around 30 dyn/cm.

This sensitivity to the shape of the air streamlines in the region *Y*, Fig. 6, also makes the theoretical results unreliable, since they are not based on the shapes of the actual liquid surfaces.

Acknowledgement—One of the authors (J.E.H.) wishes to acknowledge the support given by a Gas Council Research Scholarship.

Notation

U = air stream velocity
R_0 = radius of rod plus film
R_1 = radius of sphere plus film
a = radius of sphere
m = strength of source
p = pressure on the liquid film
r = radial distance
u = radial velocity
v = tangential velocity
θ = angle between the radius vector and the axis
ρ = density
ψ = stream function for the airflow.

Subscripts
l = liquid.
a = air.

References

[1] Davidson J. F. and Howkins J. E. *Proc. Roy. Soc.* A 1957 **240** 29.
[2] Howkins J. E. Ph.D. thesis 1957, Cambridge University.
[3] B.S.1042 *Flow Measurement*. British Standards Institution, London 1943.
[4] Ower E. *The Measurement of Air Flow* p. 194. Chapman and Hall, London 1949.
[5] Milne-Thomson L. M. *Theoretical Hydrodynamics* 2nd ed. p. 402. Macmillan, London 1949.

Chemical Engineering Science, 1958, Vol. 7, pp. 241 to 245. Pergamon Press Ltd.

Vapour–liquid equilibrium still for low pressures

AKSEL L. LYDERSEN and EGIL HAMMER
The Technical University of Norway, Chemical Engineering Laboratory, Trondheim, Norway

(*Received* 23 *August* 1957)

Abstract—A new still for vapour–liquid equilibrium measurements at pressures down to 1 mm Hg is described. The whole still is agitated in order to give vaporization from a frequently renewed falling film, and also to give good mixing of the boiler liquid and the condensate.

Possible sources of error are reviewed and tests were made to check on the different types of error. The enrichment obtained in the still appears to be approximately 98 per cent of the enrichment by complete equilibrium.

Vapour–liquid equilibrium measurements with a mixture of di-*n*-butylphthalate and di-*n*-butylsebacate at 1 mm Hg are given, showing practically ideal behaviour of the mixture.

Résumé—Les auteurs décrivent un nouvel ébulliomètre pour mesurer des pressions inférieures à 1 mm Hg. Tout l'appareil est agité de façon à provoquer l'ébullition à partir d'un film liquide constamment renouvelé, et aussi pour favoriser un bon mélange du liquide bouillant avec le condensat.

Les auteurs passent en revue les diverses sources d'erreurs et font des essais pour discerner ces diverses causes d'erreur. L'enrichissement obtenu dans l'ébulliomètre semble voisiner 98 pour cent de l'enrichissement obtenu à l'équilibre.

Les mesures de l'équilibre liquide vapeur, faits avec un mélange de di-n-butylphtalate et de di-n-butylsebacate à 1 mm Hg, montrent le comportement pratiquement idéal du mélange.

Zusammenfassung—Es wird eine neue Apparatur zur Messung des Dampf–Flüssigkeits–Gleichgewichtes bei Drücken bis herunter zu 1 Torr beschrieben. Die gesamte Apparatur ist gerührt, um eine Verdampfung aus einem häufig erneuerten Rieselfilm zu erzielen und um auch eine gute Durchmischung der siedenden Flüssigkeit und des Kondensats zu erreichen.

Die möglichen Fehlerquellen werden diskutiert und an Probeläufen die verschiedenen Fehlerarten untersucht. Die mit der Apparatur erzielte Anreicherung scheint ungefähr 98% von jener zu betragen, die bei vollständigem Gleichgewicht zu erreichen wäre.

Messungen des Dampf–Flüssigkeits–Gleichgewichts einer Mischung von Di-n-Butylphthalat und Di-n-Butylsebacat bei 1 Torr werden mitgeteilt und zeigen das praktisch ideale Verhalten des Gemisches.

INTRODUCTION

THE growing use of vacuum distillation has increased the importance of knowing low-pressure vapour–liquid equilibria. The experimental determination of equilibria at low pressures involve a number of difficulties not encountered at elevated pressures, primarily because only minor pressure drops can be tolerated, but also to some extent due to the tendency of bumping.

FOWLER [1] gives a description of the vapour–liquid equilibrium stills published in the literature up to 1948 and RIDGWAY (9) gives a corresponding review for the years 1948-55. Recent modifications of the stills are described by several authors ([3], [4], [5] and [10]).

The majority of the stills do not seem adaptable to pressures below a few mm of Hg, as the bubble formation and growth take place under an appreciable liquid head. At a pressure of 1 mm Hg in the vapour space, the pressure 2 cm under the liquid surface will be 2 to 3 mm Hg, depending on the density of the liquid.

The aim of the present authors was to build a still suitable for equilibrium measurements at pressures down to 1 mm Hg absolute. For dynamic stills only two main principles seem worth considering :

The use of an inert carrier gas, whereby a total pressure is maintained that is high compared to the partial pressure of the compounds in the

liquid mixture, thus making it possible to use a conventional type of still.

Vaporization from a liquid surface that is renewed fast enough to avoid any appreciable dilution with respect to the more volatile compound.

In the present work, the design was based on the latter principle, mainly because, firstly, the vapour pressure of the mixture can be measured directly and, secondly, because the total condensation of pure vapours is easier to obtain than the condensation from an inert, where fractional condensation will cause error.

Description of the Still

The still to be described in this paper is shown in Figs. 1 and 2. The vapours formed in the boiler *A*, Fig. 2, are condensed in the parts *D* and *E*, and the condensate flows back to the boiler through the capillary *G*. Heat flow through the inner half of the insulation of the off-take pipe *C* is prevented by electric heating of the aluminium cylinders H_1 and H_2. The heat input is manually adjusted according to the readings of the thermocouples 1–7.

The still is connected to a McLeod gauge and a rotary vacuum pump protected by the dry ice traps K_1 and K_2 as shown schematically on the right-hand side of Fig. 2. An air-bleed valve *N* and a Cartesian manostate *V* makes it possible to adjust the vacuum.

The top of the still is fastened to a universal joint *U*. During operation, the still is agitated as the shaft *Y* is rotated in a circle with radius *r*. This gives agitation of both the boiler liquid and the condensate in the sphere *F*. The capillaries for sampling and liquid return serve as baffles.

The necessary operations are adjustment of the vacuum and the heating elements in the insulation, and also checking temperatures and pressure to see that stationary conditions are maintained. At the end of the run, the vacuum is released. This instantaneously stops the boiling and forces boiler liquid and condensate into the sample flasks R_1 and R_2.

The design shown on the Fig. 1 and 2 has some resemblance to the still used by Williams [11], which again was a modification of an Othmer

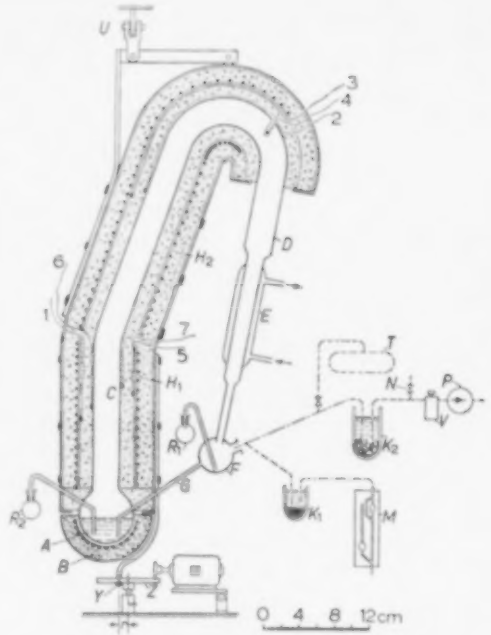

Fig. 2. A drawing of the still; the connections at the lower right are shown schematically. Legend: *A* = 6 cm dia. boiler with heating mantle *B*, *C* = vapour off-take pipe leading to aircooled condenser *D* and the water-cooled condenser *E*, *F* = condensate receiver with overflow capillary *G*; H_1 and H_2 = electrically heated aluminium cylinders; K_1 and K_2 = dry ice traps protecting the McLeod gauge *M* and the vacuum pump *P*; *N* is an air-bleed valve, *T* a surge tank and *V* a Cartesian manostate; R_1 and R_2 = sample flasks for condensate and boiler liquid, and *Y* = shaft, agitated with radius *r* by means of the rotating disk *Z*.

[7] still. Williams, however, used a filling of helices in the boiling chamber to avoid bumping, while Langdon and Keyes [6], Perry and Fuguitt [8] and later Sanders and Acciarri [10] made use of mechanical stirrers.

The type of agitation used in the present still causes the bulk of the liquid to rotate along the side of the boiler, leaving a falling liquid film on the rest of the boiler surface. This ensures vaporization from a liquid film that covers the major part of the boiler surface which at any moment is not covered by the bulk liquid. This additional surface is considerably larger than the surface over the bulk liquid.

VOL.
7
957/58

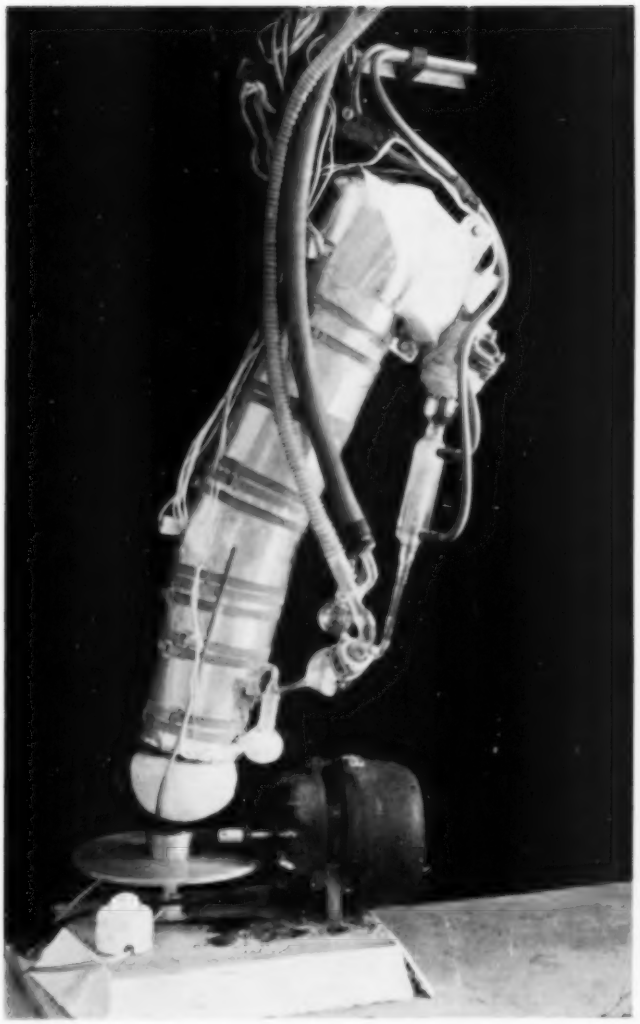

FIG. 1. A photograph of the still.

VO
7
1957

VOL. 7 957/58

Estimation of Errors

Inadequate renewal of the vaporizing surface might cause the vaporizing film to be leaner in the more volatile compound. This type of error will decrease both with decreased vaporization rate and with increased speed of the agitating disk. Fig. 3 shows the enrichment in the volatile compound obtained from a 50 mole per cent boiler mixture of di-*n*-butylphthalate and di-*n*-butylsebacate as a function of the boiling rate at three different speeds of the agitation. With a radius r (Fig. 3) of 9 mm a maximum of 260 rev/min and a minimum distillation rate of approximately 0·35 kg/hr was chosen for easy operation of the still. This boiling rate corresponds to vaporization of the boiler content 10 times an hour and renewal of the condensate sample 150 to 200 times an hour.

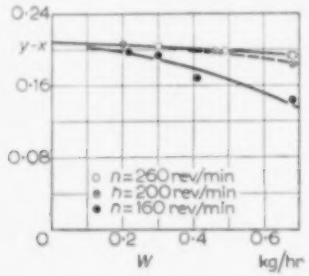

Fig. 3. The enrichment of di-*n*-butylphthalate; $y-x$, obtained from a 50 mole per cent boiler mixture of di-*n*-butylphthalate and di-*n*-butylsebacate at 1 mm Hg as a function of distillation rate W kg/hr by three different speeds of rotation n of the disk Z shown in Fig. 2.

Extrapolation in Fig. 3 to zero distillation rate indicates that the enrichment obtained at the chosen conditions should be approximately 98 per cent of the enrichment at equilibrium conditions.

Rectification effect can occur by improper heating of the insulation of the boiler off-take pipe. However, changing the temperature drop outwards through the inner half of the insulation from 0 to 7°C gave no measurable change in the composition of the condensate.

Total vaporization of boiler liquid from the boiler off-take walls may result from splashing or entrainment from the boiler in connection with superheating of the pipe C shown in Fig. 2. Tests with a temperature drop inwards through the insulation of 7°C reduced the enrichment in di-*n*-butylphthalate to only 82 per cent of the enrichment without superheating. Superheating only the upper half of the pipe C, however, gave no measurable change in condensate composition. This indicates that droplets of boiler liquid only reach the lower part of the boiler off-take pipe, and that safe operation of the still requires a slight temperature drop outwards through the lower half of the insulation.

Liquid entrainment carried over to the condenser does not seem probable as long as no vaporization of entrainment could be found from the upper part of the off-take pipe. Moreover, the correction derived from Fig. 3 should include the influence of any liquid carry-over.

The condensate sample may not be representative. Condensate draining from the condenser after the boiling stops may have a composition deviating from the average composition of the condensate. The equilibrium measurements reported in the next section indicates no systematic error. Hence, any serious error of this type does not seem reasonable.

Flashing of the low boiling condensate could occur as the condensate returns to the boiler. Substantial subcooling of the condensate and returning it under the liquid surface is believed to make errors of this type negligible.

Vaporization under a liquid head seems not to occur; visible bubble formation disappears immediately when the agitation is started.

Contamination with stop-cock grease is unlikely to occur, as no liquid comes in direct contact with the grease used on the conical joints of the sample flasks. Teflon gaskets were used for the vacuum and gauge connections.

Test runs were carried out to check the liquid filling necessary for correct operation. Only 8 cm^3 of liquid in the boiler gave an appreciable error, probably due to the fact that the bulk of the boiler liquid did not wash over the upper parts of the boiler walls. Boiler fillings from 32 to 55 cm^3, however, gave consistent results. In addition there is a condensate hold-up of 2–3 cm^3.

Vapour–Liquid Equilibria Measurements

The new still was used to determine the vapour-liquid equilibria for mixtures of di-*n*-butyphthalate and di-*n*-butylsebacate at a pressure of 1 mm Hg. This mixture is satisfactory for the calibration of low-pressure distillation columns with less than 6 theoretical stages. The chemicals are easily available, and the mixtures can be analysed by measuring the refractive index.

Also, it is reasonable to believe that this mixture should show an almost ideal behaviour. Previous vapour pressure measurements [2] gave a relative volatility α as given by the equation :

$$\log \alpha = -0{\cdot}0200 - \frac{26{\cdot}6}{T} + \frac{84800}{T^2} \qquad (1)$$

At 1 mm Hg, the boiling point of the two compounds in question is 148·8 and 164·1°C respectively, and therefore α calculated from equation (1) varies between 2·31 and 2·59.

The materials used were the same as for the vapour pressure measurements [2]. The results of the equilibrium measurements are reported in Table 1 and plotted in Fig. 4. The mole

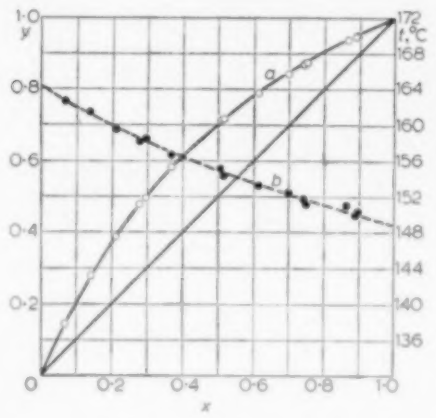

Fig. 4. The vapour–liquid equilibrium diagram for a mixture of di-*n*-butylphthalate and di-*n*-butylsebacate at 1 mm Hg. Here curve *a* gives the mole fraction y of the phthalate in the vapour as a function of the mole fraction x in the liquid as calculated for an ideal mixture. The open circles represent the experimental data. Curve *b* gives the temperature as calculated for an ideal mixture, the black dots representing the thermocouple readings.

Table 1. *Vapour–liquid equilibria for di-n-butylphthalate di-n-butylsebacate mixtures at 1mm Hg.*

1	2	3	4	5	6	7
Run No.	*Pressure* (mm Hg)	*Mole fraction of di n-butylphalate*			*Vapour temperature* (°C)	
		in liquid x	*in vapour*		t_{exp}	t_{ideal}
			y_{exp}	y_{ideal}		
52	1·000	0·065	0·143	0·139	162·6	162·7
44	1·005	0·136	0·281	0·269	161·5	161·2
45	1·000	0·138	0·279	0·272	161·4	161·2
51	1·000	0·211	0·388	0·386	159·4	159·7
50	0·995	0·276	0·477	0·474	158·1	158·6
43	1·007	0·293	0·496	0·495	158·4	158·3
49	0·998	0·366	0·582	0·579	156·6	157·1
42	1·005	0·505	0·712	0·710	155·1	154·9
53	1·000	0·514	0·716	0·718	154·3	154·8
48	0·998	0·611	0·788	0·792	153·2	153·4
46	1·000	0·698	0·842	0·850	152·4	152·3
54	1·000	0·740	0·867	0·874	151·8	151·8
57	1·000	0·750	0·874	0·880	151·1	151·7
47	1·001	0·864	0·938	0·940	151·0	150·3
56	1·000	0·888	0·947	0·951	150·0	150·0
55	1·000	0·894	0·950	0·954	150·4	150·0

fraction of phthalate in the vapour, y_{exp}, was calculated using the equation :

$$y_{exp} - x = (y - x)/0{\cdot}98 \qquad (2)$$

where y is the mole fraction actually measured in the condensate, and the factor 0·98 corrects for the deviation from equilibrium.

The mole fraction y_{ideal} in Table 1 is calculated from the relative volatility given by equation (1) assuming ideal behaviour. The temperature t_{ideal} in Table 1 is the boiling point calculated for an ideal mixture under a total pressure of 1 mm Hg.

Experimental vapour compositions and experimental boiling points are plotted in Fig. 4 as a function of the mole fraction of di-*n*-butylphthalate in the boiler liquid, x. The curves *a* and *b* in Fig. 4 correspond to values calculated for ideal mixture behaviour. The experimental points correspond to the curves for ideal behaviour within the experimental error. Hence, vapour–liquid equilibria data for the mixture in question can readily be obtained from equation (1) combined with the previously published [2] vapour-pressure data.

The equilibrium curve of Fig. 4 is a good indication that the described equilibrium still is well suited for vapour–liquid equilibria measurements in the low-pressure range.

Acknowledgment—The authors are indebted to the Royal Norwegian Council for Scientific and Industrial Research for a grant which has made this work possible.

Notation

α = relative volatility of di-*n*-butylphthalate and di-*n*-butylsebacate
n = number of rev/min for the disk *Z* shown in Fig. 2
x = mole fraction of di-*n*-butylphthalate in the boiler liquid
y = mole fraction of di-*n*-butylphthalate found in the condensate
y_{exp} = mole fraction of phthalate in the vapour calculated from equation (2)
y_{ideal} = mole fraction of phthalate in the vapour as calculated for an ideal mixture
t_{exp} = measured temperature of the saturated vapour, °C
t_{ideal} = temperature as calculated for an ideal mixture, °C
T = absolute temperature, °K
W = rate of distillation, kg/hr

References

[1] Fowler R. T. *Industr. Engng. Chem.* (*Industr.*) 1948 **24** 717, 824.
[2] Hammer E. and Lydersen A. L. *Chem. Engng. Sci.* 1957 **7** 66.
[3] Harper B. G. and Moore J. C. *Industr. Engng. Chem.* (*Industr.*) 1957 **49** 411.
[4] Jost W., Röck H., Schröder W., Sieg L. and Wagner H. Gg. *Z. phys. Chem.* 1957 **10** 133.
[5] Kümmerle K. *Chem.-Ing.-Techn.* 1956 **28** 400.
[6] Langdon W. M. and Keyes D. B. *Industr. Engng. Chem.* (*Industr.*) 1942 **34** 938.
[7] Othmer D. F. *Industr. Engng. Chem.* (*Anal.*) 1932 **4** 232.
[8] Perry E. S. and Fuguitt R. E. *Industr. Engng. Chem.* 1947 **39** 782.
[9] Ridgway K. *Industr. Chem.* 1956 **32** 59.
[10] Sanders W. W. Ph.D.Thesis, Penn. State Univ., August 1954; referred to by Acciarri J. A., Ph.D.Thesis, Penn. State Univ., June 1957.
[11] Williams F. E. *Industr. Engng. Chem.* 1947 **39** 779.

VOL. 7 1957/58

Chemical Engineering Science, 1958, Vol. 7, pp. 246 to 260. Pergamon Press Ltd.

Vapour–liquid equilibria in the ternary system ethyl acetate–benzene–*cyclo*hexane

K. C. Chao and O. A. Hougen

Chemical Engineering Department, University of Wisconsin

(*Received* 1 *August* 1957)

Abstract—The vapour–liquid equilibrium compositions and temperatures covering the entire composition range were determined experimentally under isobaric conditions of 760 mm Hg pressure for the ternary system ethyl acetate – benzene – *cyclo*hexane and its three constituent binaries.

A continuous recirculating equilibrium still combining the best features of Jones and Gillespie stills was used.

Values of activity coefficients and their ratios were correlated by Redlich–Kister equations. A modification of these equations was introduced to satisfy the Gibbs–Duhem equation at constant pressure.

Résumé—Les auteurs ont étudié expérimentalement, sous 760 mm Hg, les courbes de rosée et d'ébullition du système ternaire acétate d'éthyle–benzène–cyclohexane et des trois mélanges binaires.

Ils ont utilisé un ébulliomètre dynamique présentant les principales caractéristiques des ébulliomètres de Jones et Gillespie.

Ils ont déterminé les valeurs des coefficients d'activité et leurs rapports par les équations de Redlich–Kister.

Ils ont introduit une modification de ces équations pour satisfaire à la relation de Gibbs–Duhem.

Zusammenfassung—Zusammensetzungen und Temperaturen des Dampf-flüssig-Gleichgewichts über den ganzen Bereich der Zusammensetzungen wurden experimentell unter isobaren Bedingungen bei 760 Torr für das ternäre System Äthylazetat–Benzol–Cyclohexan und die drei darin enthaltenen Zweistoffsysteme bestimmt.

Verwendet wurde eine kontinuierliche Umlauf-Gleichgewichtsapparatur unter Ausnutzung der besten Vorschläge von Jones und Gillespie.

Werte der Aktivitätskoeffizienten und ihrer Quotienten wurden durch Gleichungen nach Redlich und Kister wiedergegeben. Diese Gleichungen waren abgeändert, um die Gibbs–Duhem–Gleichung bei konstantem Druck zu befriedigen.

Objectives

Most of the published data on vapour–liquid equilibria pertain to binary systems. Data covering the entire composition range on relatively few systems have been published. From an industrial standpoint experimental data on ternary systems are essential because of their frequent incidence in chemical processing and their growing importance in azeotropic distillation and solvent extraction. From a theoretical standpoint such investigations are also important in establishing useful relations between the behaviours of multicomponent systems and those of lower-order constituent systems.

This investigation has the following objectives: To determine the vapour–liquid composition–temperature relations at 760 mm Hg pressure of the ternary system ethyl acetate–benzene–*cyclo*hexane and its three binaries; to correlate the experimental data of activity coefficients of the ternary system and its three binaries in terms of composition; and to compare the correlation constants in equations for isobaric vaporization in conventional and corrected forms.

The particular ternary system ethyl acetate–benzene–*cyclo*hexane was selected because of its possible industrial importance in the separation of the benzene–*cyclo*hexane azeotrope by distillation with ethyl acetate. The mixture of benzene and *cyclo*hexane is an industrial product resulting from the catalytic hydrogenation of benzene to form *cyclo*hexane.

The addition of ethyl acetate to the binary system benzene–*cyclo*hexane in fractional distillation results in the separation of benzene from the binary azeotrope of *cyclo*hexane–ethyl acetate. The separation of ethyl acetate from this latter azeotrope may then be made by solvent extraction with water.

Previous Literature

The three binary systems reported in this research have been investigated by Tao [19] at pressures of 1, 10, 20 and 30 atm. The benzene–*cyclo*hexane system has been investigated by Scatchard, Wood and Mochel [16] at 39·99° and 69·98°C and by Richards and Hargreaves [14] at 739 mm Hg. Furfuraldehyde and methyl cellosolve in ternary systems with benzene–*cyclo*hexane have been studied by Thornton and Garner [20], [21]. The ternary system selected for this investigation has not been previously reported in the literature.

Equilibrium Still

The continuous equilibrium still used in this investigation (Figs. 1 and 2) is essentially a combination of the Jones [9] and Gillespie [5] types.

With reference to Fig. 1, contact between vapour and liquid is secured in the mixing chamber *A* from which vapour with entrained liquid rises to impinge on the thermowell W_2 located in the separator *D*. The liquid falls to the trap *E*, of 23 ml capacity. Liquid overflows from this trap to the mixing chamber thus completing the circuit for the liquid. Vapour escaping from the separator is totally condensed in condenser *F* and collected in the condensate trap *G* from which the condensate flows at a closely controlled rate into the vaporizer *K*. Upon complete vaporization the vapour bubbles

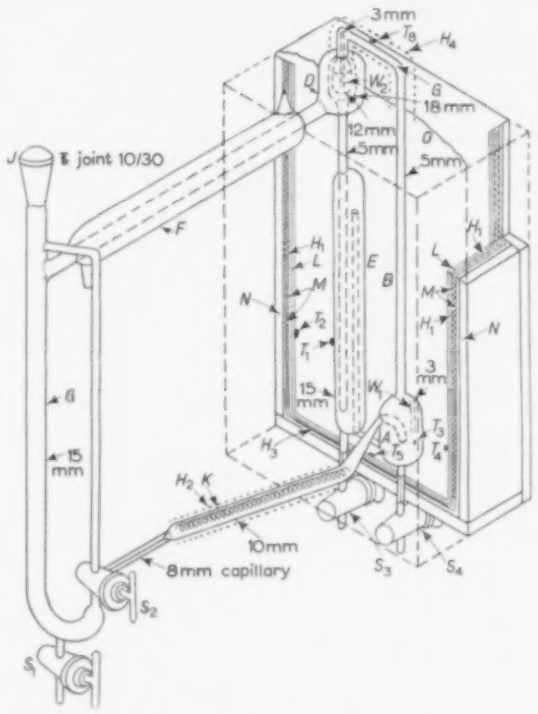

Fig. 1. Equilibrium still.

through the liquid in the mixing chamber *A*, completing its circuit.

To obtain significant data it is essential to circulate the liquid under adiabatic conditions. For this purpose an insulating jacket encloses the liquid trap and the mixing chamber. The innermost part of the jacket consists of a sheet-metal box *L* with dimensions $2\frac{1}{4}$ x $4\frac{3}{4}$ x 10 in. Two layers of asbestos fabric *M* are wrapped around this box with a chromel ribbon heater H_1 placed in between the layers. An outer box made of plywood $\frac{3}{8}$ in. thick encloses the assembly ($3\frac{1}{2}$ x 6 x $10\frac{1}{2}$ in.). The space inside the sheet metal box is filled with Santocel insulation.

The vapour–liquid tube *C* that extends above the jacket is wrapped with glass wool and wound with a heating wire H_4 to permit adiabatic performance.

Auxiliary iron–constantan thermocouples for purposes of adiabatic control are attached to the

wall of the mixing chamber, of the residue liquid trap and to the different sides of the sheet-metal box.

The equipment is heated electrically with four chromel ribbon and wire heaters controlled by three Variacs. Heater 1 consists of chromel-*A* ribbon ($\frac{1}{16}$ x 0·04 in., resistance 2·44 Ω/ft, the total resistance being 160 Ω) wound uniformly on all four sides of the adiabatic jacket which encloses the entire liquid recirculating system. Heater 2 consisting of chromel-*A* wire (size 30; 6·71 Ω/ft, the total resistance being 68 Ω) supplies heat to the vaporizer. Heater 3 supplies heat to the bottom of the adiabatic jacket. This heater consists of chromel–*A* wire having a total resistance of 20 Ω as in heater 2; the wire is enclosed between two layers of asbestos fabric as in heater 1. Heater 4 maintains adiabatic conditions in the vapour–liquid tube *C* which extends above the box enclosure.

To promote even heating a sheet of aluminium foil surrounds the vaporizer; the foil is separated from the heating coil by a layer of glass wool. A closely wound coil of 22 gauge copper wire fits tightly against the inner wall of the vaporizer to act as a liquid distributor. This coil induces a liquid film to form and wet the entire inner surface of the tube.

To maintain the still at constant pressure, a regulating device is attached to the top opening of the condensate trap of the equilibrium still through an auxiliary condenser. This control is effected by bleeding compressed air through a nozzle immersed in water, the depth of immersion being adjusted to compensate for variations in the atmospheric pressure. With this device the pressure in the still may be kept constant within an accuracy of 1·5 mm of water.

The equilibrium temperature was measured by a calibrated copper constantan thermocouple T_B located in thermowell W_2 in the separator; the thermowell being filled with liquid silicone for improved thermal contact. The accuracy of readings was within 0·1°C. Readings of thermocouple T_A located in the mixing chamber *A* were made for comparison with those of couple T_B.

All auxiliary thermocouples were iron constantan recording to an accuracy of 1°F.

Operation of the Equilibrium Still

In starting operation the adiabatic jacket and the tube to the separator are heated to the anticipated temperature, about 2 hr being required for preheating. Cooling water is admitted to the total condenser, and heat applied to the vaporizer. A voltage of 35 to 40 V is applied to heater 2 for about 5 min before admitting feed to the still. The auxiliary condenser is removed from the still and the stopcock leading to the vaporizer is slightly opened. Then a charge of known composition is fed to the condensate trap through a connection leading to the auxiliary condenser. A mixture of liquid and vapour passes into the mixing chamber; about 68 ml of total liquid charge is required. The liquid should be supplied gradually so that boiling may be continuous in the vaporizer; this insures saturation of the liquid in the liquid trap as soon as the charging operation is completed. Feeding usually takes about 15 min, after which the stopcock S_2 leading to the vaporizer *K* is partly closed to its normal operating position. The auxiliary condenser is restored and the cooling water circulated. A constant pressure of 760 mm Hg is applied to the still.

During operation adiabatic conditions are maintained by adjusting the adiabatic heaters H_1, H_3, H_4 so as to equalize the temperature readings of thermocouples T_1 and T_3 and those on the adiabatic jacket. Thermocouples T_1 and T_3 show no disagreement after a short period of operaton. Temperatures on the different parts of the adiabatic jacket may vary by 2°F, a range which is adjusted to include the temperatures of thermocouples T_1 and T_3; thus the temperature difference across the Santocel insulation is in every case less than 2°F.

Heat to the vaporizer is controlled so as to cause the last trace of condensate to disappear just at the end of the vaporizer, a condition which can be observed visually. The sensitivity of this observation is enhanced by the V-shape of the vaporizer permitting traces of liquid to be easily seen in the bottom of the V.

Equilibrium conditions were usually reached within 1 hr of operation. It was customary to

VOL.
7
957/58

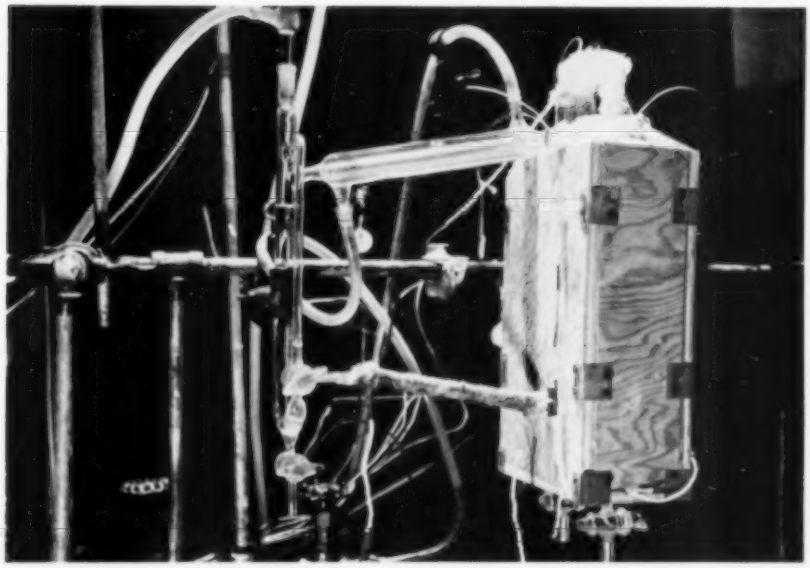

FIG. 2. Photograph of equilibrium still.

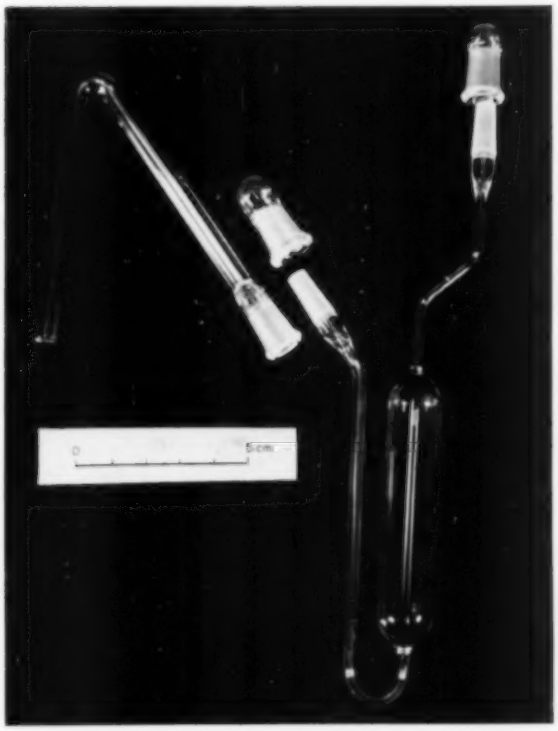

FIG. 3. Precision pycnometer.

VO
7
1957

operate 90 min before taking equilibrium readings.

At the end of each run, the stopcock S_2 leading to the vaporizer is closed and the vaporizer heater turned off. The stopcocks below the condensate trap and the liquid trap are opened to sampling bottles after purging the line with 8 ml of the liquid. When samples have been withdrawn the entire content of the still is emptied in preparation for the next run.

No difficulty was encountered in securing leak-proof operation of the two stopcocks S_1 and S_2 of the condensate trap; these stopcocks were not greased. However, difficulty was experienced with the two stopcocks S_3 and S_4 below the mixing chamber and the liquid trap. It was found necessary to use high vacuum grade cocks to obtain good service; these required lubrication. A thin layer of silicone lubricant was applied, but it was necessary to assure that no contamination resulted from this source. To verify the absence of contamination the three pure liquids used in this study were tested separately. The first 5 ml of liquid withdrawn from the sampling port were collected, but only in the case of benzene was the first 5 ml sample found different from the liquid in the trap. Further samples showed exactly the same refractive index as the original feed. Contamination of the first 5 ml in the case of benzene corresponds to a change of 0·0001 in refractive index. The capillary tube connection to the greased stopcocks prevented contamination by diffusion. To insure no contamination 8 ml of liquid were purged from the line before liquid samples were taken for analysis.

VOL. 7 957/58

Establishment of Equilibrium

An inherent advantage of the vapour recirculation still is that the two phases retain their separate compositions and flow rates, with no net vaporization or condensation. Thus a steady state attained under conditions of recirculation is an unmistakable sign of equilibrium. The following five conditions of operation were essential to assure the establishment of equilibrium conditions.

(1) One manifestation of steady state is the constancy of the boiling point of the liquid as measured by thermocouple T_B. Variation in this reading usually disappears after about 30 min operation.

(2) Constancy of composition of the vapour and liquid streams throughout is another indication of steady state and equilibrium. Since the amount of material circulating in the still must be maintained within close limits it is not possible to withdraw samples sufficiently large for analysis and to continue operating at the same time. The volume of liquid in the still is critical for proper operation of the vapour lift, and the amount of condensate is critical in furnishing the proper hydrostatic head to force the liquid into the vaporizer. A series of runs were made on about the same mixture of benzene and ethyl acetate in order to determine variation in composition of liquid in the still with residence time.

Mixtures of benzene and ethyl acetate containing about 30 mole per cent of ethyl acetate were charged to the still. Successive runs of different time intervals were made and the results are given in Table 1.

Table 1.

Length of operation (min)	x_A	$y_A - x_A$	*Run number*
30	0·308	0·025	*AB*-19
40	0·303	0·028	*AB*-17
60	0·274	0·029	*AB*-16
90	0·288	0·029	*AB*-18

Even though there is no trend in x_A values, the trend in $y_A - x_A$ is evident. Steady state conditions were obtained in from 40 to 60 min. It was concluded that 90 min of operation gave an ample margin of safety.

(3) That equilibrium was attained at the end of the runs was further confirmed by withdrawing samples from the mixing chamber. In all acceptable runs the samples showed the same composition as those taken from the liquid trap. Identity of composition in the liquid trap and in the mixing chamber indicates that equilibrium was established.

(4) In all instances constancy of the liquid level in the condensate trap gives an unmistakable

sign of thermal balance of the liquid recirculation system. This is one of the prerequisites to equilibrium and must be carefully watched throughout operation. In all acceptable runs change in the amount of condensate in the trap was scarcely noticeable, and never exceeded 0·2 ml. Even under the most unfavourable conditions where this change would take place instantly the maximum error that could be made with the most sensitive of the three systems would be 0·1 per cent.

(5). The vapour lift action in this still necessarily induces a temperature change due to variation in hydrostatic pressure with elevation. This pressure reduction is accompanied by vaporization of a portion of the liquid, and this would continuously increase the inventory in the condensate trap and deplete the inventory in the liquid trap. The change in saturation temperature due to hydrostatic head in the still is slight. Thus temperature measurements at the bottom and top of the vapour lift, using thermocouples T_A and T_B, showed a difference of 0·1 to 0·2°C between the two locations under steady conditions. That this hydrostatic effect is not appreciable, but comparable to that of imperfect adiabatic conditions around the liquid recirculation system, is conclusively shown by the constancy of the amount of material in the two separate streams.

The equilibrium pressure was maintained at a standard atmospheric pressure for all runs. Any discrepancy between the prevailing atmospheric pressure and the standard pressure was compensated for by applying compressed air to the system. That the pressure applied to the system though the auxiliary condenser actually represents the equilibrium pressure of the mixture depends on the negligible pressure difference for the vapour flow in the separator and in the condenser. This pressure drop was calculated not to exceed 0·0081 cm of water.

Analytical Procedure

Analyses of the three binary systems are readily carried out by measurements of refractive index and specific gravity. Measurements of these physical properties against mixtures of known composition were made.

For measuring refractive indices a Baush and Lomb Abbé refractometer was used. All measurements were performed at 25 ± 0·1°C, the precision of refractive index readings being ± 0·0001.

For specific gravity measurements a modified Sprengel type pycnometer was used (Fig. 3). This weighed 17 g and held 10 ml of liquid in a single bulb with capillary connection tubing of 0·7 mm bore. The reproducibility of the specific gravity measurement was ± 0·0001 at 25°C. The compositions of binary systems determined by these two measurements did not differ by more than 0·1 mole per cent.

The physical properties of the standard binary mixtures are shown in Tables 1, 2, and 3, and in Figs. 4 and 5.

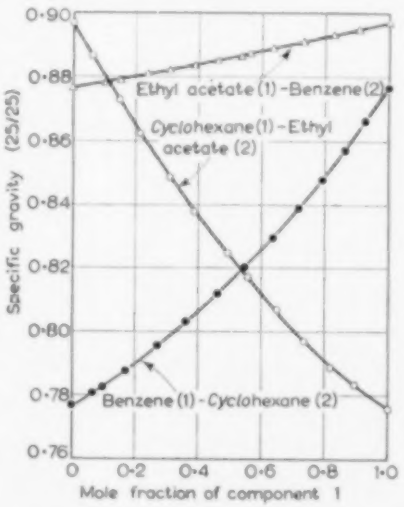

Fig. 4. Specific gravities of binary mixtures.

For calibration purposes specific gravities and refractive indices of ternary mixtures of known composition were measured over the entire composition range at intervals of 10 mole per cent for a total of 66 mixtures; the calibration data are shown in Table 4. By linear interpolation isometric lines were constructed representing loci of constant values for each physical property. (Fig. 6). The isometric lines all merge into terminals on the edge of the triangular diagram coincident with data for the binary mixtures. Linear interpolation between the contour lines

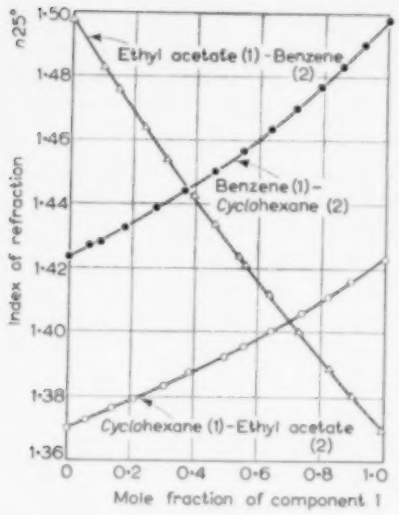

FIG. 5. Refractive indices of binary mixtures.

VOL. 7
957/58

gives the composition of an unknown sample once its refractive index and specific gravity were determined.

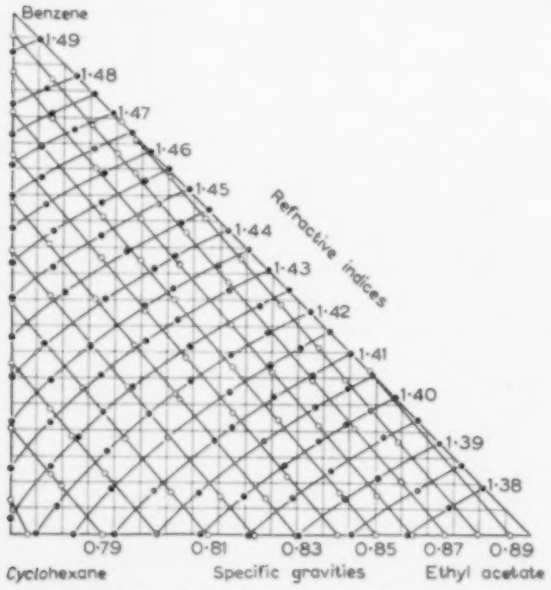

FIG. 6. Refractive indices and specific gravities of the ternary mixtures.

The precision of determining composition is ± 0·1 mole per cent for the binary mixtures and ± 0·2 mole per cent for the ternary mixture.

PREPARATION OF MATERIALS

The ethyl acetate of 99·9 per cent purity was obtained from Merck and Co., Inc. The chief impurity, water, was removed by storage over silica gel.

Benzene, of 99·9 per cent purity, was also obtained from Merck and Co. Further purification was obtained by fractional crystallization repeated three times.

*Cyclo*hexane of Research Grade (Lot Number 435), of guaranteed purity 99·94 per cent was obtained from the Phillips Petroleum Co., and used directly.

The physical properties of the purified reagents as measured are tabulated in Table 2 for comparison with literature values.

Table 2.

	Ethyl acetate	*Benzene*	Cyclo-*hexane*
Refractive index at 25°C			
Experimental	1·3698	1·4980	1·4235
Literature	1·37005 [7]	1·49790 [2]	1·42354 [3]
Specific gravity (25°/25°)			
Experimental	0·8970	0·8762	0·7759
Density (25°)			
Experimental	0·8944	0·8736	0·7736
Literature	0·89446 [8]	0·87362 [10]	0·7739 [4]
Boiling point °C			
Experimental	77·2	80·1	80·7
Literature	77·1 [17]	80·1 [17]	80·7 [17]

AZEOTROPES

Because of the very close compositions of liquid and vapour in the equilibrium mixtures of ethyl acetate and benzene at high concentrations of ethyl acetate there is some uncertainty about the existence of azeotropism for this system. RYLAND [15] in 1899 reported the absence of azeotropism. LECAT [11] in 1918 reported an azeotropic composition of 93 mole per cent of ethyl acetate, but the reliability of this finding was questioned by the same author. SWIETOSLAWSKI [18] in 1932 confirmed RYLAND'S finding. TAO [19] in 1952 reported an azeotropic composition of 91 mole

per cent of ethyl acetate. To resolve the uncertainty, both Tao's data and the data of this study were plotted in terms of γ_A/γ_B against x_A. On the same figure was plotted the ratio P_B/P_A against x_A, the experimental temperature being used for calculating the vapour pressure ratio. Azeotropism would be indicated by intersection of the two lines. The two sets of data agree up to $x_A = 0.92$. The temperature measurements also agree to within 0·1°C in both investigations. Judging by the trend of the data it is unlikely that an azeotrope exists. The one-constant equation giving a maximum deviation of 0·1 mole per cent for all the experimental measurements supports this observation in not giving any azeotropic composition.

For the binary system *benzene* – cyclo*hexane* the reported values of azeotropic composition and temperature at 1 atm pressure are shown in Table 3.

Table 3

	Benzene (mole per cent)	*Temperature* °C
Lecat [11]	55	77·5
Richards and Hargreaves [14]	51·6	77·4
Marschner and Cropper [12]	53·7	77·7
Thornton and Garner [20]	53·0	77·6
Tao [19]	50·0	77·4
This investigation	53·7	77·6

For the binary system cyclo*hexane* – *ethyl acetate* the reported values of the azeotropic composition and temperature at 1 atm pressure are given in Table 4.

Table 4.

	Acetate (mole per cent)	*Temperature* °C
Lecat [11]	33	72·8
Tao [19]	53·3	72·0
This investigation	54·9	71·6

No azeotrope was found for the ternary system. All the ternary mixtures experimentally studied boil at a higher temperature than the azeotropic mixture of *cyclo*hexane and ethyl acetate. This binary mixture is indeed the lowest boiling of all the solutions prepared with the three given components. Fig. 11 shows that there is a definite trend for all the equilibrium tie lines on the ternary diagram to converge toward the composition of this binary azeotrope. Data point *ABC*-79 was determined specifically for the purpose of ascertaining if any ternary azeotrope in the neighbourhood of this binary azeotrope might form, but the finding was negative. The liquid phase of this ternary mixture contains only 2·9 mole per cent of benzene, but the boiling point is thereby slightly increased, and the equilibrium vapour contains even less benzene.

Theoretical Considerations

Equilibrium between the vapour and liquid of a multi-component system is attained when the pressure and temperature is the same throughout the system and when the fugacity of each component in the two phases is the same, that is $f_{iv} = f_{iL}$. Under these conditions the relation of vapour composition to liquid composition for ideal solution behaviour is expressed as :—

$$y_i f_{iv}^{\circ} = x_i f_{iL}^{\circ} \qquad (1)$$

where at the temperature and pressure of the system,

f_{iv}° and f_{iL}° = fugacities of pure component i in the respective vapour and liquid phases.

Any lack of ideal solution behaviour in each phase is allowed for by arbitrary terms designated as activity coefficients, γ_{iv} and γ_{iL}, thus :—

$$\gamma_{iv}\, y_i f_{iv}^{\circ} = \gamma_{iL}\, x_i f_{iL}^{\circ} \qquad (2)$$

Here the standard state fugacities f_{iv}°, f_{iL}° are related to pressure by fugacity coefficients $\nu_{i\pi}$ and ν_{ip}, thus :—

$$f_{iv}^{\circ} = \nu_{i\pi}\pi \text{ and } f_{ip}^{\circ} = \nu_{ip} P_i \qquad (3)$$

π = total pressure

P_i = vapour pressure of pure liquid component i at the temperature of the system

At atmospheric pressure and below, the activity coefficient in the vapour phase γ_{iv} is unity and the ratio of fugacity coefficients ν_{iv}/ν_{ip} is nearly unity, hence

$$y_i \pi = \gamma_{ip} x_i P_i \qquad (4)$$

From measurements of y_i, x_i, P_i, and π the activity coefficient γ_i is evaluated.

In a binary system at constant pressure and temperature the variation of activity coefficients with composition is related by the Gibbs-Duhem equation :—

$$[(\partial \ln \gamma_1)/(\partial \ln x_1) = (\partial \ln \gamma_2)/(\partial \ln x_2)]_{pT} \qquad (5)$$

The excess free energy μ_i^E of any component i in solution is related to its activity coefficient, thus

$$\mu_i^E = RT \ln \gamma_i \qquad (6)$$

For a binary system :—

$$G^E = x_1 \mu_1^E + x_2 \mu_2^E = RT (x_1 \ln \gamma_1 + x_2 \ln \gamma_2) \qquad (7)$$

For conditions of constant temperature and pressure Redlich and Kister [13] have related excess free energy to composition by a series function using terms sufficient to fit the experimental data, thus :—

$$\{G^E = RT x_1 x_2 [B' + C' (x_1 - x_2) + D' (x_1 - x_2)^2 + \ldots]\}_{pT} \qquad (8)$$

The terms $x_1 x_2$ provide for the zero value of G^E at compositions corresponding to the separate pure components. Formulations for individual activity coefficients are obtained from equation (8) through the definition of a partial property, thus :—

$$\mu_i^E = [(\partial/\partial n_1)(n_1 + n_2) G^E]_{pT} = RT \ln \gamma_1 \qquad (9)$$

to give :—

$$\left.\begin{aligned} \ln \gamma_1 &= x_1 x_2 [B' + C' (x_1 - x_2) + D' (x_1 - x_2)^2 + \ldots] \\ &\quad + x_2 [B' (x_2 - x_1) + C' (6 x_1 x_2 - 1) + D' (x_1 - x_2)(8 x_1 x_2 - 1) + \ldots] \\ \ln \gamma_2 &= x_1 x_2 [B' + C' (x_1 - x_2) + D' (x_1 - x_2)^2 + \ldots] \\ &\quad - x_1 [B' (x_2 - x_1) + C' (6 x_1 x_2 - 1) + D' (x_1 - x_2)(8 x_1 x_2 - 1) + \ldots] \end{aligned}\right\} \qquad (10)$$

Subtracting the two parts of equation (10) gives :—

$$\ln (\gamma_1/\gamma_2) = B' (x_2 - x_1) + C' (6 x_1 x_2 - 1) + D' (x_2 - x_1)(1 - 8 x_1 x_2) + \ldots \qquad (11)$$

The same relationship for $\ln (\gamma_1/\gamma_2)$ may be obtained by differentiation of equation 8 with respect to x_1 :—

$$[(\partial/\partial x_1)(G^E/RT) = \ln \gamma_1 - \ln \gamma_2 = \ln (\gamma_1/\gamma_2)]_{pT} \qquad (12)$$

Thus experimental data on activity coefficients can be correlated by using a single equation in terms of the ratio of activity coefficients without requiring separate expressions for the individual coefficients.

Isobaric Conditions

For vapour–liquid equilibrium in a binary system at constant pressure, temperature is fixed by composition and is not an independent variable. Hence the functional form of equation (8) may also be used to express excess free energy under isobaric conditions using slightly different numerical constants. The constants in the equation are then dependent on pressure only. Thus, at constant pressure

$$\{G^E = RT x_1 x_2 [B + C (x_1 - x_2) + D (x_1 - x_2) + \ldots]\}_p \qquad (13)$$

In its conventional form the Gibbs–Duhem equation is given at conditions of constant temperature and pressure. Ibl and Dodge [6] have extended the Gibbs–Duhem equation to conditions of constant pressure and variable temperature. Since $\ln \gamma$ is at constant pressure, a continuous and single-valued function of temperature and composition, for a binary system in the liquid phase, the following exact differential equations may be written :—

$$[d \ln \gamma_1 = (\partial \ln \gamma_1/\partial T)_{px_1} dT + (\partial \ln \gamma_1/\partial \ln x_1)_{pT} d \ln x_1]_p \qquad (14)$$

and similarly for component 2.

The variations of activity coefficients with temperatures at constant pressure and composition are given as follows :—

$$(\partial \ln \gamma_1 / \partial T)_{px_1} = (H_1^* - \overline{H}_1)/RT^2 \quad (15)$$

and similarly for component 2. Combining equations (5), (14), and (15) gives :—

$$[(d \ln \gamma_1)/(d \ln x_1) = (d \ln \gamma_2)/(d \ln x_2) + Z]_p \quad (16)$$

where

$$Z = -(\Delta H/RT^2)(dT/dx_1)_p$$

$$\Delta H = H - x_1 H_1^* - x_2 H_2^*$$

H, H_1^*, H_2^* = the molal enthalpies of mixtures and components, respectively, each in the liquid phase.

The term ΔH is the integral heat of solution in dissolving liquid components in their standard states to form a liquid solution of given composition at constant pressure and corresponding temperature.

From equation (16)

$$[x_1 \, d \ln \gamma_1 + x_2 \, d \ln \gamma_2 = Z \, dx_1]_p \quad (17)$$

From equations (7) and (16) :—

$$\left.\begin{aligned}[(d/dx_1)(G^E/RT) = \\ \ln \gamma_1 - \ln \gamma_2 + (d \ln \gamma_1)/(d \ln x_1) \\ - (d \ln \gamma_2)/(d \ln x_2) \\ = \ln \gamma_1 - \ln \gamma_2 + Z]_p\end{aligned}\right\} \quad (18)$$

The values of Z are difficult to determine experimentally since they involve measurements of the variation of temperature with compositions at constant pressure and the heats of solution which involve hypothetical standard states. These measurements are circumvented by including the effect of Z in the empirical equation for the ratio of activity coefficients, thus retaining the same form as for isothermal conditions but with constants having slightly different numerical values depending upon the magnitude of Z, thus :

$$\ln \gamma_1/\gamma_2 = b(x_2 - x_1) + c(6x_1 x_2 - 1) + d(x_2 - x_1)(1 - 8x_1 x_2) + \ldots \quad (19)$$

Using identical forms for isothermal and isobaric conditions is not mandatory. This proved satisfactory for the three binary systems under investigation, but it might require additional terms for systems where Z is large. With this particular form, the integral $\int_0^1 \ln(\gamma_1/\gamma_2)\, dx_1$ is zero for both isothermal and isobaric conditions. For isobaric conditions, the integral is not necessarily zero, and might be accounted for by additional terms dissimilar to those in the isothermal equation.

Subtracting equation (18) from (7) :—

$$\ln \gamma_2 = (G^E/RT) - x_1 [(d/dx_1)(G^E/RT) - Z] \quad (20)$$

Combining equations (13), (19) and (20) :—

$$\left.\begin{aligned}\ln \gamma_2 = x_1 x_2 [B + C(x_1 - x_2) \\ + D(x_1 - x_2)^2 + \ldots] \\ - x_1 [b(x_2 - x_1) + c(6x_1 x_2 - 1) \\ + d(x_1 - x_2)(8x_1 x_2 - 1) + \ldots]\end{aligned}\right\} \quad (21)$$

Similarly,

$$\begin{aligned}\ln \gamma_1 = x_1 x_2 [B + C(x_1 - x_2) \\ + D(x_1 - x_2)^2 + \ldots] \\ + x_2 [b(x_2 - x_1) + c(6x_1 x_2 - 1) \\ + d(x_1 - x_2)(8x_1 x_2 - 1) + \ldots]\end{aligned}$$

In calculating vapour compositions, temperature sensitivity is minimized by using ratios of activity coefficients and vapour pressures by combining equation (4) for the two components, thus :—

$$\left.\begin{aligned}y_1 = (\gamma_1 x_1 P_1)/E(\gamma_2 x_2 P_2) \\ y_2 = 1/E \\ E = (\gamma_1 x_1 P_1)/(\gamma_2 x_2 P_2) + 1\end{aligned}\right\} \quad (22)$$

For calculating temperatures under isobaric conditions it is necessary to have equations for the separate activity coefficients, and then by trial and iteration to establish the temperature which satisfies the relation $y_1 \pi = x_1 \gamma_1 P_1$ in agreement with the correct value of the vapour pressure of the pure component.

Ternary Systems under Isobaric Conditions

The excess free energy of a ternary mixture is related to the activity coefficient by the expression :—

$$G_{123}^E = x_1 \mu_1^E + x_2 \mu_2^E + x_3 \mu_3^E = RT(x_1 \ln \gamma_1 + x_2 \ln \gamma_2 + x_3 \ln \gamma_3) \quad (23)$$

Under conditions of constant pressure :—

$$\left.\begin{aligned} G^E_{123} &= G^E_{12} + G^E_{23} + G^E_{31} \\ &\quad + RT\,x_1\,x_2\,x_3\,[B + C_1(x_2 - x_3) \\ &\quad + c_2(x_3 - x_1) + c_3(x_1 - x_2) + \ldots] \end{aligned}\right\} \quad (24)$$

Here the first three terms on the right side represent contributions by the separate binaries and the last term represents ternary effects. The binary contributions are related by assigning appropriate constants to equation (13), thus for G^E_{12} :—

$$G^E_{12} = RT\,x_1\,x_2\,[B_{12} + C_{12}(x_1 - x_2) + D_{12}(x_1 - x_2)^2 + \ldots] \quad (25)$$

As the temperature is fixed by composition the constants in equations (24) and (25) are dependent on pressure only.

The modified Gibbs–Duhem equation for a ternary system under isobaric conditions is given by an expansion of equation (17) thus :—

$$x_1\,d\ln\gamma_1 + x_2\,d\ln\gamma_2 + x_3\,d\ln\gamma_3 = -(\Delta H/RT^2)\,dT \quad (26)$$

On differentiating equation (23) and combining with (26) the individual activity coefficients may be expressed in terms of G^E :—

$$\left.\begin{aligned} \ln\gamma_1 = {} & \frac{G^E}{RT} + \left[\frac{\partial}{\partial x_1}\left(\frac{G^E}{RT}\right)\right]_{x_2} + \frac{\Delta H}{RT^2}\left(\frac{\partial T}{\partial x_1}\right)_{x_2} \\ & - x_1\left\{\left[\frac{\partial}{\partial x_1}\left(\frac{G^E}{RT}\right)\right]_{x_2} + \frac{\Delta H}{RT^2}\left(\frac{\partial T}{\partial x_1}\right)_{x_2}\right\} \\ & - x_2\left\{\left[\frac{\partial}{\partial x_2}\left(\frac{G^E}{RT}\right)\right]_{x_1} + \frac{\Delta H}{RT^2}\left(\frac{\partial T}{\partial x_2}\right)_{x_1}\right\} \end{aligned}\right\} \quad (27)$$

and similarly for the other components. The ratio of the activity coefficients follows :—

$$\ln(\gamma_1/\gamma_2) = [(\partial/\partial x_1)(G^E/RT)]_{x_3} + (\Delta H/RT^2)(\partial T/\partial x_1)_{x_3} \quad (28)$$

and similarly for the other ratios.

Expressions of activity coefficients and their ratios explicitly in terms of compositions result upon substituting equation (24) into equations (27) and (28), respectively. The difficulties with the correction terms $(\Delta H/RT^2)(\partial T/\partial x)$ are circumvented by modifying the constants as done with the binary system, thus :—

$$\left.\begin{aligned} \ln\gamma_1 = {} & (G^E_{123}/RT) + [x_2(x_2 + x_3) - x_1x_2][b_{12} + c_{12}(x_1 - x_2) + \ldots] \\ & - 2x_2x_3[b_{23} + c_{23}(x_2 - x_3) + \ldots] \\ & + [(x_3 - x_1)(x_2 + x_3) + x_1x_2][b_{31} + c_{31}(x_3 - x_1) + \ldots] \\ & + [x_1x_2(x_2 + x_3) + x_1x_2^2](c_{12} + \ldots) \\ & + [x_2x_3(x_2 + x_3) - 2x_2^2x_3](c_{23} + \ldots) \\ & + [-2x_3x_1(x_2 + x_3) + x_1x_2'x_3](c_{31} + \ldots) \\ & + [(x_2 + x_3)(x_2x_3 - x_1x_2) - x_2(x_1x_3 - x_1x_2)][b + c_1(x_2 - x_3) + c_2(x_3 - x_1) + c_3(x_1 - x_2) + \ldots] \\ & + x_1x_2x_3[(x_2 + x_3)(c_1 - 2c_2 + c_3) - x_2(2c_1 - c_2 - c_3) + \ldots] \end{aligned}\right\} \quad (29)$$

where G^E_{123} is given by equation (24).

$$\left.\begin{aligned} \ln(\gamma_1/\gamma_2) = {} & -b_{12}(x_1 - x_2) + c_{12}[2x_1x_2 - (x_1 - x_2)^2] + \ldots \\ & + x_3\{b_{31} - b_{23} - c_{23}(2x_2 - x_3) + c_{31}(x_3 - 2x_1) + \ldots \\ & - b(x_1 - x_2) - c_1[x_1(2x_2 - x_3) + x_2(x_3 - x_2)] \\ & - c_2[x_1(2x_2 - x_1) + x_3(x_1 - x_2)] \\ & + c_3[2x_1x_2 - (x_1 - x_2)^2] + \ldots\} \end{aligned}\right\} \quad (30)$$

Similarly expressions for the other components are obtained by cyclic advancement of the subscripts in the order 1, 2, 3, 1.

In calculating vapour composition from these equations, temperature sensitivity is minimized by using ratios of activity coefficients and vapour pressures by combining equation (4) for the three components, thus :—

$$\left.\begin{aligned} y_1 &= 1/E \\ y_2 &= (\gamma_2x_2P_2/\gamma_1x_1P_1)\,E \\ y_3 &= (\gamma_3x_3P_3/\gamma_1x_1P_1)\,E \\ E &= 1 + \{(\gamma_2x_2P_2)/(\gamma_1x_1P_1)\} + \{(\gamma_3x_3P_3)/(\gamma_1x_1P_1)\} \end{aligned}\right\} \quad (31)$$

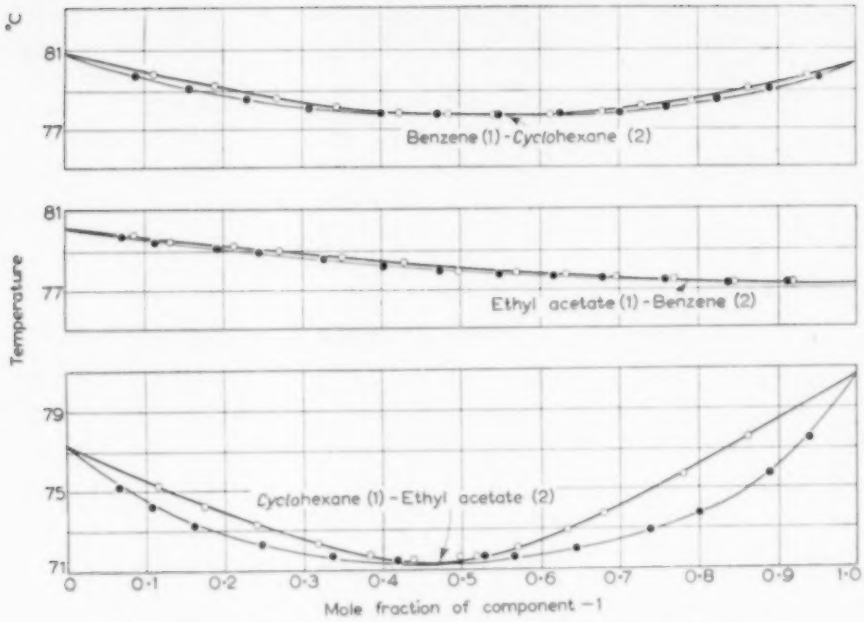

Fig. 7. Equilibrium temperatures and compositions in the binary systems.

Binary Data and Correlation

A total of 13 $x - y - t$ values were measured for each of the three binary systems at 760 mm Hg pressure and for nearly equal intervals of liquid composition. These are presented in Tables 5, 6, and 7 and Figs. 7, 8, 9 and 10. For each binary system the data were correlated with a series of Redlich-Kister equations of increasing complexity, namely, with 1, 2 and 3 constants. These constants were in each case evaluated by the method of least squares using all experimental data.

The following constants were evaluated for equations relating activity coefficient ratios, using logarithms to the base 10 :—

$$\log(\gamma_1/\gamma_2) = b(x_2 - x_1) + c(6x_1 x_2 - 1) + d(x_2 - x_1)(1 - 8x_1 x_2) \qquad (32)$$

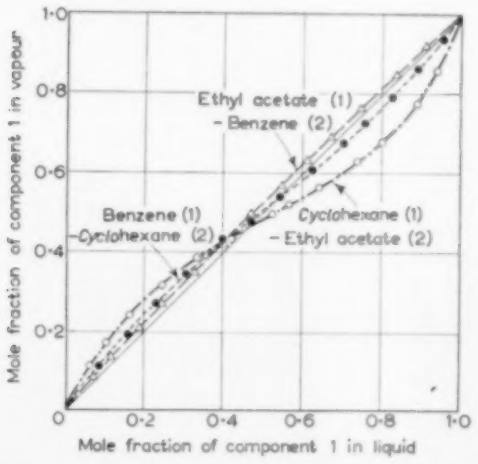

Fig. 8. Equilibrium compositions in the binary systems.

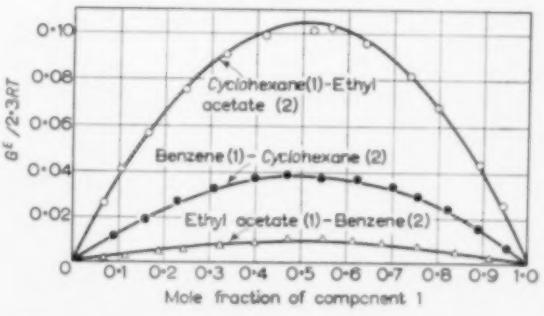

Fig. 9. Excess free energy of the binary mixtures.

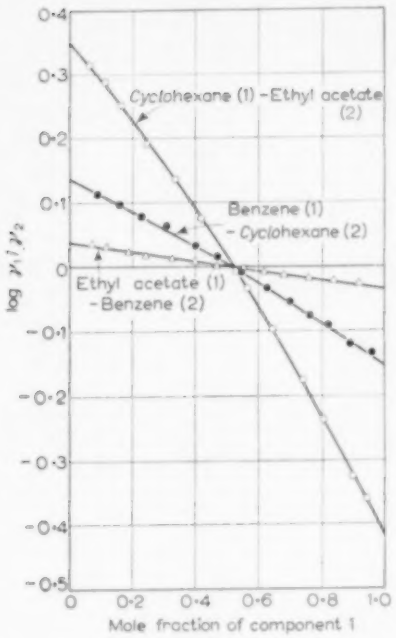

FIG. 10. Ratio of activity coefficients in the binary systems.

Table 5.

		1-*Constant*	2-*Constant*	3-*Constant*
For ethyl acetate [1] – benzene [2]	*b*	0·0372	0·0369	0·0369
	c	—	− 0·0041	− 0·0042
	d	—	—	− 0·0028
For benzene [1] – *cyclo*hexane [2]	*b*	0·1454	0·1443	0·1444
	c	—	0·0100	0·0104
	d	—	—	− 0·0029
For *cyclo*hexane [1] – ethyl acetate [2]	*b*	0·3850	0·3849	0·3848
	c	—	0·0321	0·0318
	d	—	—	0·0076

Calculated values of vapour composition were compared with experimental values for each binary system, using each correlating equation. The root mean square deviations of calculated values from experimental values of vapour compositions expressed in mole fractions were obtained (Table 6). In these calculations vapour pressure ratios were based upon experimental equilibrium temperatures.

Table 6. Root mean square deviations of $(y_{calc.} - y_{exp.})$

	1-*Constant equation*	2-*Constant equation*	3-*Constant equation*
Ethyl acetate – benzene	0·0007	0·0009	0·0010
Benzene – *cyclo*hexane	0·0022	0·0012	0·0010
*Cyclo*hexane – ethyl acetate	0·0059	0·0022	0·0020

An examination of the above deviations indicates that for the ratio of activity coefficients an optimum correlation is obtained with 2-constant equations for the benzene – *cyclo*hexane and *cyclo*hexane – ethyl acetate systems, and that a 1 – constant equation suffices for the ethyl acetate – benzene system. By optimum correlation is meant that the use of additional terms does not give significant improvement to justify the extra work involved.

For simultaneous correlation of vapour – liquid composition with equilibrium temperature at constant pressure a trial and iteration procedure was employed. Calculation of separate activity coefficients as well as their ratios were required for this purpose. The procedure followed was to calculate vapour pressures of the separate pure components at an assumed temperature from the vapour pressure equations. The vapour composition calculated thus from equation (22) was subsituted into equation (4) to verify the assumed vapour pressure; the second temperature to be assumed was then obtained from this vapour pressure through an equation for vapour pressure. The process was repeated until successive trials gave the same temperature within 0·01°C.

The following equations were obtained for expressing individual activity coefficients in terms of logarithms to the base 10 :—

$$\left.\begin{aligned} \log \gamma_1 &= x_1 x_2 \left[B + C\,(x_1 - x_2)\right] \\ &\quad + x_2 \left[b\,(x_2 - x_1) + c\,(6x_1 x_2 - 1)\right] \\ \log \gamma_2 &= x_1 x_2 \left[B + C\,(x_1 - x_2)\right] \\ &\quad - x_1 \left[b\,(x_2 - x_1) + c\,(6x_1 x_2 - 1)\right] \end{aligned}\right\} \quad (33)$$

A comparison of calculated with experimental

Table 7.

	b	c	B	C
For ethyl acetate [1] – benzene [2]	0·0372	0	0·0359	0
For benzene [1] – *cyclo*hexane [2]	0·1443	0·0100	0·1507	0·0100
For *cyclo*hexane [1] – ethyl acetate [2]	0·3849	0·0321	0·4190	0·0149

values for these three equations is shown in Figs. 7, 8, 9 and 10.

The root mean square deviations of calculated from experimental values of temperature and vapour composition are tabulated herewith. A comparison with deviation obtained from the conventional method of correlation is also given. The conventional method does not recognize the difference between the constants in the free energy expression and those in the activity coefficient ratio expression. Those constants are

Table 8.

	$y_{calc.} - y_{exp.}$ mole fractions		$t_{calc.} - t_{exp.}$ C°	
System	*Isobaric*	*Conventional*	*Isobaric*	*Conventional*
Ethyl acetate – benzene	0·0007	0·0007	0·07	0·07
Benzene – *cyclo*hexane	0·0012	0·0012	0·06	0·13
*Cyclo*hexane – ethyl acetate	0·0022	0·0022	0·13	0·37

then solely determined from the expression of the activity coefficient ratios as in equation (19).

It will be seen that the correlations are nearly the same with isobaric and conventional equations. The calculated temperatures deviate from the experimental values by about 0·1°C for all three systems. Employing two sets of constants did not improve the calculated values of vapour composition but slightly improved the calculated values of temperature.

Ternary Systems

Experimental values of vapour–liquid compositions at atmospheric pressure are shown by the lines connecting the vapour with the equilibrium liquid composition (Fig. 11). Values of x, y, and t were measured at 760 mm Hg pressure for 77 ternary compositions uniformly distributed over the entire range of ternary compositions. These were in addition to the 39 compositions for the three binary systems, and were recorded in Table 14.

Table 9. Constants for the ternary system for use in expressing $\log \gamma_1/\gamma_2$

	3-*Constant equation* (1 *for each pair*)	6-*Constant equation* (2 *for each pair*)	9-*Constant equation* (3 *for each pair*)	5-*Constant equation*
b_{AB}	0·0372	0·0369	0·0369	0·0372
b_{BC}	0·1454	0·1443	0·1444	0·1443
b_{CA}	0·3850	0·3849	0·3848	0·3849
c_{AB}		− 0·0041	− 0·0042	
c_{BC}		0·0010	0·0104	0·0100
c_{CA}		0·0321	0·0318	0·0321
d_{AB}			− 0·0028	
d_{BC}			− 0·0029	
d_{CA}			0·0076	

Correlations of ternary data were made similarly to those for the three binary systems, basing them first upon experimental measurements of temperature and then correcting the temperature to give complete correlation for all equilibrium conditions. The first correlation was made with experimental temperature values, using 1-, 2- and 3-constants for each binary pair with corresponding 3-, 6- and 9-constants for the ternary solution. No additional constants were required for ternary effects.

The root mean square deviations of $y_{calc.} - y_{exp.}$ in mole per cent are shown in Table 10.

The accepted equation for relating all three activity coefficient ratios in the ternary system required only 5-constants; for individual activity coefficients at constant pressure, 5 additional constants permitted accurate calculation of temperature. With reference to equations (29) and (30) for activity coefficient

VOL.
7
957/58

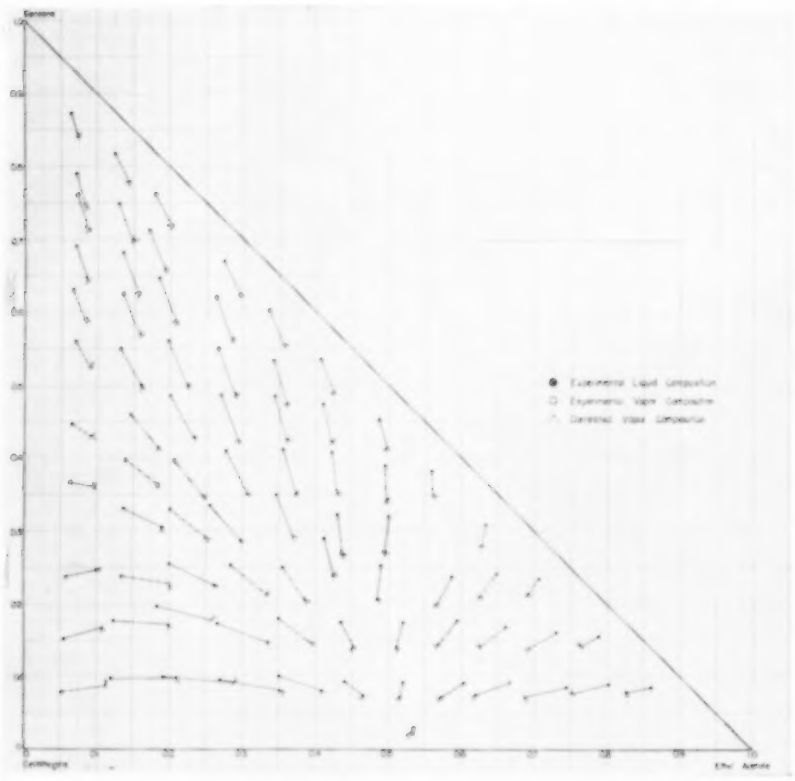

FIG. 11. Equilibrium compositions in the ternary system.

VO
7
1957

Table 10.

3-*Constant equation*	6-*Constant equation*	9-*Constant equation*	5-*Constant equation*
0·22	0·13	0·16	0·13

ratios and activity coefficients, the following constants apply. They are given for use with logarithms to the base 10 instead of natural logarithms.

Table 11.

b_{12}	0·0372	B_{12}	0·0359
b_{23}	0·1443	B_{23}	0·1507
b_{31}	0·3849	B_{31}	0·4190
c_{12}	0	C_{12}	0
c_{23}	0·0100	C_{23}	0·0100
c_{31}	0·0321	C_{31}	0·0149

Here 1 = ethyl acetate (also designated as component *A*), 2 = benzene (component *B*), and 3 = *cyclo*hexane (component *C*).

The root mean square deviation of calculated values from experimental measurements are presented in Table 12.

Table 12.

	$y_{calc.} - y_{exp.}$ (mole per cent)	$t_{calc.} - t_{exp.}$ °C
Isobaric equation	0·13	0·13
Conventional equation	0·13	0·34

It will be seen that the correlations are nearly the same with isobaric and conventional equations. The temperatures calculated with the isobaric equations deviate from the experimental values by about 0·1°C. Employing two sets of constants did not improve the calculated values of vapour composition but slightly improved the calculated values of temperature.

Acknowledgements—Credit is acknowledged to the Wisconsin Alumni Research Foundation and the C. T. Loo Fellowship Fund for financial aid and to the Numerical Analysis Laboratory of the University of Wisconsin for use of high speed electronic digital computers.

A more detailed form of this paper (or extended version, or material supplementary to this article) has been deposited as Document number 5424 with the ADI Auxiliary Publications Project, Photoduplication Service, Library of Congress, Washington 25, D.C. A copy may be secured by citing the Document number and by remitting $5.00 for photoprints, or $2.25 for 35 mm microfilm. Advance payment is required. Make checks or money orders payable to: Chief, Photoduplication Service, Library of Congress.

References

[1] Dodge B. F. *Chemical Engineering Thermodynamics* p. 106. McGraw-Hill, New York 1944.
[2] Faraday J. E. *Encyclopedia of Hydrocarbons* Sheet 06016.11.01. Chemical Publishing Co.
[3] Faraday J. E. *Encyclopedia of Hydrocarbons* Sheet 06082.90. Chemical Publishing Co.
[4] Forziati A. F., Glasgow A. R., Willingham C. B. and Rossini F. D. *J. Res. Nat. Bur. Stand.* 1946 **36** 129.
[5] Gillespie D. T. C. *Industr. Engng. Chem.*, (*Anal.*) 1946 **18** 574.
[6] Ibl N. V. and Dodge B. F. *Chem. Engng. Sci.* 1953 **2** 120.
[7] *International Critical Tables* Vol. VII p. 81. McGraw-Hill, New York 1933.
[8] *International Critical Tables* Vol. III p. 33. McGraw-Hill, New York 1933
[9] Jones C. A., Schoenborn E. M. and Colburn A. P. *Industr. Engng. Chem.* 1943 **35** 666.
[10] Kailan A. *Z. Phys. Chem.* 1914 **88** 67.
[11] Lecat M. *L'Azeotropisme.* Henri Lamertin, Libraire-Editeur, Bruxelles, 1918.
[12] Marschner R. F. and Cropper W. P. *Industr. Engng. Chem.* 1946 **38** 262.
[13] Redlich O. and Kister A. T. *Industr. Engng. Chem.* 1948 **40** 345.
[14] Richards A. R. and Hargreaves E. *Industr. Engng. Chem.* 1944 **36** 805.

VOL. 7 957/58

[15] Ryland G., *J. Amer. Chem. Soc.* 1899 **22** 390.

[16] Scatchard G., Wood S. E. and Mochel J. M. *J. Phys. Chem.* 1939 **43** 119.

[17] Stuhl D. R. *Industr. Engng. Chem.* 1947 **39** 517.

[18] Swietoslawski W. *Roczn. Chem.* 1932 **12** 48.

[19] Tao, L. C. Ph.D. Thesis, University of Wisconsin 1952.

[20] Thornton J. D. and Garner F. H. *J. Appl. Chem.* 1951 **1** S61.

[21] Thornton J. D. and Garner F. H. *J. Appl. Chem.* 1951 **1** S68.

Chemical Engineering Science, 1958, Vol. 7, pp. 261 to 264. Pergamon Press Ltd.

The error in thermodynamic predictions as a function of the displacement from equilibrium

R. P. Rastogi and K. G. Denbigh
Dept. of Chemical Technology, West Mains Road, Edinborough 9

(*Received* 17 *September* 1957)

Abstract—The paper is concerned with the extent to which a thermodynamic prediction of the effect of temperature or pressure on the yield of a reaction is in error, due to the non-attainment of equilibrium. The magnitude of the error is evaluated as a function of the fractional attainment of equilibrium and is shown to be surprisingly large under conditions such as might be encountered in industrial practice.

Résumé—Cet article traite des écarts intervenant dans les prédictions thermodynamiques des effets de température ou de pression sur le rendement d'une réaction quand l'équilibre n'est pas atteint. L'auteur évalue l'erreur en fonction de l'approche de l'équilibre et il montre que dans le cas des installations industrielles elle est étonnament grande.

Zusammenfassung—Die Arbeit beschäftigt sich mit der Frage, wieweit eine thermodynamische Voraussage des Temperatur- oder Druckeinflusses auf die Ausbeute einer Reaktion fehlerhaft sein kann, bedingt durch die Nichterreichung des Gleichgewichtes. Die Grösse dieses Fehlers wird als Funktion der Annäherung an das Gleichgewicht errechnet und erweist sich als überraschend gross unter Bedingungen, wie sie in der industriellen Praxis auftreten können.

VOL. 7 1957/58

One of the useful applications of thermodynamics is the prediction of the effect of changes of temperature, pressure or concentration on the state of physical and chemical systems. The equations used for this purpose are based on the second law and are thus strictly applicable only if there is true equilibrium—a condition never actually attained in industry, due to the time factor. The question arises: What is the error in these predictions, as a function of the degree of attainment of the equilibrium state?

This problem, which it seems has not been discussed previously, is obviously of greater significance in chemical than in physical processes. In ammonia synthesis or sulphur dioxide oxidation, for example, the chemical engineer uses Van't Hoff's equation,

$$\frac{d \ln K}{dT} = \frac{\Delta H}{RT^2}, \tag{1}$$

for the purpose of predicting the effect of temperature on the yield of the reaction. This prediction is inevitably somewhat in error whenever the contact time in the plant is less than infinite. A more exact prediction must be based on chemical kinetics, which allows for the finite speed of the forward and backward reactions. This can be done only when the form of the kinetics is known, together with experimental data on the temperature coefficients of the velocity constants.

In the present note we shall compare the prediction based on thermodynamics with the more exact prediction based on chemical kinetics. For this purpose it is convenient to examine reactions whose kinetics are sufficiently simple.

Consider the reversible reaction

$$A + B = X + Y$$

which will be assumed to be second order in both directions. The reagents A and B will be taken as being present in equimolar amounts, their initial concentrations being a_0. Let x and x_e be the concentrations of X (or Y) at time t and at equilibrium respectively. The reaction yield at time t is

$$\phi \equiv x/a_0 \tag{2}$$

and the equilibrium yield is

$$\phi_e \equiv x_e/a_0. \tag{3}$$

Assuming that the system forms a perfect gaseous mixture, the equilibrium constant is

$$K = \frac{x_e^2}{(a_0 - x_e)^2} \tag{4}$$

or

$$K = \frac{\phi_e^2}{(1 - \phi_e)^2} \tag{5}$$

Hence by differentiation and using equation (1):

$$\frac{d\phi_e}{dT} = \frac{\Delta H\, K^{\frac{1}{2}}}{2RT^2\,(1 + K^{\frac{1}{2}})^2} = \frac{\Delta H}{2RT^2}\,\phi_e\,(1 - \phi_e) \tag{6}$$

and this equation shows how the yield varies with temperature if there is true equilibrium.

Consider the matter now according to chemical kinetics :

$$\frac{dx}{dt} = k_1\,(a_0 - x)^2 - k_2\,x^2 \tag{7}$$

where k_1 and k_2 are the velocity constants of the forward and reverse reactions respectively. Integrating we obtain

$$t = \frac{K^{\frac{1}{2}}}{2k_1 a_0} \times \ln\left\{\left(\frac{K^{\frac{1}{2}} - 1}{K^{\frac{1}{2}} + 1}\right)\left(\frac{Kx - x - Ka_0 - K^{\frac{1}{2}}\,a_0}{Kx - x - Ka_0 + K^{\frac{1}{2}}\,a_0}\right)\right\} \tag{8}$$

Hence solving equation (8) for the ratio $\phi = x/a_0$, which is the yield at time t, we obtain

$$\phi = \frac{K^{\frac{1}{2}}\left[1 - \exp\left(2k_1\,a_0\,t\,K^{-\frac{1}{2}}\right)\right]}{K^{\frac{1}{2}} - 1 - (K^{\frac{1}{2}} + 1)\exp\left(2k_1\,a_0\,t\,K^{-\frac{1}{2}}\right)} \tag{9}$$

Differentiating with respect to temperature and using equation (1), together with

$$\frac{d\ln k_1}{dT} = \frac{E_1}{RT^2}, \tag{10}$$

where E_1 is the activation energy for the forward reaction, we obtain,

$$\left(\frac{\partial\phi}{\partial T}\right)_t = \frac{4a_0 k_1\,t\,(2E_1 - \Delta H)\exp\left(2k_1\,a_0\,t\,K^{-\frac{1}{2}}\right) - K^{\frac{1}{2}}\,\Delta H\left[1 - \exp\left(4k_1\,a_0\,t\,K^{-\frac{1}{2}}\right)\right]}{2RT^2\left[(K^{\frac{1}{2}} - 1) - (K^{\frac{1}{2}} + 1)\exp\left(2k_1\,a_0\,t\,K^{-\frac{1}{2}}\right)\right]^2} \tag{11}$$

From this equation the time t can be eliminated by substitution from equation (8). Let the *fractional attainment of equilibrium* be defined as

$$f \equiv \frac{x}{x_e} = \frac{\phi}{\phi_e} \tag{12}$$

Then we finally obtain

$$\left(\frac{\partial\phi}{\partial T}\right)_t = \left.\begin{aligned}&\frac{\phi_e}{4RT^2\,(1 - \phi_e)}\left\{2\,\Delta H f\,(1 - \phi_e)\,(1 - f\phi_e)\right.\\&+ (2E_1 - \Delta H)\,(1 - f)\,(1 + f - 2f\phi_e)\ln\\&\left.\left.\left[\frac{1 + f - 2f\phi_e}{1 - f}\right]\right\}\right\} \tag{13}$$

where ϕ_e is related to K through equation (5). This equation shows how the yield varies with temperature as a function of f, and it reduces to equation (6) when $f = 1$ — i.e. at thermodynamic equilibrium.

The ratio r of the true temperature coefficient of the yield to the temperature coefficient which would be predicted on the assumption that the system is at equilibrium, is thus obtained by dividing equation (13) by equation (6) and is

$$r \equiv \frac{(\partial\phi/\partial\,T)_t}{d\phi_e/dT} = \left.\begin{aligned}&\frac{1}{(1 - \phi_e)^2}\left\{f\,(1 - \phi_e)\,(1 - f\phi_e)\right.\\&+ \left(\frac{E_1}{\Delta H} - \tfrac{1}{2}\right)\left[1 - 2\phi_e f(1 - f) - f^2\right]\ln\\&\left.\left.\left[\frac{1 - f\,(2\phi_e - 1)}{1 - f}\right]\right\}\right\} \tag{14}$$

This equation is also applicable to reactions whose stoichiometry is

$$2A = X + Y,$$

provided that these also have second order kinetics. A well-known example for which experimental data are available is the decomposition of hydrogen iodide :

$$2\mathrm{HI} = \mathrm{H_2} + \mathrm{I_2}.$$

For this reaction the equilibrium constant, K, has a value of $2{\cdot}18 \times 10^{-2}$ at 763·8°K* and E_1 and ΔH have values of 44,000 cal/mole and 3000 cal/mole respectively†.

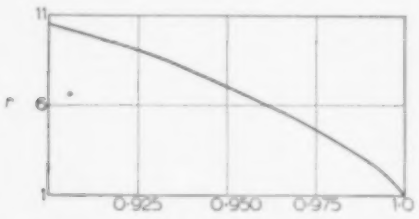

FIG. 1. The ratio r as a function of the fractional attainment of equilibrium in the reaction $2\,HI = H_2 + I_2$.

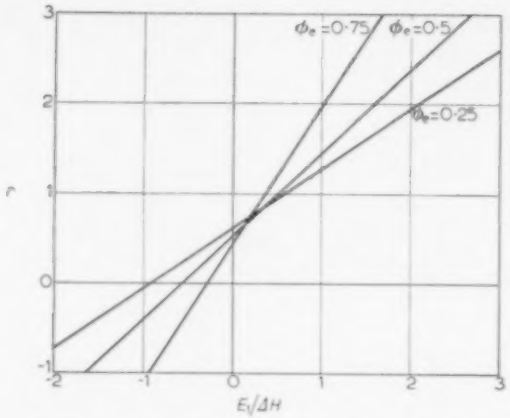

FIG. 2. Influence of the relative magnitudes of E and ΔH.

These figures have been used in a numerical solution of equation (14). The results are shown in Fig. 1, where the ratio r is plotted as a function of f, the fractional attainment of equilibrium. It will be seen that, for a value of f of 0·9, the true temperature coefficient of the yield is 10·6 times the value predicted thermodynamically on the supposition of equilibrium. When the system is 1 per cent from equilibrium (f = 0·99) the corresponding factor is still as much as 2·8. In this instance, at least, the effect of a few per cent displacement from equilibrium clearly gives rise to a disproportionately large error in the thermodynamic prediction. The reason for this is that the temperature coefficient of the equilibrium yield is determined by ΔH, whilst the temperature coefficient of the yield when the reaction is far from equilibrium is mainly determined by E_1, the activation energy of the forward reaction. Thus whenever E_1 and ΔH differ by an order of magnitude, as in the case of the decomposition of hydrogen iodide, the ratio r may be expected to be fairly large at comparatively small departures from equilibrium.

This has been confirmed by solving equation (14) for various values of the ratio $E_1/\Delta H$ at a fixed value of f equal to 0·9, and for fixed values of ϕ_e. The results are shown in Fig. 2. As expected, the ratio r has a large (positive or negative) value whenever E_1 and ΔH differ considerably. Higher values of ϕ_e also tend to increase the magnitude of r.

In addition to the temperature coefficient, $d\phi/dT$, it is of interest to consider also the pressure coefficient, $d\phi/dP$, and the extent to which its equilibrium value differs from its value prior to the attainment of equilibrium. For this purpose consider a reaction of the type

$$A + B = X,$$

taking place in a perfect gas mixture. For simplicity, it will be supposed that the reaction takes place in a closed system of constant volume (and temperature) rather than in a flow system. For this reason the pressure P varies during the course of the reaction and is not, properly speaking, an independent variable. Instead we shall choose P_0, the initial pressure in the vessel before reaction commences – or, which comes to the same thing, the initial concentration a_0 of the two reagents, taken as equal.

Let ϕ and ϕ_e be the yield of product at time t and at equilibrium respectively. The variation of the equilibrium yield with the initial concentration is given by

$$\frac{d\phi_e}{da_0} = \frac{\phi_e(1-\phi_e)}{a_0(1+\phi_e)} \qquad (15)$$

*TAYLOR A. H. and CRIST R. H. *J. Amer. Chem. Soc.* 1941 **63** 1376.

†For a reaction of the type $2A = X + Y$, the relationship between K and ϕ_e is $4K = \phi_e^2/(1-\phi_e)^2$, in place of equation (5). But equation (14) applies unchanged.

where ϕ_e is calculable from the equilibrium constant :

$$\frac{\phi_e}{a_0(1-\phi_e)^2} = K \qquad (16)$$

If the reaction kinetics happen to correspond to the stoichiometry, we have

$$\frac{d\phi}{dt} = k_1 a_0 (1-\phi)^2 - k_2 \phi \qquad (17)$$

which may be integrated to give ϕ as a function of t. Proceeding as in the preceding example, we finally obtain r, the ratio of the true dependence of the yield on the initial concentration, to the thermodynamic value as given by equation (15):–

$$\left.\begin{aligned} r &\equiv \frac{(\partial\phi/\partial a_0)_t}{d\phi_e/da_0} \\ &= f + \frac{2\phi_e(1-f)}{(1-\phi_e^2)^2} \times \\ &\left\{(1-f\phi_e^2)\ln\left[\frac{(1-f\phi_e^2)}{1-f}\right] + f\phi_e(1-\phi_e^2)\right\} \end{aligned}\right\} \qquad (18)$$

where f, the fractional attainment of equilibrium is defined as in equation (12).

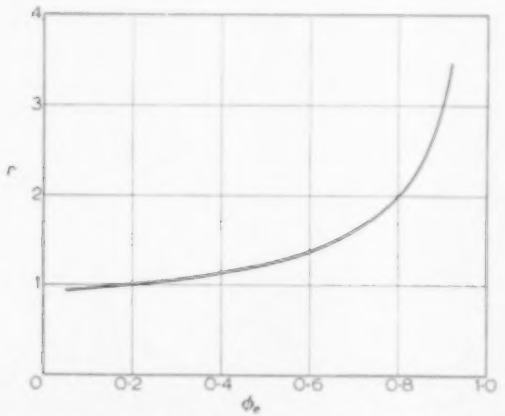

Fig. 3. The value of r in a reaction influenced by the pressure.

Using equation (18), the value of r has been plotted in Fig. 3 as a function of ϕ_e (which is determined by K and a_0), for a fixed value of f equal to 0·9 – which is about as high a value as might be expected under normal industrial conditions. It will be seen that as ϕ_e, the equilibrium yield, becomes greater the larger the error in the thermodynamic prediction. This is as might be expected : in a reaction of stoichiometry $A + B = X$ the effect of an increase in pressure, or concentration, is to raise the rate of the forward reaction more than that of the reverse reaction, and thus to increase ϕ. If ϕ_e is large, the effect is almost entirely due to the forward reaction, the backward reaction being relatively insignificant. Thus, under these conditions, a prediction based on equation (15), which implies that the forward and backward processes are proceeding equally, would be a great deal in error.

The result of this short survey is to show that a thermodynamic prediction can be considerably in error when a chemical system is, say, 10 per cent away from equilibrium ($f = 0{\cdot}9$). In the case of the temperature coefficient of the yield, especially, the error can be quite large whenever the ratio $E_1/\Delta H$ is large.

The comparison has been extended to other types of reaction, of different kinetic orders, and similar results have been obtained. The general conclusion to be drawn is that thermodynamic predictions are to be used with a good deal of caution, whenever the system in question is appreciably displaced from equilibrium. Of course the great advantage in the use of thermodynamics is that it requires a minimum of experimental data—and also it shows the limiting value of what is attainable. To apply kinetics requires a much larger amount of information, in particular a knowledge of the kinetic order of the reaction and also—for a prediction of the effect of temperature—a knowledge of the activation energies. Nothing that has been said in this short paper need be taken as diminishing the great value of thermodynamics in chemical engineering.

Acknowledgements—One of the authors (R.P.R.) is grateful to the Royal Society and Nuffield Foundation Commonwealth Bursaries Committee for the award of a bursary.

Chemical Engineering Science, 1958, Vol. 7, pp. 265 to 268. Pergamon Press Ltd.

A note concerning turbulent exchange of heat or mass with a boundary

E. RUCKENSTEIN

Bucharest Polytechnical Institute, Roumanian People's Republic

(*Received* 18 *September* 1957)

Abstract—A renewal model is proposed which allows the derivation, at large Prandtl numbers, of the equation

$$Nu \sim Re \sqrt{\frac{f}{2}}\, Pr^{\frac{1}{2}},$$

where Nu, Re and Pr are Nusselt's, Reynolds' and Prandtl's numbers, and f is the friction factor.

Résumé—L'auteur propose, dans le cas des nombres de Prandtl élevés, une forme nouvelle de l'équation :

$$Nu \sim Re \sqrt{\frac{f}{2}}\, Pr^{\frac{1}{2}}$$

propre à la dérivation où, Nu, Re, Pr, sont les nombres de Nusselt, Reynold et Prandtl, et f le coefficient de frottement.

Zusammenfassung—Es wird ein Austauschmodell vorgeschlagen, das die Erweiterung der Gleichung

$$Nu \sim Re \sqrt{\frac{f}{2}}\, Pr^{\frac{1}{2}},$$

auf grosse Prandtl-Zahlen gestattet. Hierin bedeuten Nu, Re und Pr die Nusselt-, Reynolds- und Prandtl-Zahlen und f den Reibungsfaktor.

VOL. 7 957/58

In their recent papers HANRATTY [1] and JOHNSON and HUANG [2] extended the model of continuous renewal of the interface layer, as given by DANCKWERTS [3], to the case of mass exchange with a boundary. A similar idea has been used independently by the author in [4], with a more complete result than the one obtained in [1] and [2].

In these papers it is assumed that, owing to turbulence, the liquid layer near the boundary is continuously replaced by other liquid layers, each of them remaining at the boundary for a very short time.

Observations made by FAGE and TOWNEND [5] in the immediate vicinity of the wall on a turbulent fluid in which they traced—by the aid of an ultra-microscope—the motion of dust particles, perhaps provide experimental support for a renewal mechanism. These authors noticed the existence of large lateral displacements of groups of these particles, and mentioned the fact that the motion can be regarded as practically rectilinear only during the interval between two such displacements. This experimental evidence is in contradiction with the model of the laminar sublayer which implies the existence of a region within which the motion should be rectilinear, but is consistent with a renewal mechanism.

In [4] the author obtained for the coefficient of heat transfer at large Prandtl numbers, in the case of a tube,

$$Nu \sim Re \sqrt{\frac{f}{2}}\, Pr^{\frac{1}{2}}, \qquad (1)$$

Nu being Nusselt's number, Re Reynolds' number, Pr Prandtl's number and f the friction

factor. In deriving equation (1), dimensional considerations were used besides DANCKWERTS' renewal mechanism.

Within the framework of classical theory one obtains for Nusselt's number, at large Prandtl numbers [6], [7],

$$Nu \sim Re \sqrt{\frac{f}{2}}\, Pr^{\frac{1}{2}}. \tag{2}$$

It should be stressed though that (2) has been derived on the assumption that in the close neighbourhood of the wall the eddy diffusivity is proportional to the third power of the distance from the wall :

$$\frac{\varepsilon}{\nu} \sim \left(\frac{y\sqrt{\frac{\tau_0}{\rho}}}{\nu}\right)^3. \tag{3}$$

Here ν is the kinematic viscosity, y the distance from the wall, τ_0 the shear stress at the wall and ρ the density. This assumption is needed to obtain agreement with experimental data.

In this note a renewal model differing in some respects from the one used in [1], [2], and [4] is proposed ; thus equation (2) may be derived without making use of the above assumption. It will be assumed that the boundary is divided along the direction of flow into short sections of length x_0. A certain part of the liquid flows along the wall a distance x_0, after which it mixes with the bulk of the liquid. This process is repeated at intervals x_0 apart. Let it be assumed that the liquid layer which flows along the wall in each section is non-turbulent and that the " path-length " x_0 is small enough to render the thickness of the laminar boundary layer corresponding to the flow along a plate smaller than the thickness z_0 of the liquid layer. Then the velocity distribution in this layer can be approximated by the velocity distribution in the case of a flow along a plate [8] :

$$u = \frac{u_0}{2}\left(\alpha\,\eta - \frac{\alpha^2\,\eta^4}{4\,!} + \cdots\right)$$

$$\approx \frac{1{\cdot}33\,u_0}{4}\left(\frac{u_0\,y^2}{\nu\,x}\right)^{\frac{1}{4}} = 1{\cdot}73\,\frac{u_0\,y}{\delta} \tag{4a}$$

$$v \approx \frac{\alpha}{4}\left(\frac{u_0\,\nu}{x}\right)^{\frac{1}{4}}\eta^2. \qquad \left[\eta \equiv \frac{1}{2}\left(\frac{u_0\,y^2}{\nu\,x}\right)^{\frac{1}{4}}\right] \tag{4b}$$

Here u_0 is the velocity of the liquid layer at the beginning of each section, x is, for each section, the distance from its beginning, and δ the thickness of the boundary layer, given by :

$$\delta = 5{\cdot}2\left(\frac{\nu\,x}{u_0}\right)^{\frac{1}{2}}. \tag{5}$$

The equation of heat transfer in a liquid layer which flows along the wall in a section is :

$$u\,\frac{\partial T}{\partial x} + v\,\frac{\partial T}{\partial y} = a\,\frac{\partial^2 T}{\partial y^2}, \tag{6}$$

where T is the temperature and a the thermal diffusivity.

If Prandtl's number is large enough, the temperature does not vary sensibly except close to the wall, and we can assume the temperature of the liquid layer which flows at the wall to be the same, for $x = 0$, to the average temperature. If the thickness δ_T of the thermal boundary layer (under conditions of laminar flow) is smaller than the thickness of the layer flowing along the wall in a section, the temperature distribution may be approximated by one for a semi-infinite medium. (Since $\delta_T < \delta$ if $Pr > 1$, it is evident that for $Pr > 1$ $\delta_T < z_0$ if also $\delta < z_0$). Hence, we have the following boundary conditions :

$$\left.\begin{aligned} T &= T_p \text{ for } y = 0 \\ T &= T_m \text{ for } y = \infty \\ T &= T_m \text{ for } x = 0. \end{aligned}\right\} \tag{7}$$

The solution of equation (6) with boundary conditions (7) has been given by POHLHAUSEN [8], [9], [10] :

$$\frac{T - T_p}{T_m - T_p} \approx \left(\int_0^{\frac{1}{2}\left(\frac{u_0\,y^2}{\nu\,x}\right)^{1/3}} \exp\left\{-0{\cdot}22\,Pr\,z^3\right\} dz\right) \Big/ \int_0^{\infty} \exp\left\{-0{\cdot}22\,Pr\,z^3\right\} dz. \tag{8}$$

Since

$$\int_0^{\infty} \exp\left\{-0{\cdot}22\,Pr\,z_0\right\} dz = \frac{0{\cdot}89}{(0{\cdot}22\,Pr)^{\frac{1}{3}}},$$

equation (8) becomes

$$\frac{T - T_p}{T_m - T_p} = \frac{(0{\cdot}22\ Pr)^{\frac{1}{3}}}{0{\cdot}89} \int_0^{\frac{1}{2}\left(\frac{u_0 y^2}{\nu x}\right)^{1/2}} \exp\left\{-0{\cdot}22\ Pr\ z^3\right\} dz. \quad (9)$$

For the heat transfer coefficient we obtain easily :

$$h_x = 0{\cdot}34\ \lambda \left(\frac{u_0}{\nu x}\right)^{\frac{1}{2}} Pr^{\frac{1}{3}}. \quad (10)$$

The average value h of h_x is given by :

$$h = \frac{1}{x_0} \int_0^{x_0} h_x\, dx. \quad (11)$$

Hence,

$$\frac{h}{\lambda} = 0{\cdot}68 \left(\frac{u_0}{\nu x_0}\right)^{\frac{1}{2}} Pr^{\frac{1}{3}}. \quad (12)$$

Taking into account that the " path-length " x_0 is very small, h may be regarded as a quasi-local quantity, the quasi-local coefficient of heat transfer.

The " path-length " x_0 as well as the velocity u_0 are hydrodynamical quantities. In other words x_0 and u_0 are functions only of τ_0, ρ, and ν, which characterize the hydrodynamical state of the fluid in the vicinity of the boundary, and not of λ, for instance. Dimensional considerations permit writing :

$$u_0 \sim \left(\frac{\tau_0}{\rho}\right)^{\frac{1}{2}} \quad (13)$$

$$x_0 \sim \nu/(\tau_0/\rho)^{\frac{1}{2}}. \quad (14)$$

Taking into account (13) and (14), equation (12) becomes

$$\frac{h}{\lambda} \sim \frac{\left(\frac{\tau_0}{\rho}\right)^{\frac{1}{2}}}{\nu} Pr^{\frac{1}{3}}. \quad (15)$$

Using the expression,

$$\frac{\tau_0}{\rho} = \frac{f}{2} u_m^2,$$

where u_m is the average velocity, and the usual dimensionless groups, equation (15) becomes :

$$Nu \sim Re \sqrt{\frac{f}{2}}\, Pr^{\frac{1}{3}}. \quad (16)$$

In what follows the assumption that x_0 is constant in time will be abandoned ; for a given value of x_0, equation (12) will be used to give the approximate coefficient of heat transfer. Consider an infinitesimal region chosen at random at the boundary, and let $\phi\, dx_0$ be the number of cases in which this region belongs to a path-length between x_0 and $x_0 + dx_0$.

Dimensional considerations lead to :

$$\phi = F\left(\frac{x_0}{x_1}\right), \quad (17)$$

where

$$x_1 \sim \frac{\nu}{\left(\frac{\tau_0}{\rho}\right)^{\frac{1}{2}}}. \quad (18)$$

It can easily be shown that x_1 is proportional to the average value of x_0.

The quasi-local coefficient of heat transfer $\bar{h}$ can be defined as the average value of h.

This treatment of the problem holds true only if ϕ takes finite values in a sufficiently narrow interval about the average value of x_0 and practically vanishes outside this interval. Only in this case can the motion in the vicinity of the wall be considered as quasi-stationary, and hence equation (12) may be used. Using equations (12) and (17) we obtain

$$\bar{h} = 0{\cdot}68\ \lambda \left(\frac{u_0}{\nu x_1}\right)^{\frac{1}{2}} Pr^{\frac{1}{3}} \frac{\int_0^\infty \left(\frac{x_0}{x_1}\right)^{-\frac{1}{2}} F\left(\frac{x_0}{x_1}\right) d\frac{x_0}{x_1}}{\int_0^\infty F\left(\frac{x_0}{x_1}\right) d\frac{x_0}{x_1}}. \quad (19)$$

Since the ratio of the integrals is a constant, by using equations (13), (18) and (19), an equation of the same form as equation (16) is obtained for $\bar{h}$.

Notation

a = thermal diffusivity
f = friction factor
T = temperature
T_p = temperature at the wall
T_m = average temperature
u = x component of velocity
v = y component of velocity
x = co-ordinate in flow direction

y = distance from wall
h = coefficient of heat transfer
ϵ = eddy diffusivity
λ = thermal conductivity
ν = kinematic viscosity
ρ = density
τ_0 = shear stress at the wall
Re = Reynolds number
Nu = Nusselt number
Pr = Prandtl number

REFERENCES

[1] HANRATTY J. T. *Amer. Inst. Chem. Engrs. J.* 1956 **2** 359.

[2] JOHNSON A. I. and HUANG C. J. *Amer. Inst. Chem. Engrs. J.* 1956 **2** 412.

[3] DANCKWERTS P. V. *Industr. Engng. Chem.* 1951 **43** 1460.

[4] RUCKENSTEIN E. *Rev. Chim.* 1957 in press (in Roumanian).

[5] FAGE A. and TOWNEND H. C H *Proc. Roy. Soc.* 1932 A **135**, 656 (quoted in [1]).

[6] RUCKENSTEIN E. *Stud. Cercet. Fiz.* 1954 **4** 123 (in Roumanian).

[7] RIBAUD G. *C. R. Acad. Sci. Paris.* 1956 **242** 959.

[8] LEVICI V. G. *Fiziko-khimicheskaia gidrodinamica.* Izd. Alcad. Nauk. SSSR, Moscow, 1952.

[9] BRUN E. A. *Introduction a l'étude de la couche limite.* Gauthier-Villars, Paris, 1955.

[10] POHLHAUSEN E. *Z. Angew. Math. Mech.* 1921 **1** 115.

Discussion of the paper "Fugacities in simple gas mixtures"

J. M. Prausnitz*

(*Received* 3 *May* 1957)

VOL. 7 957/58

The paper mentioned above presents an interesting and useful method for estimating the fugacities of individual components in a particular type of gas mixture, and it is correctly represented as such.

To illustrate the method, Prof. Prausnitz chooses the $N_2 - C_2H_4$ system, for which extensive $p - v - T$ data are available at 50°C [2]. He compares the results of fugacity calculations by his simplified method with the smoothed results of Bennett [1]. It is not pointed out, however, that the method used by Bennett for smoothing his results is based on the same general assumption of the type of mixture as is made by Prausnitz. Hence the comparison made is between two approximate sets of results. It is true, of course, that Prausnitz' method is based on a principle of corresponding states, whereas Prof. Bennett's method makes use of the actual $p - v - T$ data. But both methods are limited by the assumption that the volume change of mixing is a symmetrical function of the composition. A better test of Prausnitz' method would be a comparison of his results with the more accurate values of activity coefficients for this system given in a paper by the writer [4].

Prof. Bennett's calculations [1] were carried out by entirely graphical methods, and the differentiations involved are inherently inaccurate. He fully recognized this difficulty, and pointed out that his calculated results did not meet the test of thermodynamic consistency as made according to the method of Redlich and Kister [3]. In order to get a consistent set of results from his calculations, he smoothed his calculated values by arbitrarily drawing straight lines on the Redlich and Kister plot of $\ln (\gamma_{N_2}/\gamma_{C_2H_4})$ vs. y_{N_2}.

Such straight lines correspond to a system of Type II as described by Redlich and Kister [3], and are truly representative only of systems whose volume change of mixing curves are symmetrical functions of mole fraction. This is not strictly true for the $N_2 - C_2H_4$ system as may be seen from Bennett's Fig. 1. Prof. Bennett clearly stated that his *calculated* values might be more accurate than his *smoothed* values even though thermodynamically inconsistent. The equations for $\ln \gamma$ which result when the straight-line relationship is assumed for the Redlich and Kister plot are given by Bennett as :—

$$\ln \gamma_1 = By_2^2 \text{ and } \ln \gamma_2 = By_1^2$$

These are identical with the Prausnitz' equations (16) and (19). Prof. Prausnitz has presented us with a new method of calculating B (K in his paper). However, the comparison of his results with Bennett's smoothed values begs the issue of their accuracy. He is comparing two methods of calculating a constant for an equation which is not strictly valid for the system considered, although it is admittedly a good approximation over much of the range to which it was applied by Prausnitz.

The more accurate results calculated by the writer [4] met the test of thermodynamic consistency without smoothing, but did not result in straight lines on the Redlich and Kister plot. The curves that were obtained could certainly be approximated by straight lines over a considerable portion of the concentration range, and the method presented by Prausnitz apparently is equivalent to such an approximation in the pressure range to which he has applied it. However, there may well exist regions of concentration in which the straight-line approximation

Table 1.

y_{N_2}	γ_{N_2}			$\gamma_{C_2H_4}$		
	Bennett [1]	Prausnitz	Van Ness [4]	Bennett [1]	Prausnitz	Van Ness [4]
0·0	1·45	1·41	1·79	1·00	1·00	1·00
0·2	1·27	1·25	1·30	1·01	1·01	1·03
0·4	1·14	1·11	1·13	1·06	1·06	1·09
0·6	1·06	1·06	1·05	1·14	1·11	1·18
0·8	1·01	1·01	1·01	1·27	1·25	1·27
1·0	1·00	1·00	1·00	1·45	1·41	1·37

* *Chem. Engng. Sci.* 1957 **6** 112.

does not give very good results. For example, in the $N_2 - C_2H_4$ system at 100 atm the approximate values of both BENNETT and PRAUSNITZ for γ_{N_2} at low concentrations of nitrogen are appreciably different from the values determined by the writer. It should be noted that BENNETT was unable to calculate the limiting values of γ at infinite dilution of either component. Hence his smoothed values of γ at this condition represent extrapolated values. A comparison of γ values for a pressure of 100 atm obtained by the three different authors is tabulated below.

Certainly the new method proposed by PRAUSNITZ should be useful to those who require easy estimations of fugacities for the components of simple gas mixtures, but it should not be used with quite the confidence suggested by Prof. PRAUSNITZ' comparison of results.

HENDRICK C. VAN NESS

Department of Chemical Engineering,
Rensselaer Polytechnic Institute,
Troy, New York, U.S.A.

REFERENCES

[1] BENNETT C. O. *Chem. Engng. Prog. Symposium Series No.* 7 1953 **49** 45.

[2] HAGENBACH W. P. and COMINGS E. W. *Industr. Engng. Chem.* (*Industr.*) 1953 **45** 606.

[3] REDLICH O. and KISTER A. T. *Industr. Engng. Chem.* (*Industr.*) 1948 **40** 345.

[4] VAN NESS H. C. *Amer. Inst. Chem. Engrs. J.* 1955 **1** 100.

Book Reviews

Chemical Engineering Practice. Edited by H. W. Cremer (Managing Editor Trefor Davies). Vol. I: **General** xiv + 494 pp. 95s. Vol II: **Solid State** vi + 632 pp., Butterworths Scientific Publications, London, 1956. 95s.

VOL.
7
957/58

Volume I

The Origins of Chemical Engineering
The Chemical Engineer
Economics of Production as Exemplified in Process Industries
Investigation and Development of an Industrial Process :—
Preparation of Materials Balances
Preparation of Energy Balances
Pilot Plants and Semi-Commercial Units
The Preparation of Flow Diagrams for Full-Scale Production
Units, Dimensions and Calculations.

Volume II

Fundamental Concepts of Matter in the Solid State
Metals and Metallic Alloys
Mechanical and Physical Properties of Plastics and Glasses
Corrosion of Metals
Porous Masses
Porous Powder Metallurgical Products for Filtration and Related Uses
Powder Metallurgy
Important Industrial Uses of Porous Masses
Transpiration Cooling

The two volumes under review are the first of a set of twelve. The object of the series is stated in the Preface :

" Thus, commercial success in translating a laboratory method of a preparation into a full-scale manufacturing process depends as much upon the careful study of plant and plant design as upon consideration of the precise chemical reactions to be employed ; in short, industrial efficiency and the profits expected to accompany this can only be realized by sound chemical engineering.

" In order to achieve this end and to meet the intensive competition of the present age, the closest co-operation between the more strictly theoretical worker and the technologist is essential. Furthermore, it is necessary for both the pure and the applied scientist in industry to have an awareness of the significance of the economic background of processes which they are engaged in bringing into being. In addition, an administrative and financially minded class must be participants, the education of which is sufficiently broad to enable its members to recognize the sure foundations on which sound scientific conclusions rest. It is the object of the present publication to assist all three kinds of individuals . . . ."

" A study of the lists of contents of the twelve volumes which will eventually comprise the present series will indicate that an attempt is being made to acquaint the reader with the various stages of development of a manufacturing process from the laboratory bench to the completed factory. There are other matters, however, which must be taken into account if the factory is to be brought into successful operation and if its efficiency is to be ensured. Consideration has been given, therefore, to Works Administration, Supervision and Maintenance. The equally significant items of Works Safety and of Medical, First Aid and Welfare Services will also be included. Patent Legislation is another matter to which consideration has been given, an acquaintance with which may be all important to the chemical engineer in the course of exercising his wider functions."

The project is, therefore, an ambitious one, and one must admire the courage and enterprise of the editors in attempting it, and their success, so far, in obtaining contributions from well-informed authors. The completed work will be unique in chemical engineering literature, and will be found in all well-stocked academic and industrial libraries in this country, and many abroad.

I suppose that any given well-informed reader whose interests lie somewhere in the chemical engineering spectrum will get novel information from about one-third of the work. Another third he will use as an *aide-memoire* in respect of matters with which he is familiar but not concerned frequently ; and the rest he will read as an expert—that is critically and suspiciously. It is essential, therefore, that the standard of all the contributions should be high enough to compel the respect of the expert if he is to have confidence in the parts with which he is less familiar.

A further requirement is that each contribution should be comprehensible to any potential reader (postulated by the editors to have reached degree standard in the pure or applied physical sciences). Finally, it is desirable to avoid too much overlapping, unevenness in presentation, diffuseness and the temptation to include more than can be adequately treated.

No symposium has ever achieved perfection in these respects. A certain inconsequence and disjointedness, an invertebrate quality, is always apparent. For this reason one might speculate whether such talent and time as is available for writing technical books (all publishers will know how little there is) might not be more profitably used in producing a series of authoritative monographs.

In the present instance, might it have been more useful to promote a series similar to (but better than) the McGraw-Hill Chemical Engineering Series? However, a reviewer's task lies with the books he is given, and not with hypothetical alternatives.

The contributors to the present volumes, many of whose names are well known, have on the whole done a good job. Most of the information they give, as far as I have checked it, is factually correct and the general level of presentation is good considering the difficulties involved in compressing the subject into the required compass. In a number of cases the treatment of topics is necessarily so condensed that it might have been better to take the working results for granted and refer to text-books for the theoretical background. The treatment of Second-Law thermodynamics and of adsorption in "The Preparation of Energy Balances", and of wave mechanics in "Concepts of Matter in the Solid State" are examples.

On the other hand there are places where the editors, to my mind, have allowed too much space to generalities with a rather low content of information. For instance, the philosophy and methodology of pilot-plant work have been treated far too liberally, and the authors have plenty of space for stating the obvious, in sharp contrast to those mentioned above.

The more technical side of the section on pilot-plants is probably the most valuable part of these two volumes, although many of the topics dealt with under "Design" will presumably also be covered in Vol. IV: "Design and Construction of Chemical Plant," and elsewhere. Similarly, much of the thermodynamics dealt with in Vol. I is to be covered again in Vol. IV. This tendency to duplication is probably inevitable in a multi-volume work if each volume is to be reasonably self-contained. Nevertheless, it will add considerably to the total bulk of the published work, and it is to be hoped that the editors will do all they can to co-ordinate the work of different authors.

A further danger which can be foreseen after looking at the first two volumes is that chapters may be included because expert authors are available rather than because their contributions are really relevant to the theme of the volume or of the work as a whole. For instance, Eisenklam *et al.* contribute an admirable chapter to Vol. II on "Transpiration Cooling"; this technique may one day find an application in chemical engineering, but the only applications at present are apparently to rocket motors and gas-turbine blades. A chapter on "Porous Masses" is followed by "Important Industrial Uses of Porous Masses". The latter consists of three expert articles on the purification of coal gas, combustion in a fuel bed, and the filtration of water and sewage; although interesting as accounts of particular industrial processes, these articles (except, to a certain degree, the last) make little reference to the principles discussed at length in the earlier chapter.

These criticisms are coupled with congratulations to the editors for the way in which they have largely overcome the inevitable difficulties of their task, and for the amount of solid value they have provided in their first two volumes. If they do as well or better with the remaining volumes, their work will become the *vade-mecum* of practising chemical engineers.

P. V. Danckwerts

International News

Volume 1 of *Les Annales du Génie Chimique* has been received. The series is intended to make available the results of work carried out in the Research Department of Institut du Génie Chimique of the University of Toulouse. Further volumes will be published annually.

Volume 1 (140 pp. 3,200 fr.) describes with detailed calculations the design of a process for the production of anhydrous sulphur trioxide. It also contains a foreword by Professor Cathala, Directeur de L'Institut du Génie Chimique.

The journal may be obtained from:

Editions Édouard Privat,
14, Rue des Arts,
Toulouse (France)

VOL.
7
957/58

END